

ANTICANCER ACTIVITY OF PLUMBAGIN ON STEM-LIKE CHARACTERISTICS,  
TUMOR ANGIOGENESIS AND METASTATIC POTENTIAL  
IN ENDOCRINE RESISTANT BREAST CANCER



A Dissertation Submitted in Partial Fulfillment of the Requirements  
for the Degree of Doctor of Philosophy in Medical Sciences

Common Course

Faculty of Medicine

Chulalongkorn University

Academic Year 2018

Copyright of Chulalongkorn University

ฤทธิ์ด้านมะเร็งของพลัมบาจินต่อลักษณะคล้ายเซลล์ต้นกำเนิดมะเร็ง การสร้างหลอดเลือดใหม่  
และการแพร่กระจายในเซลล์มะเร็งเต้านมที่ดื้อยาต้านฮอร์โมน



วิทยานิพนธ์นี้เป็นส่วนหนึ่งของการศึกษาตามหลักสูตรปริญญาวิทยาศาสตรดุษฎีบัณฑิต

สาขาวิชาวิทยาศาสตร์การแพทย์ ไม่สังกัดภาควิชา/เทียบเท่า

คณะแพทยศาสตร์ จุฬาลงกรณ์มหาวิทยาลัย

ปีการศึกษา 2561

ลิขสิทธิ์ของจุฬาลงกรณ์มหาวิทยาลัย





## 5874769330 : MAJOR MEDICAL SCIENCES

KEYWORD: Plumbagin, Angiogenesis, FGF2, Cancer stem-like cells, Wnt signaling pathway,  
Endocrine resistant breast cancer

Nithidol Sakunrangsit : ANTICANCER ACTIVITY OF PLUMBAGIN ON STEM-LIKE CHARACTERISTICS, TUMOR ANGIOGENESIS AND METASTATIC POTENTIAL IN ENDOCRINE RESISTANT BREAST CANCER. Advisor: Asst. Prof. WANNARASMI KETCHART, M.D., Ph.D.

Plumbagin (PLB), a naphthoquinone compound and vitamin K<sub>3</sub> derivative, was shown its potent cytotoxicity and anti-invasion in anti-hormonal resistant cells through the inhibition of Snail-induced epithelial mesenchymal transition (EMT). Overexpression of Snail leads to decrease E-cadherin and increase of beta-catenin, resulting in the activation of Wnt pathway that increases cancer stem-like characteristics in these resistant cells. This study was aimed to investigate the inhibitory effects of PLB on cancer stem-like cells (CSLCs), angiogenesis and Wnt signaling-mediated cell proliferation and invasion. In addition, our study also focused on the anticancer activity of PLB in anti-hormonal resistant breast cancer *in vivo*. Both anti-hormonal resistant LCC2 and LCC9 cells increased beta-catenin and dysregulated Wnt signaling. Thus, these two cell lines were able to form mammospheres with elevated stem cell markers. This property is the characteristic of CSLCs. Our study showed that PLB significantly diminished the colony and mammosphere formation in a concentration-dependent manner. PLB also dramatically reduced angiogenic factors, stem cell markers and p-Akt expression. Our findings demonstrated the anti-proliferative and anti-invasive properties of PLB were partly mediated by Wnt signaling. Importantly, the inhibitory effects of PLB in cell lines were consistent with the result in xenograft mice. PLB at the doses of 2 mg/kg/day and 4 mg/kg/day significantly inhibited tumor growth without any adverse effects on body weight and blood coagulation. Moreover, PLB treatment not only repressed tumor angiogenesis, but also inhibited lung metastasis. Overall, these findings supported the role of PLB as an anti-cancer agent for anti-hormonal resistant breast cancer.

Field of Study: Medical Sciences

Student's Signature .....

Academic Year: 2018

Advisor's Signature .....

## ACKNOWLEDGEMENTS

First and foremost, I would like to express my gratitude to my advisor, Assist. Prof. Wannarasmee Ketchart M.D., at the Department of Pharmacology for her support, patience, and encouragement throughout my doctoral student. It is not often that one finds a mentor and colleague that always finds the time for listening to any problems and roadblocks that perforce appear in the course of performing research. Her editorial advice was essential to the fulfillment of this dissertation and has taught me inestimable lessons and insights in working as an excellent academic researcher.

I am sincerely grateful to the members of my dissertation committee, Prof. Vilai Chentanez M.D., Assist. Prof. Wacharee Limpanasithikul, Assist. Prof. Depicha Jindatip, and Dr. Pongpun Siripong for reading previous drafts of this dissertation and providing many valuable comments that improved the presentation and contents of this work. I wish to acknowledge the 100th Anniversary Chulalongkorn University for doctoral scholarship and the Department of Pharmacology at the Faculty of Medicine, Chulalongkorn University for making it possible for me to study here.

My thanks also go to everyone who contributed in the completion of my journey in 4 year for Ph.D study and thanks myself to energetic, patience, and responsible to work really hard. I would like to give special thanks to Prof. Mana Taweewisit M.D., at the Department of Pathology for his assistance to standardize methods for immunohistochemical analysis and my thanks to Intouch Kiatkongla at Laboratory Animal Center, Faculty of Medicine for helping to access animal facilities. This research was partially supported by the 90th Anniversary of Chulalongkorn University Ratchadaphiseksomphot Endowment Fund.

Last but not least, I would like to thank my family, my parents, and younger sister to receive my deepest gratitude for their understanding, love and their dedication in the many years of support mental health during my graduate education experience.

Nithidol Sakunrangsit

## TABLE OF CONTENTS

	Page
.....	iii
ABSTRACT (THAI) .....	iii
.....	iv
ABSTRACT (ENGLISH) .....	iv
ACKNOWLEDGEMENTS .....	v
TABLE OF CONTENTS .....	vi
LIST OF TABLES .....	x
LIST OF FIGURES .....	xi
LIST OF ABBREVIATIONS .....	15
CHAPTER I INTRODUCTION .....	20
Background and Rationale .....	20
Research Questions .....	23
Hypothesis .....	23
Research Objectives .....	24
Expected Benefit and Application .....	24
Keywords .....	24
CHAPTER II LITERATURE REVIEWS .....	25
Breast Cancer .....	25
Molecular Subtypes of Breast Cancer .....	25
Hormonal therapy for ER-positive Breast Cancer .....	26
Anti-hormonal Resistance .....	28

Anti-Hormonal Resistance in ER-positive Breast Cancer.....	28
Anti-hormonal Resistant Breast Cancer and Metastasis .....	29
Cancer Stem-like Features in Anti-hormonal Resistance .....	30
Wnt Signaling.....	31
Wnt Signaling and EMT.....	31
Wnt Signaling and Tumor Angiogenesis .....	34
Wnt Signaling and Cancer Stem-like Features.....	36
Plumbagin.....	37
Anticancer Effects.....	38
Drug Resistant Reversal Effects.....	39
Antiangiogenic Effects.....	40
Inhibitory Effects on Cancer Stem Cells.....	40
Pharmacokinetics.....	43
Safety and Toxicity.....	44
Rationale for the Study.....	46
Conceptual Framework .....	47
CHAPTER III MATERIALS AND METHODS .....	49
Cell Lines and Cultures .....	49
Tested Compound.....	50
Chemicals and Reagents .....	50
Instruments and Equipment.....	51
Subculturing Adherent Cells.....	53
Cell Counting.....	53



Clonogenic Assay.....	54
Mammosphere Formation Assay.....	55
MTT assay.....	56
Matrigel Invasion Assays.....	56
Tumor Growth in Xenograft Mice.....	57
H&E Staining of Lung Tissues.....	59
Immunohistochemistry Staining (PECAM).....	60
Blood Coagulation.....	61
RNA Extraction and cDNA preparation.....	61
Quantitative real-time PCR (qRT-PCR).....	63
Protein Extraction and SDS-PAGE Preparation.....	65
Western Blot Analysis.....	66
Ethical Statement.....	67
Statistical analysis.....	68
CHAPTER IV RESULTS.....	69
Characterization of cancer stem-like features in anti-hormonal resistant breast cancer cell lines.....	69
Aberrant activation of Wnt/beta-catenin signaling in anti-hormonal resistant breast cancer cell lines.....	74
PLB inhibited cell proliferation and the expression of Wnt-targeted genes in anti-hormonal resistant breast cancer cell lines.....	79
PLB decreased stem-like features and the expression of cancer stem cell genes in anti-hormonal resistant breast cancer cell lines.....	88

PLB decreased Akt phosphorylation in anti-hormonal resistant breast cancer cell lines. ....	94
PLB abrogated Wnt-mediated proliferation and invasion via the modulation of <i>CCND1</i> and <i>MYC</i> in anti-hormonal resistant cell lines. ....	98
PLB significantly inhibited tumor growth without serious adverse effects in anti-hormonal resistant breast cancer orthotopic xenografts in mice. ....	108
PLB inhibited tumor angiogenesis and metastasis in anti-hormonal resistant breast cancer orthotopic xenograft mice. ....	113
CHAPTER V DISCUSSION AND CONCLUSION.....	122
Discussion .....	122
Conclusion.....	127
Future Perspective.....	129
REFERENCES .....	130
APPENDIX.....	156
VITA .....	163

## LIST OF TABLES

	Page
Table 1. Cancer stem cells (CSCs) biomarkers in several tumors.....	31
Table 2. A summary of previous studied on pharmacological activities of PLB. ....	41
Table 3. The PK parameters of PLB after oral administration in Wistar rats.....	44
Table 4. The characterization of cell lines used this study. ....	50
Table 5. Primer sequences used for quantitative real-time PCR analysis.....	63



## LIST OF FIGURES

	Page
Figure 1. EMT associated with drug resistance and stemness .....	30
Figure 2. Wnt/beta-catenin signaling in tumor metastasis .....	32
Figure 3. VEGF signaling in tumor angiogenesis .....	35
Figure 4. The 2D structure of plumbagin .....	37
Figure 5. Characterization of cancer stem-like features in anti-hormonal resistant breast cancer cell lines.....	70
Figure 6. <i>ALDH1</i> mRNA expression of anti-hormonal resistant cells grown under adherent monolayer and mammosphere cultures.....	71
Figure 7. <i>NANOG</i> mRNA expression of anti-hormonal resistant cells grown under adherent monolayer and mammosphere cultures.....	72
Figure 8. <i>OCT4</i> mRNA expression of anti-hormonal resistant cells grown under adherent monolayer and mammosphere cultures.....	73
Figure 9. Protein expression of beta-catenin in breast cancer cell lines .....	75
Figure 10. The canonical Wnt-targeted gene expression involved in cell proliferation ( <i>CCND1</i> and, <i>MYC</i> ) in anti-hormonal resistant cells.....	76
Figure 11. The canonical Wnt-targeted gene expression involved in angiogenesis and invasion ( <i>VEGF</i> and <i>AXIN2</i> ) in anti-hormonal resistant cells.....	77
Figure 12. The canonical Wnt-targeted gene expression involved in EMT and metastasis ( <i>TCF4</i> and <i>DKK1</i> ) in anti-hormonal resistant cells.....	78
Figure 13. The inhibitory effect of PLB on colony formation of LCC2 and LCC9 cells....	80
Figure 14. <i>AXIN2</i> mRNA expression in anti-hormonal resistant cells after the treatment with 0.5 and 1.0 $\mu$ M of PLB for 24 hours.....	81

Figure 15. <i>TCF4</i> mRNA expression in anti-hormonal resistant cells after the treatment with 0.5 and 1.0 $\mu$ M of PLB for 24 hours.....	82
Figure 16. <i>DKK1</i> mRNA expression in anti-hormonal resistant cells after the treatment with 0.5 and 1.0 $\mu$ M of PLB for 24 hours.....	83
Figure 17. Protein expression of beta-catenin in anti-hormonal resistant LCC9 cells after the treatment with 0.5 and 1.0 $\mu$ M of PLB for 24 hours.....	84
Figure 18. Protein expression of FGF2 in breast cancer cell lines.....	85
Figure 19. Protein and mRNA expression of FGF2 in anti-hormonal resistant cells after the treatment with 0.5 and 1.0 $\mu$ M PLB for 24 hours.....	86
Figure 20. <i>VEGF</i> mRNA expression in anti-hormonal resistant cells after the treatment with 0.5 and 1.0 $\mu$ M of PLB for 24 hours.....	87
Figure 21. The inhibitory effect of PLB on the secondary mammospheres-forming efficiency (MFE) of LCC2 and LCC9 cells. ....	89
Figure 22. The inhibitory effect of PLB on the tertiary mammospheres-forming efficiency (MFE) of LCC2 and LCC9 cells.....	90
Figure 23. <i>ALDH1</i> mRNA expression in anti-hormonal resistant LCC2 and LCC9 cells after treatment with 0.5 and 1.0 $\mu$ M PLB for 24 hours.....	91
Figure 24. <i>NANOG</i> mRNA expression in anti-hormonal resistant LCC2 and LCC9 cells after treatment with 0.5 and 1.0 $\mu$ M PLB for 24 hours.....	92
Figure 25. <i>OCT4</i> mRNA expression in anti-hormonal resistant LCC2 and LCC9 cells after treatment with 0.5 and 1.0 $\mu$ M PLB for 24 hours.....	93
Figure 26. Protein expression of Akt phosphorylation at Ser473 in breast cancer cell lines .....	95
Figure 27. Protein expression of phosphorylated Akt in anti-hormonal resistant LCC2 cells after treatment with 0.5 and 1.0 $\mu$ M of PLB for 24 hours. ....	96

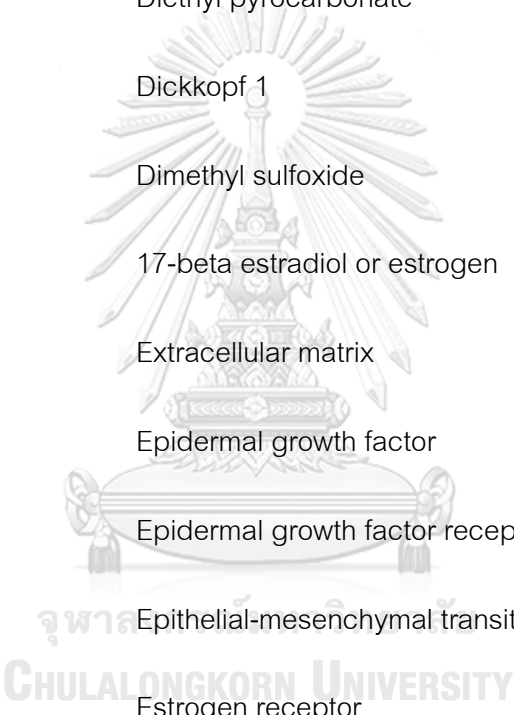
Figure 28. Protein expression of phosphorylated Akt in anti-hormonal resistant LCC9 cells after the treatment with 0.5 and 1.0 $\mu$ M of PLB for 24 hours. ....	97
Figure 29. Cell viability of LCC2 and LCC9 treated with 0.5, 1.0, and 1.5 $\mu$ M of PLB for 24 hours with or without the pre-treatment with 100 ng/mL Wnt1 ligand. ....	100
Figure 30. Cell viability of LCC2 and LCC9 treated with 0.5, 1.0, and 1.5 $\mu$ M of PLB for 24 hours with or without the 5 $\mu$ M IWP2 (Wnt inhibitor). ....	101
Figure 31. <i>CCND1</i> mRNA expression after the treatment with 0.5 and 1.0 $\mu$ M of PLB with or without pre-treatment with 5 $\mu$ M IWP2 (Wnt inhibitor) for 24 hours. ....	102
Figure 32. <i>MYC</i> mRNA expression after the treatment with 0.5 and 1.0 $\mu$ M of PLB with or without pre-treatment with 5 $\mu$ M IWP2 (Wnt inhibitor) for 24 hours. ....	103
Figure 33. Cell invasion of LCC2 treated with 0.5 and 1.0 $\mu$ M of PLB for 48 hours with or without the pre-treatment with 100 ng/mL Wnt1 ligand. ....	104
Figure 34. Cell invasion of LCC9 treated with 0.5 and 1.0 $\mu$ M of PLB for 48 hours with or without the pre-treatment with 100 ng/mL Wnt1 ligand. ....	105
Figure 35. Cell invasion of LCC2 treated with 0.5 and 1.0 $\mu$ M of PLB for 48 hours with or without the pre-treatment with 5 $\mu$ M IWP2 (Wnt inhibitor). ....	106
Figure 36. Cell invasion of LCC9 treated with 0.5 and 1.0 $\mu$ M of PLB for 48 hours with or without the pre-treatment with 5 $\mu$ M IWP2 (Wnt inhibitor). ....	107
Figure 37. Time schedule of treatments and tumor volume in mice treated with 0.1% DMSO in normal saline (control), 2 mg/kg/day PLB (low-dose) and 4 mg/kg/day PLB (high-dose), ....	109
Figure 38. The body weight in grams of mice treated with 0.1% DMSO in normal saline (control), 2 mg/kg/day PLB (low-dose) and 4 mg/kg/day PLB (high-dose) was monitored every other day throughout the treatment. ....	110
Figure 39. The average of tumor weight in mice treated with 0.1% DMSO in normal saline (control), 2 mg/kg/day PLB (low-dose) and 4 mg/kg/day PLB (high-dose). ....	111

Figure 40. The prothrombin time (PT) in seconds in blood sample collected from mice treated with PLB on the sacrificed day .....	112
Figure 41. The micrometastasis and the incidence of lung metastasis in mice treated with 0.1% DMSO in normal saline (control), 2 mg/kg/day PLB (low-dose) and 4 mg/kg/day PLB (high-dose).....	115
Figure 42. The mean lung weight in grams of mice treated with 0.1% DMSO in normal saline (control), 2 mg/kg/day PLB (low-dose) and 4 mg/kg/day PLB (high-dose).....	116
Figure 43. <i>SDF1</i> mRNA expression levels in lung tissues of mice after treatment with 0.1% DMSO in normal saline (control), 2 mg/kg/day PLB (low-dose) and 4 mg/kg/day PLB (high-dose).....	117
Figure 44. <i>MMP9</i> mRNA expression levels in lung tissues of mice after treatment with 0.1% DMSO in normal saline (control), 2 mg/kg/day PLB (low-dose) and 4 mg/kg/day PLB (high-dose).....	118
Figure 45. PECAM staining showed the relative microvessel area of PECAM/CD31 in tumor tissues.....	119
Figure 46. <i>VEGF</i> mRNA expression levels in lung tissues of mice after treatment with 0.1% DMSO in normal saline (control), 2 mg/kg/day PLB (low-dose) and 4 mg/kg/day PLB (high-dose).....	120
Figure 47. <i>FGF2</i> mRNA expression levels in lung tissues of mice after treatment with 0.1% DMSO in normal saline (control), 2 mg/kg/day PLB (low-dose) and 4 mg/kg/day PLB (high-dose).....	121

## LIST OF ABBREVIATIONS

ng/mL	Nanogram per milliliter
v/v	Volume by volume
w/v	Weight by volume
mM	Millimolar
mL	Milliliter
$\mu$ M	Micromolar
$\mu$ L	Microliter
4-OHT	4-hydroxytamoxifen
Als	Aromatase inhibitors
AKT	Protein kinase B
ALDH1	Aldehyde dehydrogenase 1
APC	Adenomatous polyposis coli
AXIN2	Axis inhibition protein 2
BCRP	Breast cancer resistance protein
CD44	Cluster of differentiation 44
CDH1	E-cadherin
CDK4/6	Cyclin-dependent kinase 4/6
CK1	Casein kinase 1





CYP	Cytochromes P450
CSLCs	Cancer stem-like cells
CTGF	Connective tissue growth factor
CTNNB1	Beta-catenin
DAB	3,3'-diaminobenzidine tetrahydrochloride
DAPC	Diethyl pyrocarbonate
DKK1	Dickkopf 1
DMSO	Dimethyl sulfoxide
E2	17-beta estradiol or estrogen
ECM	Extracellular matrix
EGF	Epidermal growth factor
EGFR	Epidermal growth factor receptor
EMT	Epithelial-mesenchymal transition
ER	Estrogen receptor
ERK1/2	Extracellular signal-regulated kinase 1/2
FGF2	Fibroblast growth factor 2
GAPDH	Glyceraldehyde-3-phosphate dehydrogenase
GSK3	Glycogen synthase kinase 3
H&E	Haematoxylin and eosin
HER2	Human epidermal growth factor receptor 2

IHC	Immunohistochemistry
IWP2	Inhibitor of Wnt protein 2
KDR	Kinase insert domain receptor
LCC2	Tamoxifen-resistant breast cancer cell line
LCC9	Fulvestrant/tamoxifen-resistant breast cancer cell line
LRP5/6	Low-density lipoprotein receptor-related protein 5/6
MAPK	Mitogen-activated protein kinase
MCF-7	ER-positive breast cancer cell line
MEM	Minimal essential medium
MMP2	Matrix metalloproteinase 2
MMP9	Matrix metalloproteinase 9
MTT	Methylthiazolyldiphenyl tetrazolium bromide
NANOG	Nanog homeobox
NCOA3	Nuclear receptor coactivator 3
NCOR1	Nuclear receptor corepressor 1
NF- $\kappa$ B	Nuclear factor kappa B
OCT4	Octamer-binding transcription factor 4
P21	Cyclin-dependent kinase (CDK) inhibitor
p38 MAPK	p38 mitogen-activated protein kinase
PBS	Phosphate buffered saline

PDGF	Platelet-derived growth factor
PECAM/CD31	Platelet endothelial cell adhesion molecule/CD31
PI3K	Phosphoinositide-3-kinase
PKC	Protein kinase C
PLB	Plumbagin
PR	Progesterone receptor
RT-qPCR	Real-time quantitative polymerase chain reaction
RAC	Ras-related C3 botulinum toxin substrate
ROS	Reactive oxygen species
RNA	Ribonucleic acid
RTK	Receptor tyrosine kinase
SDF-1	Stromal-derived factor 1
SEM	Standard error of the mean
SERDs	Selective estrogen receptor degraders
SERMs	Selective estrogen receptor modulators
SFM	Serum-free medium
SLUG	Zinc finger protein <i>SNAI2</i>
SNAI1	Snail family transcriptional repressor 1
SSM	Serum-supplemented medium
STAT3	Signal transducer and activator of transcription 3

TCF/LEF1	T-cell factor/lymphoid enhancing factor 1
TCF4	Transcription factor 4
TLEs	Transducin-like enhancer proteins
TWIST	Twist family BHLH transcription factor
VEGF	Vascular endothelial growth factor
VEGFR2	Vascular endothelial growth factor receptor 2
WNT1	Wingless-type MMTV integration member 1
ZEB1/2	Zinc finger E-box binding homeobox 1/2



## CHAPTER I

### INTRODUCTION

#### Background and Rationale

Breast cancer is the most common and the leading cause of death in women around the world and Thailand [1, 2]. Breast cancer patients are categorized into three major subtypes depending on their hormonal receptor expression including estrogen receptor (ER), progesterone receptor (PR) and human epidermal growth factor receptor 2 (HER2). Tamoxifen, a selective ER modulator (SERM), is commonly used as adjuvant therapy for ER-positive breast cancer [3]. However, approximately 40 percent of advanced stage breast cancer developed acquired resistance after taking tamoxifen for five years [4].

Increased expression of nuclear receptor coactivator-3 (NCOA3) and a loss of nuclear receptor corepressor-1 (NCOR1) were established as hallmarks of anti-hormonal-resistant breast cancer resulted in tumor recurrence and metastasis [5, 6]. The overexpression of NCOA3 is often detected in approximately 60% of breast cancer patients and associated with short overall survival [5]. Ao et al. demonstrated that NCOA3 overexpression was able to induce AKT signaling pathway involved in cell proliferation, apoptosis and drug resistance in breast cancer [7]. These findings are similar to Sakunrangsit et al. [8] which reported that NCOA3 protein level was

significantly higher in anti-hormonal resistant cell lines when compared to wild-type ER-positive breast cancer cells [8].

Accumulating evidences showed that tamoxifen-resistant breast cancer (TAM-R) cells over-expressed important angiogenic factor which is vascular endothelial growth factor (VEGF) leading to increased tumor angiogenesis [9, 10]. Likewise, Guo et al [11] reported cancer stem cells increased tumor recurrence and liver metastasis in tamoxifen resistant breast cancer [11]. Hence, the dual targeting of cancer stem-like features and tumor angiogenesis in anti-hormonal resistant phenotype may provide a promising strategy to improve survival in breast cancer patients.

A recent study has demonstrated that plumbagin, a plant-derived naphthoquinone which isolated from *Plumbago indica*, has the potent effects on tumor growth inhibition, drug resistance reversal and anti-invasion in anti-hormonal resistant breast cancer cells. Plumbagin altered epithelial-mesenchymal transition (EMT) markers by increasing an epithelial marker E-cadherin and decreasing mesenchymal markers including Vimentin and Snail expression [8]. Snail, a transcriptional repressor of E-cadherin, is a critical determinant of tumor growth, EMT and distant metastasis [12, 13]. A recent report indicated that both mRNA and protein of Snail expression are triggered by VEGF and its receptor Neuropilin-1 via the inhibition of glycogen synthase kinase-3 (GSK-3) in breast cancer [10].

In addition, Snail also triggered cancer stem-like phenotypes and promoted blood vessel formation in several types of tumor including breast [14-16]. Abundant evidence demonstrated that Wnt/beta-catenin signaling plays an essential role in EMT and contributes to cancer stem cell-like properties [17]. In the absence of Wnt ligand, beta-catenin interacts with E-cadherin which located in the plasma membrane. Snail is the transcription factor that activates EMT transition and Wnt pathway through the nuclear accumulation of beta-catenin and a loss of E-cadherin [16]. Moreover, Loh et al. [18] demonstrated that upregulation of Wnt-targeted genes in TAM-R cells resulted in increased metastatic abilities [18].

Our previous studies found that plumbagin can inhibit EMT and tumor invasion through the reduction of Snail expression which may decrease the activation of Wnt/beta-catenin signaling. Furthermore, the activity of plumbagin on tumor angiogenesis in breast cancer, especially in anti-hormonal resistant cells have not been studied. Therefore, this study purposes to investigate the activity of plumbagin on cancer stem-like characteristics, tumor angiogenesis and Wnt-mediated EMT in anti-hormonal resistant breast cancer *in vitro* and *in vivo*.

### Research Questions

1. Does plumbagin inhibit cancer stem-like features and angiogenesis in anti-hormonal resistant breast cancer *in vitro*?
2. Does plumbagin inhibit AKT signaling pathway in anti-hormonal resistant breast cancer *in vitro*?
3. Does plumbagin decrease the cell proliferation and invasion in anti-hormonal resistant breast cancer *in vitro* through Wnt signaling pathway?
4. Does plumbagin exhibit anti-tumor and anti-angiogenic effects in anti-hormonal resistant breast cancer *in vivo*?

### Hypothesis

1. Plumbagin inhibits cancer stem-like features and angiogenesis in anti-hormonal resistant breast cancer *in vitro*.
2. Plumbagin inhibits AKT signaling pathway in anti-hormonal resistant breast cancer *in vitro*.
3. Plumbagin decreases the cell proliferation and invasion in anti-hormonal resistant breast cancer *in vitro* through Wnt signaling pathway.
4. Plumbagin exerts anti-tumor and anti-angiogenic effects in anti-hormonal resistant breast cancer *in vivo*.



### Research Objectives

1. To investigate the effect of plumbagin on cancer stem-like features and angiogenesis in anti-hormonal resistant breast cancer *in vitro*.
2. To investigate the effect of plumbagin on AKT signaling pathway in anti-hormonal resistant breast cancer *in vitro*.
3. To investigate the effect of plumbagin on the cell proliferation and invasion in anti-hormonal resistant breast cancer *in vitro* through Wnt signaling pathway.
4. To investigate the inhibitory effects of plumbagin on tumor growth and angiogenesis in anti-hormonal resistant breast cancer *in vivo*.

### Expected Benefit and Application

Our findings could provide new insights on the potential therapeutic effects and mechanism of plumbagin in anti-hormonal resistant breast cancer by decreasing cancer stem-like features and inhibiting tumor growth, angiogenesis and metastasis. Therefore, plumbagin may use as a treatment to prevent tumor recurrence and improve survival rate of anti-hormonal resistant breast cancer patients.

### Keywords

Plumbagin, Wnt/beta-catenin signaling, Anti-hormonal resistance, Cancer stem-like cells, FGF2-mediated angiogenesis, Metastasis.

## CHAPTER II

### LITERATURE REVIEWS

#### Breast Cancer

According to World Health Organization (WHO) reports, breast cancer is indicated as the highest numbers of new cases in women worldwide in 2019 [1, 19]. Approximately 29% of women aged over fifty are commonly diagnosed with breast cancer. Breast cancer can occur in men accounting for 1% of total population. Globally, breast cancer is the second leading cause of death which is estimated of 14% (40,450) of all patients [1]. The evidence from National Cancer Institute (NCI) of Thailand demonstrated that approximately 21.6% of Thai women was diagnosed with breast cancer which is the most common sites of tumor [2, 20]. Recently, the mortality rate of advanced-stage breast cancer patients remains high and very challenge for new treatment strategies.

#### Molecular Subtypes of Breast Cancer

Breast cancer is divided into 5 categories based on the molecular profiling expression. There are luminal (A and B), human epidermal growth factor receptor 2 (HER2)-overexpressed, claudin-low and basal-like tumors. Luminal A is the most common type of breast cancer showing hormone receptor such as

estrogen receptor (ER) and progesterone receptor (PR)-positive and HER2-negative. Luminal B is hormone receptors (ER and PR)-positive with the presence or absence of HER2 and higher proliferation markers such as Ki-67 (*MKI67*). In addition, basal-like breast cancer is a highly aggressive phenotype which is lack of ER, PR and HER2 expression (also known as triple-negative). Lastly, claudin-low is a recently proposed subtype of breast tumor characterized by the absence of proteins involved in tight junction such as claudin 3, E-cadherin, and exhibited high expression of mesenchymal markers and low expression of luminal biomarkers [3]. The molecular profiling is used to classified the treatment for each subtype such as hormonal therapy for ER-positive breast cancer patients.

### Hormonal therapy for ER-positive Breast Cancer

Most cases of breast cancer will receive systemic treatment after surgery with either radiation therapy or pharmacotherapy. These patients also received hormonal (also known as anti-hormonal or endocrine) therapy, HER2-targeted drugs or chemotherapy regarding to their intrinsic molecular expression or breast cancer subtypes. Anti-hormonal therapy is often used to treat estrogen receptor (ER)-positive breast cancer patients. There are selective estrogen

receptor modulators (SERMs), aromatase inhibitors (AIs), and selective estrogen receptor degraders (SERDs) [21].

Tamoxifen (TAM) is commonly used as the first-line drug in ER-positive breast cancer patients. TAM metabolism is mediated by cytochrome P450 (CYP) with major contribution from CYP2D6 and CYP3A4 isoforms for the formation of active metabolites 4-hydroxytamoxifen (4-OHT) and endoxifen [22]. 4-OHT is a nonsteroidal SERM acts as an ER-antagonist in breast tissues, while it functions as an ER-agonist in bone and endometrium [3, 22]. Fulvestrant is used to treat metastatic estrogen receptor (ER)-positive breast cancer, which functions by binding competitively to ER, acts as an antagonist and stimulates ER degradation [23]. Aromatase inhibitor (AIs) works as an inhibitor of aromatase enzyme which converts estrone ( $E_1$ ) or androstenedione (as a precursor to testosterone and  $E_1$ ) to estradiol ( $E_2$ ) such as Anastrozole, Letrozole, and Exemestane [24]. Hormonal therapy has common adverse drug reactions (ADRs) including hot flashes, night sweats, irregular menstruation and vaginal dryness. In addition, tamoxifen treatment is correlated with an increased incidence of vaginal bleeding, endometrial polyps and thromboembolic events, while ADRs of fulvestrant and AIs include nausea, bone pain and risk of bone fractures [3, 24].

## Anti-hormonal Resistance

### Anti-Hormonal Resistance in ER-positive Breast Cancer

Approximately 40% of advanced-stage ER-positive breast cancer patients who received tamoxifen more than five years developed tumor recurrence which led to high aggressive disease and low survival rate [4]. Almost all patients developed distant metastasis which resulted from poor response to anti-hormonal therapy (endocrine resistance). Several mechanisms involved in anti-hormonal resistant breast cancer include (i) loss of ER function and expression [5, 25], (ii) alteration of ER coregulator proteins such as increased nuclear receptor coactivator (NCOA1 or NCOA3) and decreased corepressor (NCOR1) proteins [26, 27], (iii) crosstalk between ER-independent signaling and other growth factors such as MAPK ERK1/2 and PI3K-AKT pathways [7, 28] and (iv) cancer stem-like features and expression of putative breast cancer stem cell pathways, especially Wnt signaling [6, 25, 29].

Our previous study confirmed that anti-hormonal resistant breast cancer (LCC9) cell line which developed the resistance to both tamoxifen and fulvestrant treatment exhibited EMT-like behaviors through the downregulation of epithelial biomarker (e.g. E-cadherin) and upregulation of mesenchymal markers (e.g. Snail and Vimentin) at the mRNA and protein levels, resulting in more aggressive invasive phenotype [8].

### Anti-hormonal Resistant Breast Cancer and Metastasis

An epithelial-mesenchymal transition (EMT) is a hallmark of tumor metastasis in advanced-stage ER-positive breast cancer [13]. EMT process is the cause of cancer cell migration and invasion from primary tumor where epithelial cells lose their polarity and cell-cell interaction. The invaded cells gain fibroblast-like behaviors with the low expression of epithelial markers (such as E-cadherin, claudins, cytokeratin) and the high expression of mesenchymal biomarkers including N-cadherin, Fibronectin, Snail and Vimentin [30].

Several growth factors and cytokines play roles in regulating EMT progression including Snail, Slug, Zeb1/2 and Twist transcription factors led to the change in phenotypes of cancer cell from epithelial to mesenchymal-like cells resulted in tumor invasion, metastasis, and drug resistance (**Figure 1**) [31].

Our previous study indicated Snail mRNA and protein were increased in anti-hormonal resistant breast cancer cells [8]. These data suggested that these cell line had mesenchymal-like properties, resulted in increased metastatic ability and resistance to anti-hormonal tamoxifen which may contribute to cancer stem-like characteristics.

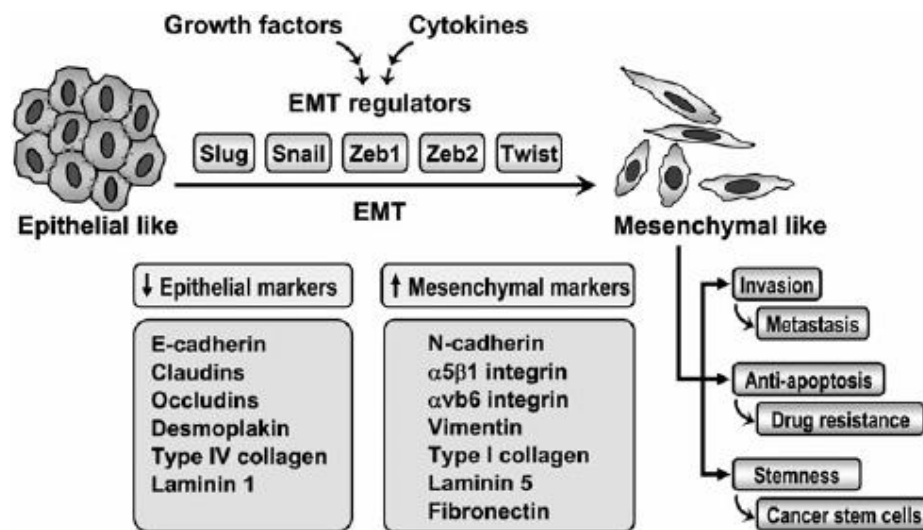


Figure 1. EMT associated with drug resistance and stemness [31].

#### Cancer Stem-like Features in Anti-hormonal Resistance

Many studies reported that drug resistance developed from cancer stem-like cells (CSLCs) surviving in the bulks tumor after treatment of conventional or hormonal therapy [13]. Moreover, EMT characteristics contribute tumor cells to increase migration and invasion in breast cancer [16, 32]. EMT-like phenotypes can also generate tumor cells with stem-like features [16]. The properties of CSLCs include increased proliferative potential *in vitro* and tumorigenicity *in vivo*, self-renewal capacity, apparent resistance to hormonal therapy or chemotherapeutic agents, and altered profile of cell surface cancer stem cell (CSC) markers depending on distinct types of cancer [33] as listed in **Table 1**. In case of breast cancer, expression of the cell surface molecule (high level of the CD44 expression and low level of CD24) with high aldehyde

dehydrogenase 1 (ALDH1) activity are well-established markers for identifying breast CSLCs [34].

**Table 1.** Cancer stem cells (CSCs) biomarkers in several tumors [33].

Type of cancer	Phenotype of CSCs markers
Leukemia	CD34 <sup>+</sup> , CD38 <sup>-</sup> , HLA-DR <sup>-</sup> , CD71 <sup>-</sup> , CD90 <sup>-</sup> , CD117 <sup>-</sup> , CD123 <sup>+</sup>
<b>Breast</b>	<b>ESA<sup>+</sup>, CD44<sup>+</sup>CD24<sup>-/low</sup>, ALDH1<sup>high</sup></b>
Liver	CD133 <sup>+</sup> , CD49f <sup>+</sup> , CD90 <sup>+</sup>
Brain	CD133 <sup>+</sup> , BCRP1 <sup>+</sup> , A2B5 <sup>+</sup> , SSEA1 <sup>+</sup>
Lung	CD133 <sup>+</sup> , ABCG2 <sup>high</sup>
Colorectal	CD133 <sup>+</sup> , CD44 <sup>+</sup> , CD166 <sup>+</sup> , EPCAM <sup>+</sup> , CD24 <sup>+</sup>

## Wnt Signaling

### Wnt Signaling and EMT

Tamoxifen resistant breast cancer cells underwent EMT which is activated by Wnt signaling pathways [18, 35]. When Wnt ligand is absent (Figure 2, left), the destruction complex is formed. This complex is consisted of APC (adenomatous polyposis coli), Axin1, GSK-3 (glycogen synthase kinase 3) and CK1 (casein kinase 1). the complex binds and phosphorylates cadherin-associated beta-catenin and can be targeted for destruction by the proteasome. In the nucleus, DNA-binding proteins of the T cell factor (TCF) and lymphoid enhancer-binding factor 1 (LEF1) family are bound by transducin-like enhancer



proteins (TLEs) resulted in transcriptional repression in breast cancer [36]. The right of Figure 2 represents the canonical Wnt pathway activation when secreted Wnt ligands (e.g. Wnt1 or Wnt3a) bind to Frizzled cognate receptor which is conjugated with lipoprotein receptor-related protein 5/6 (LRP5/6) then the complex changes its conformation and leads to the phosphorylation of the LRP6 coreceptor. The affinity of Axin1 binding site is increased which promotes the disruption of APC-GSK3-CK1 complex. beta-catenin can accumulate in cytoplasm and then translocate into the nucleus. beta-catenin binds to TCF which causes TLE repressor to dislocate from TCF, resulting in the transcriptional activation of Wnt target genes (e.g. *Cyclin D1*, *MYC*, *AXIN2*, *VEGF* and *CD44*) involved in tumor growth, angiogenesis, and metastasis [37, 38].

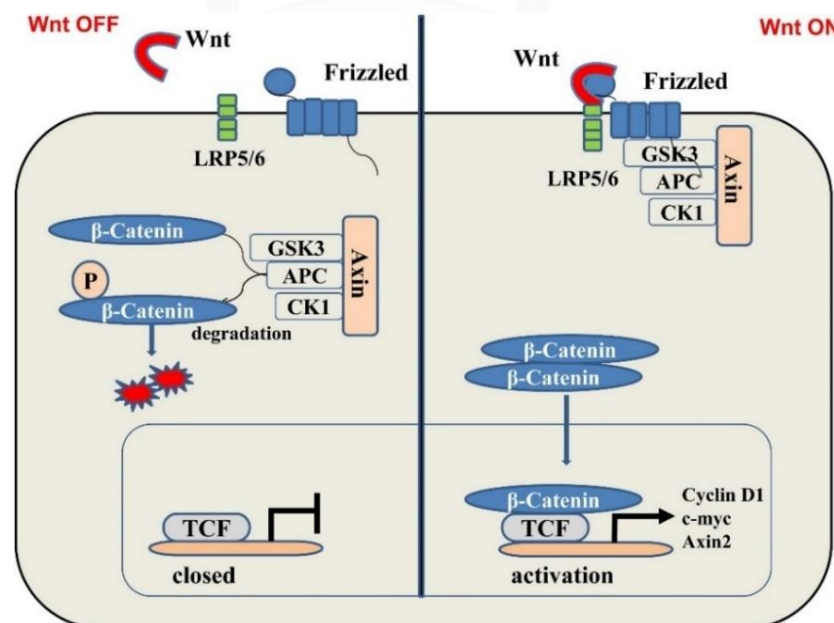


Figure 2. Wnt/beta-catenin signaling in tumor metastasis [37].

Loh et al. [18] demonstrated that Wnt-related genes were upregulated and increased EMT-like behaviors in tamoxifen-resistant TAM-R cells [18]. A study also showed the overexpression of Snail was able to induce EMT and enhance stem cell-like phenotypes with mammosphere formation in non-tumorigenic epithelial breast MCF-10A cells [12]. Our previous study demonstrated that the increase of *Snail* and decrease of *E-cadherin* mRNA expression were observed in anti-hormonal resistant breast cancer cells [8]. Moreover, Snail was able to induce EMT-like behaviors and triggered Wnt signaling activation through the downregulation of E-cadherin [16].

Our previous study also reported that plumbagin reduced the expression of Snail mRNA and protein in anti-hormonal resistant breast cancer cells [8]. Snail is a transcription factor which acts as a repressor of the E-cadherin (*CDH1*) expression and is regulated by Wnt signaling. Snail is also involved in tumor cell invasion and metastasis [37]. Hence, we hypothesized that plumbagin may inhibit Wnt/beta-catenin signaling that regulates stem-like characteristics and drug resistance in ER-positive breast cancer.

### Wnt Signaling and Tumor Angiogenesis

Angiogenesis plays a significant role in tumor growth and metastasis and involves in both primary and metastatic sites of cancer. This process includes endothelial cell migration, growth, vessel sprouting, vessel branching and stabilization as in **Figure 3**. Vascular endothelial growth factor (VEGF), a direct target of Wnt signaling, is a key angiogenic factor that induces the growth of new blood vessels from pre-existing vessels or tumor angiogenesis [10]. *VEGF* expression significantly increased in several types of cancer including colorectal, prostate, liver, and breast cancers [37]. Furthermore, activated stromal cells in microenvironment can release VEGF which induces angiogenesis in ER-positive breast cancer *in vitro* and *in vivo* [39]. *VEGF* and fibroblast growth factor (*FGF2*) increased expression in ER-negative breast cancer [37].

As illustrated in **Figure 3** shows the role of VEGF in tumor angiogenesis. VEGF interacts with its cognate receptors (such as VEGFR1 and VEGFR2) or Neuropilin-1 (NRP-1 as a co-receptor for VEGF) on endothelial cells and pericytes. In parallel, activated proteases MMPs (such as MMP2 and MMP9) degrade the extracellular matrix (ECM), resulting in tumor cell intravasation and forming vasculature. Endothelial cells secrete platelet-derived growth factor (PDGF) to recruit pericytes. Endothelial cells and other perivascular

mesenchymal cells secrete angiopoietin 1 (Ang1) which binds tyrosine kinase receptor (Tie1) on tumoral endothelial cells and promote vessel stability [40].

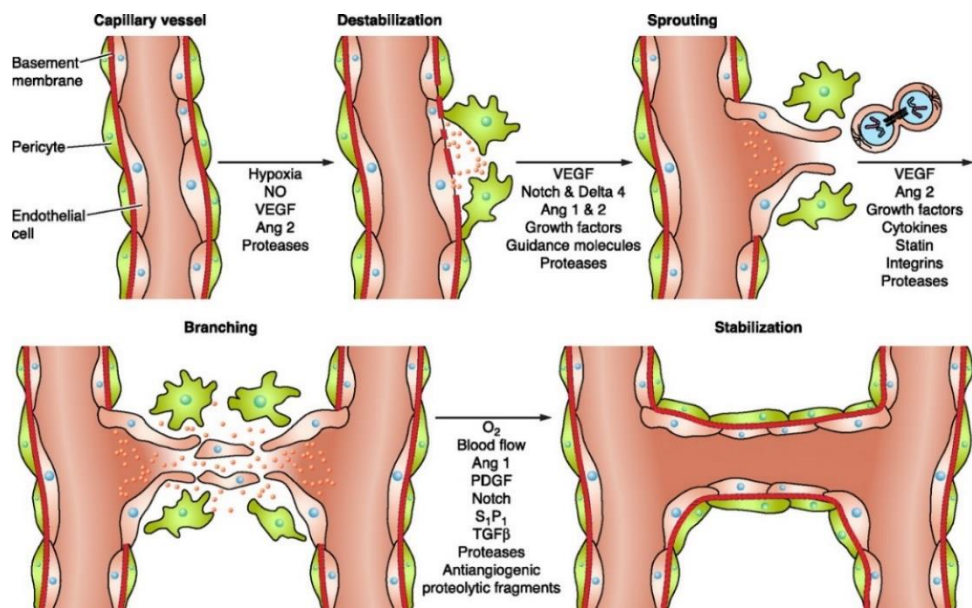


Figure 3. VEGF signaling in tumor angiogenesis [40].

The upregulation of VEGF expression in TAMR cells and breast cancer tissues from patients contributed to tumor metastasis and angiogenesis [10, 39].

Bevacizumab was used to inhibit angiogenesis in breast cancer patients.

However, this VEGF inhibitor decreased overall survival of breast cancer patients due to the enhancement of metastasis. Thus, the indication of this drug

to use in breast cancer was withdrawn in 2011 by the United States Food and Drug Administration (US FDA) [40]. Since there are so many pathways involved

in angiogenesis, inhibition of only VEGF may cause the crosstalk to other

redundant pathways. Approximately 60% of breast tumors upregulated FGF2 expression which is the other important pro-angiogenic factor [41]. Consequently, the ongoing studies on the safety and efficacy of anti-angiogenic agents for the treatment of breast cancer are still required.

### Wnt Signaling and Cancer Stem-like Features

Cancer stem-like cells (CSLCs) can survive from traditional cancer therapies, resulting in tumor recurrence and drug resistance in many types of tumor including colorectal, prostate and breast cancers [42-44]. Drug resistant phenotypes acquired the characteristics of CSLCs and undergone EMT through numerous signaling cascades include the Wnt pathway [18, 45]. As mentioned, Snail acts as a negative regulator of E-cadherin which causes beta-catenin accumulation in cytoplasm and leads to the activation of Wnt signaling that promotes transcription of Wnt-targeted genes involved in CSC-like features [13, 14, 46]. Therefore, eradication of CSC-like features in resistant breast cancer is an effective anti-cancer therapeutic strategy.

## Plumbagin

Plumbagin (PLB) is the major bioactive naphthoquinone compound which isolated from the root of *Plumbago indica* in Plumbaginaceae family. The 2-dimensional (2D) structure of PLB as showed in Figure 4 [47]. PLB exerts several therapeutic activities in the treatment of human diseases in preclinical studies. According to NCBI databases, PLB is one of the most studied compounds from 1968 to 2016. The pharmacological activities of PLB include antibacterial properties [48-52], antifungal effects [53-55], antimalarial effects [56, 57], cardioprotective effect [58], neuroprotective effects [59, 60], antidiabetic properties [61, 62], antioxidant activities [59, 63, 64], anti-inflammatory [65-67], anti-invasive [8, 68, 69], anti-metastatic effects [70-72], and anti-proliferative activities [73, 74] in cell cultures and animal models.

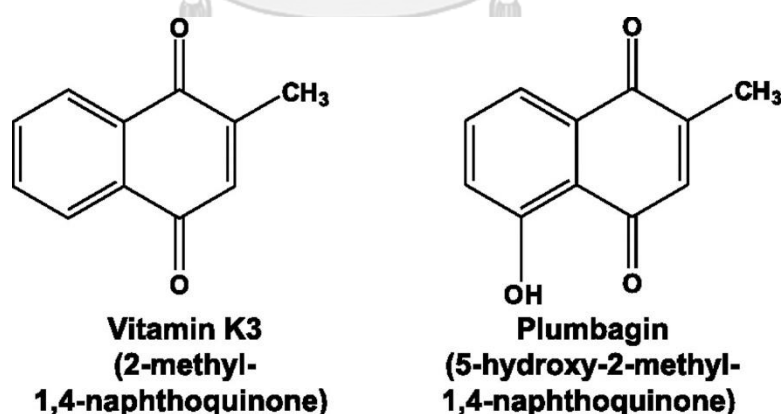


Figure 4. The 2D structure of plumbagin [47].

### Anticancer Effects

PLB has been studied as an anti-cancer agent with anti-angiogenesis and the inhibition of cancer stem-like cells (CSCs) in several types of cancer including brain [75-78], pancreas [79, 80], gastric [81, 82], liver [83-85], ovarian [86], bone [73, 87], skin [74, 88], blood cells [89-92], head and neck [93-95], colon [96-99], lung [100-103], prostate [70, 104-106], and breast cancers [107-113] which are concluded in **Table 2**.

The anti-tumor effects of PLB were studied in some types of breast cancer. PLB reduced G1 cell cycle regulators and increased expression of p53 and p21 levels in MCF-7 cells [107]. PLB also caused DNA damage, telomere dysfunction and genome instability in breast cancer cells [108]. Dandawate et al. [109] reported that PLB derivative exhibited anti-cancer effect associated with autophagy, mTOR and Notch signaling pathways by using molecular docking method in ER-positive MCF-7 and triple negative MDA-MB-231 breast cancer cell lines [109]. Moreover, PLB inhibited the proliferation of MCF-7 breast cancer cell line and stimulated apoptosis induction of SKBR3 and BT474 breast cancer cells through the mitochondrial-mediated pathway [112-114]. Interestingly, Yan et al. [110] reported that PLB suppressed cell migration and invasion by inhibiting IL-1 $\alpha$ , MMP2/9 expression and downregulating

STAT3/TGF-beta crosstalk in triple negative breast cancer MDA-MB-231 cells and intracardially bone metastatic model [110]. Similar cellular responses were observed *in vivo* studies that PLB reduced osteolytic lesions and inhibited the growth of MDA-MB-231 tumor-bearing mouse [115].

### Drug Resistant Reversal Effects

PLB has synergistic effects with some chemotherapeutic drugs in overcoming resistance in human cancers [8, 116-119]. Gowda et al. [118] demonstrated the combination of celecoxib and PLB significantly reduced cell viability by the inhibition of cyclooxygenase 2 (COX2) and signal transducer and activator of transcription 3 (STAT3) in melanoma cells [116]. Additionally, Qiao et al. [117] reported that PLB combined with zoledronic acid (ZA) inhibited MDA-MB231 cell line [117]. PLB had synergistically cytotoxic effect with ZA (combination index (CI) = 0.26) through the modulation of mitogen-activated protein kinase (MAPK)/JNK/ERK pathways [119]. In our study also demonstrated that a fixed low concentration of PLB and tamoxifen resulted in synergistic effect (CI = 0.58) in LCC2 cell line and additive effect (CI = 0.94) in anti-hormonal resistant breast cancer LCC9 cells [8].



### Antiangiogenic Effects

Wei et al. [83] demonstrated that PLB inhibited angiogenesis by decreasing endothelial cell migration and invasion through the regulation of PI3K/AKT, VEGF/KDR and Angiopoietins/Tie2 in hepatocellular carcinoma [83]. PLB suppressed tumor angiogenesis in ovarian cancer cell line and animal models via the downregulation of VEGF expression [86]. Additionally, Lai et al. [120] reported that PLB inhibited VEGF-induced cell proliferation and migration of human umbilical vein endothelial cells (HUVECs) and decreased angiogenesis in mouse corneal and chicken chorioallantoic membrane (CAM) neovascularization in prostate cancer *in vivo* by reducing RAS/RAC and RAS/MEK pathways [120].

### Inhibitory Effects on Cancer Stem Cells

PLB can inhibit cancer stem cells (CSCs) of head and neck cancer through the suppression of EMT via the reduction of Keap1-Nrf2 expression in SCC25 cells [14]. According to the study of Somasundaram et al. [34], PLB inhibited breast CSCs by inducing ROS generation in BRCA1-mutated triple negative HCC1937 cell line [34]. Furthermore, Reshma et al. [121] demonstrated that PLB suppressed prostate CSCs and induced cell apoptosis of BRCA1/2 silencing PC-3 and DU145 cells [121].

Table 2. A summary of previous studied on pharmacological activities of PLB.

Types of cancer	Main mechanisms	<i>In silico</i>	<i>In vitro</i>	<i>In vivo</i>	Ref.
<b>Anticancer Effects</b>					
Leukemia	- c-Myb and BCL2 expression - p65 and NF- $\kappa$ B signaling		/		[89-91]
Multiple myeloma	- PI3K/AKT/mTOR		/		[92]
Skin	- BCL2 - TRAIL and DR5 expression		/		[74, 88]
Liver	- Glutathione reductase and thioredoxin reductase - uPA and MMP2		/		[84, 85]
Glioma	- Apoptosis induction - FOXM1 expression - Telomere dysfunction, PTEN, and caspase-3/7 activity		/	/	[75-78]
Lung	- PI3K/AKT/mTOR pathway - AP1, NF- $\kappa$ B and MAPK ERK		/		[100-103]
Gastric	- SHP1, STAT3, BCL2 and NF- $\kappa$ B		/		[81, 82]
Pancreas	- PI3K/AKT/mTOR and EMT - EGFR, STAT3 and NF- $\kappa$ B		/	/	[79, 80]
Head and neck	- PI3K/AKT and p38 MAPK - Caspase-3/7 activity - BAX/BCL2 ratio		/		[93, 94, 122]

Colorectal	- p53-independent signaling - COX2 and ROS generation - AMPK signaling pathway		/		[96-99]
Osteosarcoma	- Apoptosis induction		/		[117]
Prostate	- AMPK/p38 MAPK and PI3K/AKT/mTOR signaling - PKC/STAT3/COX2 crosstalk - Interacted with 78 proteins involved in cell proliferation, apoptosis, autophagy and EMT	/	/	/	[104-106, 123]
Breast	- p53 and p21 expression - Telomere dysfunction and genome instability - Diminished osteolytic lesions - STAT3, TGF-beta, MMP2/9 - mTOR and Notch pathway - ROS generation	/	/	/	[107, 108, 110-113, 115]
<b>Antiangiogenic Effects</b>					
Liver	- VEGF, FGF2, connective tissue growth factor CTGF, ET-1, PI3K/AKT, KDR and AGO/TIE2		/		[83]
Ovarian	- VEGF signaling		/	/	[86]
Prostate	- RAS/RAC and RAS/MEK signaling pathways		/	/	[120]

Inhibitory Effects of Cancer Stem Cells					
Head and neck	- EMT and NRF2		/		[95]
Prostate	- Apoptosis induction		/		[121]
Breast	- ROS generation		/		[34]

### Pharmacokinetics

The pharmacokinetic profile of PLB includes absorption, distribution, metabolism and excretion has been studied in human volunteers and animal model. PLB was able to moderately cross the colon epithelial Caco2 cells and was transported by passive transport. Oral bioavailability of PLB was 38.78% in Spragu-Dawley rats [124]. After mice taking single dose of PLB at 100 mg/kg body weight (b.w.) via oral route, the area under the curve (AUC) was 271.9 mg/kg b.w.  $C_{max}$  was 0.35 mg/ml at 1 hour and then declined quickly.  $T_{max}$  was 2 hours 30 minutes. PLB was excreted about 49% through feces. Conjugated metabolites were detected in the urine [124]. Sumsakul et al. also observed these parameters in Wistar rats as shown in **Table 3** [125].

In addition, the effects of PLB on drug metabolism by several cytochrome P450 enzymatic activities were studied [125, 126]. Chen et al. demonstrated that PLB was the mixed inhibition of CYP1A2, CYP2D1, and competitive inhibition of CYP2B1, CYP2C11 and CYP2E1 with  $K_i$  values less than 9.93  $\mu$ M in rodent. Moreover, PLB was CYP2B6, CYP2C9, CYP2D6, CYP2E1 and

CYP3A4 mixed inhibitor and of CYP1A2 non-competitive inhibitor with less  $K_i$  values  $2.16 \mu\text{M}$  in humans [126].

**Table 3.** The PK parameters of PLB after oral administration in Wistar rats.

Parameters	PLB 100 mg/kg bw (Median $\pm$ interquartile range)
$T_{1/2}$ (half-life)	$9.63 \pm 3.04$ h
$T_{\text{max}}$	$5.00 \pm 0.00$ h
$C_{\text{max}}$	$0.46 \pm 0.15$ $\mu\text{g/mL}$
$\text{AUC}_{0-48 \text{ hours}}$	$6.51 \pm 1.16$ $\mu\text{g h/mL}$
$\text{AUC}_{0-\text{infinity}}$	$6.71 \pm 1.41$ $\mu\text{g h/mL}$
MRT (mean residence time)	$12.88 \pm 2.49$ h
Vd/F (volume of distribution)	$2.2 \pm 0.00$ mL/mg dose/kg bw
CL/F (oral clearance)	$0.15 \pm 0.30$ L/h/mg dose/kg bw

### Safety and Toxicity

PLB, a vitamin  $K_3$  derivative, is a medicinal plant-derived naphthoquinone compound that has been showed anti-cancer properties in preclinical studies with no evidence of normal cells and tissue toxicity [70-72, 115, 120]. Vitamin  $K_3$ , a synthetic water-soluble compound, is functionally like vitamin K which associated with an increased risk for clotting [54]. Based on toxicity testing, Sumsakul et al. [125] demonstrated that oral PLB-feeding rats

(25 mg/kg body weight) had normal behaviors, body weights without changes in blood chemistry and hematology for 28 days [125]. Similarly, Vijayakumar et al. [127] indicated that 4-weeks after treatment with PLB (2 mg/kg body weight) showed no change in the platelet counts in the treated group [127].

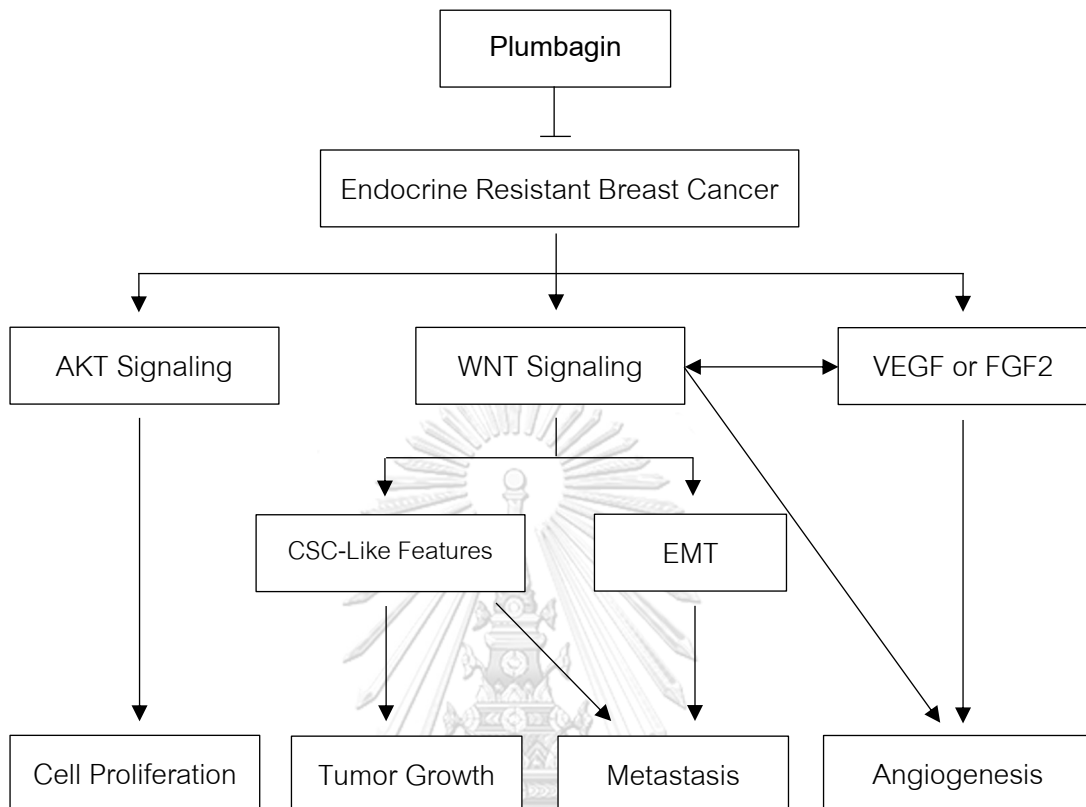
*In vitro* studies, PLB significantly inhibited human breast cancer cell growth with no effect on human peripheral blood mononuclear (PBMC) cells [89, 99] and non-tumorigenic epithelial breast MCF-10A cells [128]. These results consisted with Aziz et al. [129] that PLB was unable to induce normal prostate epithelial RWPE-1 cell death [129]. The recent study confirmed that PLB has a potent cytotoxicity in several types of tumor with a high selectivity index (SI) in breast cancer MCF-7 cells (SI = 1,128) and showed non-toxic effect on human CRL2120 normal fibroblasts [130]. Therefore, PLB has a safety profile in cell line and animal models to investigate further for anti-cancer activity.

## Rationale for the Study

The acquisition of anti-hormonal resistance is still a critical problem for the treatment of breast cancer due to limited choices of drug. In our previous study, PLB displayed growth inhibition, drug resistance reversal and anti-invasive effects in anti-hormonal resistant LCC9 cells by the reduction of EMT process [8]. We also found that PLB significantly increased E-cadherin and significantly decreased Snail protein expression [8] which Snail is well-known as a transcription factor that is modulated by Wnt signaling pathway [131]. More evidences suggested that Wnt signaling contributed to EMT, cancer stem-like features and metastasis. Moreover, tamoxifen-resistant (TAM-R) cells expressed high-level expression of VEGF which led to increased tumor growth and angiogenesis [9, 39].

However, the effects of PLB in targeting cancer stem-like characteristics and tumor angiogenesis in breast cancer remains to be studied, especially in anti-hormonal resistant phenotype. Taken together, more animal-based and molecular mechanistic studies need to be performed. Therefore, this study aimed to investigate the biological and pharmacological activities of PLB on stem cell-like properties, tumor angiogenesis and Wnt-mediated EMT in anti-hormonal resistant breast cancer *in vitro* and *in vivo*.

## Conceptual Framework



**Abbreviations:** ER, estrogen receptor; SERMs, selective estrogen receptor modulators;

AIs, aromatase inhibitors; SERDs, selective estrogen receptor degraders; CSC, cancer

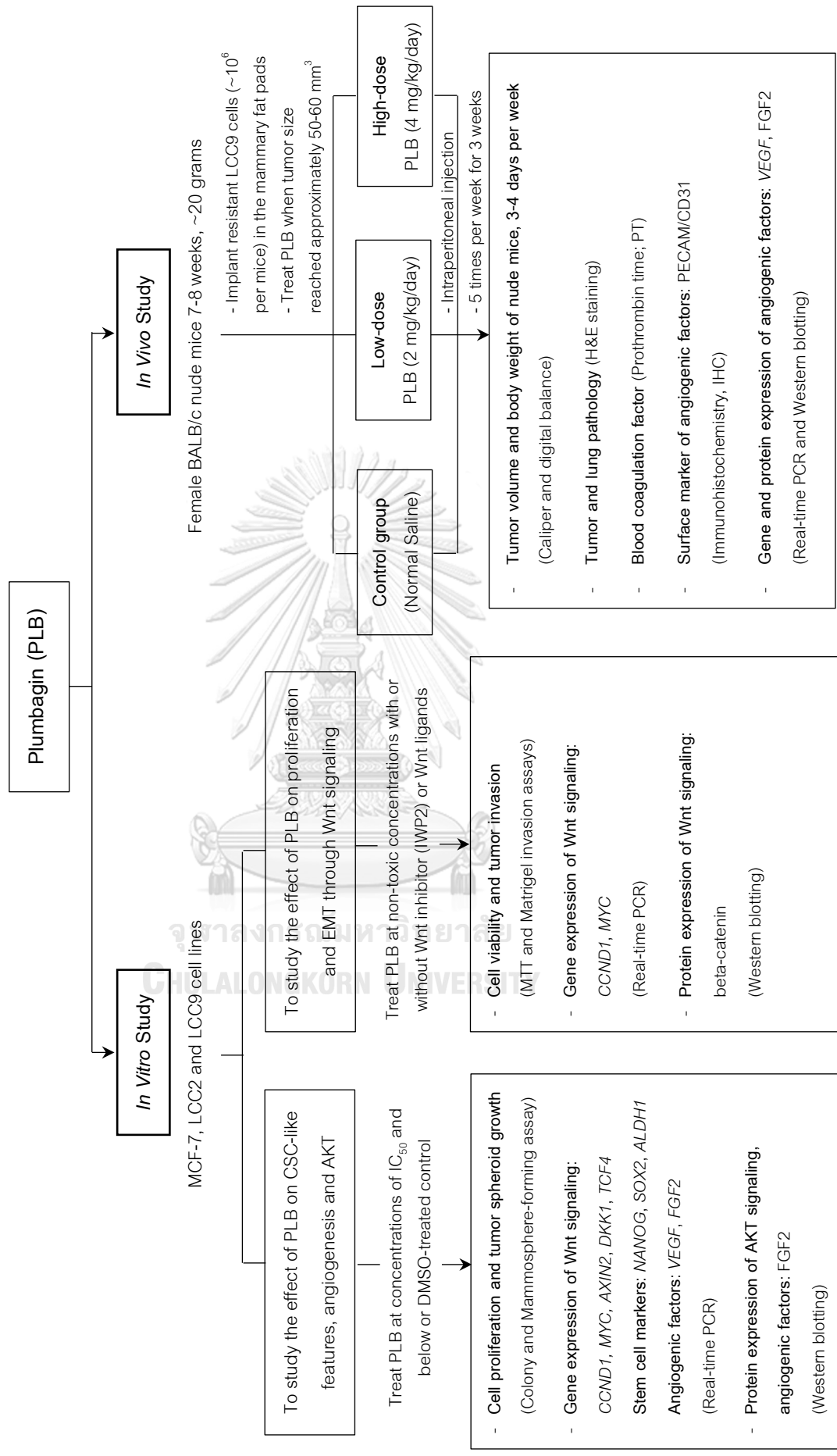
stem cells; AKT/PKB, protein kinase B; WNT, wingless-related integration; EMT,

epithelial-mesenchymal transition; FGF2, fibroblast growth factor 2; VEGF, vascular

endothelial growth factor.



Experimental design of this study



## CHAPTER III

### MATERIALS AND METHODS

#### Cell Lines and Cultures

Wild-type MCF-7 cells (ER-positive breast cancer cell line) was purchased from American Type Culture Collection (ATCC, Manassas). Anti-hormonal resistant cell lines consist of LCC2 cells (tamoxifen-resistant cell line) and LCC9 cells (fulvestrant/tamoxifen-resistant cell line). The details of each cell line were summarized in the **Table 4**. The anti-hormonal resistant cells were kindly provided by Prof. Dr. Robert Clarke (Georgetown University School of Medicine). Cell lines were maintained in MEM medium supplemented with 5% heat-inactivated fetal bovine serum (FBS) (Hyclone, USA), 1% penicillin-streptomycin and 0.1% amphotericin B (Gibco, USA) in a humidified incubator (95% air, 5% CO<sub>2</sub>) at 37°C.

**Table 4.** The characterization of cell lines used this study.

Cell line	Expression					Morphology of cells in culture
	ER	PR	HER2	Snail	E-cadherin	
MCF-7	/	/	-	/	/	Epithelial-like cells
LCC2	↓	↓	↑	↑	↓	Mesenchymal-like cells
LCC9	↓	↑	↑	↑	↓	Mesenchymal-like cells
Ref.	(unpublished data)			[8]		[8]

**Note:** ( / ) represents the presence of hormone receptors or EMT markers. ( ↑ ) and ( ↓ ) denote upregulation and downregulation, respectively when compared to MCF-7 cells.

#### Tested Compound

Plumbagin (PLB, 98% purity) was purchased from Sigma-Aldrich (Missouri, USA). PLB powder was dissolved in dimethyl sulfoxide (DMSO) to obtain a concentration of 10 mM, and then was stored at -20°C and protected from the light. The final concentration of DMSO of 0.1% (v/v) was used as a negative control.

#### Chemicals and Reagents

The following chemicals and reagents were used in this study; amphotericin B (Gibco, USA), chloroform (Merck, Germany), crystal violet dye (Sigma-Aldrich, USA), deoxynucleotide (dNTP) solution mix (Promega, USA), diethyl pyrocarbonate; DEPC-treated water (Molekula, UK), dimethyl sulfoxide; DMSO (Sigma-Aldrich, USA), absolute ethanol (Merck, Germany), fetal bovine serum; FBS (Hyclone, USA), hematoxylin and

eosin (Abcam, UK), human recombinant Wnt1 ligand (Peprotech, USA), Improm-II™ reverse transcription system (Promega, USA), isopropanol (Merck, Germany), MammoCult™ serum-free (Human) basal medium (STEMCELL Technologies Inc, USA), Matrigel® growth factor reduced (GFR) matrix (Corning, USA), minimum essential medium eagle; MEM (Gibco, USA), penicillin-streptomycin,100X (Gibco, USA), phosphate buffer saline; PBS (Sigma-Aldrich, USA), proliferation supplement (Human) medium (STEMCELL Technologies Inc, USA), recombinant human insulin zinc solution (Gibco, USA), soluble Wnt inhibitor IWP2 (Sigma-Aldrich, USA), Thiazolyl blue tetrazolium bromide; MTT (Sigma-Aldrich, USA), TRIzol reagent (Invitrogen, USA), 0.25% Trypsin/EDTA (Gibco, USA), 0.4% Trypan blue solution (Sigma-Aldrich, USA), 10% Neutral buffered formalin NBF (Sigma-Aldrich, USA), 4% formaldehyde solution (Sigma-Aldrich, USA).

#### Instruments and Equipment

The following instruments and equipment were used in this study; autopipette (Brand, USA), bunsen burners (Thomas Scientific, USA), C-DiGit blot scanner (LI-COR Biosciences, USA), 15-mL, 50-mL centrifuge tubes (Corning, USA), CO<sub>2</sub> incubator (Thermo Scientific, USA), coverslips (Menzel Glaser, Germany), cryogenic freezing container (Thermo Scientific, USA), digital balance (Thomas Scientific, USA), digital Vernier Caliper 0-150mm (Invech, China), disposable pipette tip (Corning, USA),

disposable syringe (Terumo, Japan), 5804R refrigerated centrifuge (Eppendorf, USA), Mastercycler nexus thermal cycler (Eppendorf, USA), freezers (-20, -80°C), glass slide 25 mm x 75 mm (Sigma-Aldrich, USA), hemacytometer (Hausser Scientific, Germany), insulin syringe with needle, 1-mL 27G (0.4 mm) x 12.7mm (Terumo, Japan), laminar flow hood (Labconco, USA), phase contrast microscope with digital Nikon camera (Carl Zeiss, Germany), liquid nitrogen (N<sub>2</sub>) storage (Linde, Thailand), microcentrifuge (Hettich zentrifugen, Germany), microcentrifuge tube (Corning, USA), microplate reader (MTX Lab Systems, USA), minicentrifuge (Alic, UK), Mice cages (Techniplast, USA), NanoDrop One UV-Vis spectrophotometer (Thermo Scientific, USA), needle 25G x 16mm (Terumo, Japan), normal saline, 0.9% NSS (A.N.B. Laboratories, Thailand), PCR tube (Corning, USA), pH-meter (Knick, Germany), pipette gun (Gilson, USA), refrigerators (4-8°C) (Toshiba, Thailand), reservoir for cell culture (Thermo Scientific, USA), sodium citrate vacuum tubes (Becton Dickinson, USA), StepOnePlus Real-Time PCR system (Applied Biosystems, USA), invasion chamber, 8.0 µm PET membrane 24-well plates (Corning, USA), ultra-low attachment 6-well plates (Corning, USA), vacuum aspirator pump (Thermo Scientific, USA), vortex (Scientific Industries, USA), water bath (Thermo Scientific, USA), waste containers (Thermo Scientific, USA), 25-cm<sup>2</sup> tissue culture (T25) flasks (Corning, USA), 75-cm<sup>2</sup> tissue culture (T75) flasks (Corning, USA), 6-wells culture plate (Corning, USA), 24-wells culture plate (Corning, USA), 96-wells culture plate (Corning, USA), 100-mm culture plates (Corning, USA).

### Subculturing Adherent Cells

The cells were split into the new culture container after three days of culture or eighty percent confluence in the culture container. First, the media were removed and the cells were washed by sterile 1X PBS to remove the remaining FBS. After washing, cells were trypsinized by adding 0.25% Trypsin-EDTA (Gibco, USA) and incubated at 37 °C for 3 minutes. The reaction was stopped by adding the complete media and transferred into conical tube for centrifugation at 1500 rpm for 5 min. The supernatant was removed and fresh media were added to cells. After mixing, cells were transferred into the new culture container and incubated in 5% CO<sub>2</sub> incubator.

### Cell Counting

After trypsinization and centrifugation, 10 µL of the resuspended cells were aliquoted and transferred in equal volume. 0.4% trypan blue solution (Gibco, USA) was added to cells in 1.5-mL microcentrifuge tube and mixed up and down several times by using a micropipette. 10 µL microliters of trypan blue-staining cells were further added to a hemacytometer chamber (Hausser Scientific, Germany) with cover slip. The number of cells were counted by using the light microscope with 10x objective. Unstained and stained trypan blue cells represented live and dead cells, respectively.

The viability and density of cells were calculated as follow;

$$\% \text{Cell viability} = \frac{\text{the number of live cells}}{\text{the number of live and dead cells}} \times 100$$

$$\text{Total cells/mL} = \frac{\text{the number of live and dead cells}}{4} \times 2 \text{ (dilution factor)} \times 10^4$$

Over 95% percentage of cell viability in the exponential growth phase was accepted to use in each experiment. All cell-based assays were achieved at least three independent experiments in triplication.

#### Clonogenic Assay

Colony-forming (clonogenic) assays were performed to determine the inhibitory effect of PLB on cell proliferation in anti-hormonal resistant breast cancer cells in 2-dimensional (2D) culture. LCC2 and LCC9 cells at the density of  $1 \times 10^3$  cells were seeded into a 6-well plate (Corning, USA) with the 0.5, 0.75, and 1  $\mu\text{M}$  of PLB. 0.1% dimethyl sulfoxide (DMSO) was used as the negative control. After that, the plates were incubated for 7 days. After washing with PBS, cells were fixed and stained with 4% formaldehyde and 0.1% crystals violet, respectively. The colonies were observed under a digital microscope camera. Large colony containing at least 50  $\mu\text{m}$  was counted by using ImageJ (NIH).

The inhibitory effect of PLB on colony formation was analyzed as the percentage of colony-forming ability (%CFA) as follow;

$$\%CFA = \frac{\text{Mean of colonies number in treated cells}}{\text{Mean of colonies number in untreated control}} \times 100$$

### Mammosphere Formation Assay

3D mammosphere assays were performed to determine the inhibitory effect of PLB on cancer stem-like features in non-adherent condition and serum-free media (SFM) in anti-hormonal resistant breast cancer *in vitro*. LCC2 and LCC9 cells at the density of  $2 \times 10^3$  cells were seeded in ultra-low attachment 6-well plate (Corning, USA) in MammoCult™ basal and proliferation supplement medium (StemCell Technologies). At the same time, resuspended cells were treated with the 0.5 or 1  $\mu\text{M}$  of PLB for 7-10 days. 0.1% DMSO was used as a negative control. After the culture period, the mammospheres were photographed by an inverted microscope with a digital Nikon camera (Carl Zeiss, Germany). Mammospheres with the diameter greater than 50  $\mu\text{m}$  were counted using ImageJ software (NIH). The inhibitory effect of PLB on stem-like features was analyzed as the percentage of mammosphere-forming efficiency (%MFE) which was calculated as follow:

$$\%MFE = \frac{\text{Mean of mammospheres number in treated cells}}{\text{Mean of mammospheres number in untreated control}} \times 100$$



### MTT assay

MTT assays were performed to determine the inhibitory effect of PLB on Wnt-mediated cell viability in anti-hormonal resistant breast cancer *in vitro*. LCC2 and LCC9 cells at the density of  $5 \times 10^3$  cells were seeded into a 96-well plate (Corning, USA) with the different concentrations of PLB at 0.5, 1.0, and 1.5  $\mu\text{M}$  with or without Wnt inhibitor IWP2 (5  $\mu\text{M}$ ) or Wnt1 ligand (200 ng/mL). 0.1% DMSO was used as a negative control. The plates were incubated for 24 and 48 hours for Wnt inhibitor and Wnt1 ligand, respectively. After adding MTT (5 mg/ml), cells were incubated for 4 hours at 37°C. After 4-h incubation, formazan crystals were dissolved by DMSO. Viable cells were evaluated by absorbance measurements at 570 nm using Synergy HTX multi-mode microplate reader (BioTek, USA). The values of optical density (OD570) in triplicate were proportional to the degree of survival rate. The inhibitory effect of PLB on tumor cell growth was analyzed as the percentage of cell viability relative to control as follow:

$$\% \text{Cell viability} = \frac{\text{Mean of OD570 in treated cells}}{\text{Mean of OD570 in untreated control}} \times 100$$

### Matrigel Invasion Assays

Matrigel invasion assays were performed to determine the inhibitory effect of PLB on Wnt pathway-mediated cell invasion in anti-hormonal resistant breast cancer *in vitro*. Upper chambers of transwells were coated with Matrigel (1:30 dilution) in serum-

free MEM before seeding. LCC2 and LCC9 cells at the density of  $5 \times 10^4$  cells were seeded into the upper chamber and treated with PLB (0.5 and 1  $\mu\text{M}$ ) with or without Wnt inhibitor (5  $\mu\text{M}$ ) or Wnt1 ligand (200 ng/mL), while 5% FBS in MEM was added in the lower chamber. After treatment for 48 h, Non-invaded cells in the insert were rinsed with PBS and swiped out with a cotton swab. Invaded cells were fixed and stained with 4% formaldehyde and 0.1% crystal violet, respectively. Images were taken by a light microscope with digital camera at least 5 random fields per chamber. For data analysis, invaded cells were counted using ImageJ (NIH) software. The inhibitory effect of PLB on cancer cell invasion was analyzed as the percentage of cell invasion relative to control which was calculated as follow:

$$\% \text{Cell invasion} = \frac{\text{Mean of invaded cells in treated group}}{\text{Mean of invaded cells in untreated control}} \times 100$$

#### Tumor Growth in Xenograft Mice

Eighteen female BALB/c nude mice at 7-8 weeks of age (approximately weight 20 grams) were used to determine the anti-cancer effect of PLB on tumor growth of anti-hormonal resistant breast cancer in orthotopic xenografts. Nude mice were obtained from the Nomura Siam International company which jointly established by Central Institute for Experimental Animals (CLEA) Japan, Inc. Each mouse was housed under 12 h light and 12 h dark controlled light at  $24 \pm 2$  °C room temperature and 55–60% humidity

in the animal house facility at the Faculty of Medicine, Chulalongkorn University. All animals were fed with a standard diet and water ad libitum. Healthy mice were implanted with anti-hormonal resistant breast cancer (LCC9) cells under general anesthesia with isoflurane. A million cells of LCC9 cell line in 1:1 proportion of complete medium and Matrigel (Corning, USA) were implanted into mammary fat pads of each mouse. Treatment of PLB was started when the tumors reached volume at least 50-60 mm<sup>3</sup>. The sample sizes of mice were 6 animals per group which were calculated by using G-Power statistical power analysis v3.1.9.4 software (<http://www.psych.uni-duesseldorf.de/abteilungen/aap/gpower3/>) [125]. Animals were randomly separated into three groups.

**Group 1:** Normal saline alone (Control)

**Group 2:** PLB 2 mg/kg/body weight (Low-dose)

**Group 3:** PLB 4 mg/kg/body weight (High-dose)

Twenty microliters of PLB or normal saline was injected through intraperitoneal (i.p.) route for 5 times a week [115, 132]. Body weight and tumor size of each mouse was monitored every other day using digital balance and caliper. Measurement of primary tumor volume in mm<sup>3</sup> was calculated by the following equation:

$$\text{Tumor volume} = 0.5 \times \text{the length diameter} \times (\text{the width diameter})^2 \quad [133].$$

After 3 weeks of PLB treatment, anti-hormonal resistant breast tumor-bearing mice were sacrificed by overdosing isoflurane inhalation (4% v/v for 5 minute), Tumor mass, major organs such as lung tissues and blood plasma were collected. Tumor samples were weighted and divided for real-time PCR, western blot and histological studies. For histopathological assessment, the thin-sliced sections of tumors and lung were stained for Hematoxylin and Eosin staining. PECAM/CD31 staining was performed in tumor section for angiogenesis.

#### **H&E Staining of Lung Tissues**

Hematoxylin and Eosin (H&E) sections were carried out to determine the inhibitory effect of PLB on lung metastasis of anti-hormonal resistant breast cancer in orthotopic xenograft mice. For micrometastasis examination, the lung tissues were stained with hematoxylin solution for 10 minutes at a temperature of 60-70°C and were washed in tap water until the water was colorless. Next, 10% acetic acid and 85% ethanol in water were used 2 times, and the tissue sections were rinsed with tap water. The sample was soaked in saturated lithium carbonate solution for 2 hours and then washed with tap water. Lastly, staining was performed with eosin Y solution for 5 minutes. Sliced sections were dehydrated, cleared and mounted, respectively. The stained tissues were scanned using a Leica ScanScope CS slide scanner (Aperio Technologies, USA). The inhibitory effect of PLB on metastasis was analyzed as the

incidence of mice observed with lesions containing tumor cells in the lung tissues relative to control group.

### **Immunohistochemistry Staining (PECAM)**

PECAM/CD31 is platelet-endothelial cell adhesion molecule/CD31 which is highly expressed in endothelial cells. Hence, staining with PECAM/CD31 has also been widely accepted to measure angiogenesis in tumor sections. PECAM staining was performed to determine the anti-cancer effect of PLB on angiogenesis of anti-hormonal resistant breast cancer in orthotopic xenografts. The paraffin-embedded tumor sections were stained with anti-PECAM/CD31 (clone JC70A, 1:100) in 10% human serum and incubated for 2 hours at room temperature. Alkaline phosphatase labeling was performed by HRP-polymer linked secondary antibody (Thermo Scientific, USA) following 3,3'-diaminobenzidine (DAB) substrate and then counterstained with hematoxylin (nuclear). The slides were scanned using a Leica ScanScope CS slide scanner (Aperio Technologies, USA) with 40x magnification. For data analysis, brown spots showing vessels density of angiogenesis in tumor xenografts were chosen at least 5 random fields per slide and analyzed using the Microvessel algorithm by ImageScope (Aperio Technologies) software. The inhibitory effect of PLB on tumor angiogenesis was analyzed as the percentage of microvessel area (MVA) relative to control which was calculated as follow:

$$\%MVA = \frac{\text{Mean of PECAM/CD31 staining in treated group}}{\text{Mean of PECAM/CD31 staining in control group}} \times 100$$

### Blood Coagulation

PLB is a vitamin K<sub>3</sub> derivative that may affect the bleeding time in blood samples of mice. A prothrombin time (PT) was used to determine the extrinsic pathway (factor VII) and common pathway (Factor I, II or thrombin and X) of coagulation which is activated by adding tissue factor [134]. The blood plasma was collected in 3.2% citrate tubes and centrifuged at 1500 g for 10 minutes. The time was optically recorded until a clot formed using a semi-automated Sysmex CA104 analyzer (Sysmex Europe GmbH) as described in the manufacturer's instructions. The citrated plasma (100 µL) of each mouse was used to estimate PT value.

The mean ± S.E.M of PT is 11.9 ± 0.30 seconds in healthy female mice (Normal range = 10.0-15.2 seconds) [134, 135].

### RNA Extraction and cDNA preparation

The total RNA was extracted from cell lines and tissues by using Trizol reagent (Invitrogen, USA). A260/A280 value of RNA was analyzed to prove the isolation efficacy. The accepted range should be between 1.8-2. One microgram of RNA and Oilgo(dT)<sub>15</sub> primers were mixed and the volume was brought up to 5 µL per reaction with DEPC-treated water. The samples were plated on ice followed by mixing and spinning down.

PCR tubes were tightly closed and placed into a Mastercycler<sup>®</sup> thermocycler (Eppendorf, USA), incubated at 70°C for 5 minutes and immediately chilled on ice at least 5 minutes. PCR tubes were vortexed and spun down for 20 seconds. While the master mix solutions were prepared, tubes were kept on ice at all time.

The reverse transcription reaction master mix was prepared by adding the following components of the ImProm-II<sup>™</sup> Reverse Transcription System in a sterile 1.5-mL microcentrifuge tube. Master mix solutions were frequently vortexed and kept on ice prior to aliquot into the reaction tubes. The reverse transcription reaction master mix contained the following reagents;

1) Nuclease-Free Water (to a final volume of 15 $\mu$ L)	7.3 $\mu$ L
2) ImProm-II <sup>™</sup> 5X Reaction Buffer	4.0 $\mu$ L
3) 25 mM MgCl <sub>2</sub> (final concentration 2.0 mM)	1.2 $\mu$ L
4) dNTP Mix (0.5 mM each of dATP, dCTP, dGTP and dTTP)	1.0 $\mu$ L
5) Recombinant RNasin <sup>®</sup> Ribonuclease Inhibitors (20U)	0.5 $\mu$ L
6) ImProm-II <sup>™</sup> Reverse Transcriptase	1.0 $\mu$ L
<u>Total volume</u>	<u>15 <math>\mu</math>L</u>

Each reaction tube was added with 15  $\mu$ L master mix solutions on ice for a total reaction volume of 20  $\mu$ L per tube. The reaction tubes were placed into a Mastercycler nexus thermal cycler (Eppendorf, USA) to generate cDNA using the following

conditions; annealing step at 25°C for 5 minutes, extension step at 42°C for 90 minutes, and inactivated Reverse Transcriptase at 70°C for 15 minutes. The cDNA sample was kept at -20°C to use for the determination of mRNA expression.

#### Quantitative real-time PCR (qRT-PCR)

Table 5 represents the primer sequences used for quantitative real-time PCR analysis to investigate the effect of PLB on gene expression involved in cancer stem-like features (*NANOG*, *OCT4* and *ALDH1*), angiogenic factors (*VEGF* and *FGF2*) and Wnt-targeted genes (*AXIN2*, *DKK1* and *TCF4*). The PCR products were amplified by using SYBR green master mix and StepOnePlus real-time PCR system (Applied Biosystems). For data analysis, the expressions of interested genes were analyzed using  $2^{-\Delta\Delta CT}$  method normalized to beta-actin (*ACTIN*) or glyceraldehyde-3-phosphate dehydrogenase (*GAPDH*) which is used as the loading control.

**Table 5.** Primer sequences used for quantitative real-time PCR analysis.

Gene	Primer sequences
<i>GAPDH</i>	Forward: 5'-GAG AAG GCT GGG GCT CAT TT-3'
	Reverse: 5'-AGT GAT GGC ATG GAC TGT GG-3'
<i>ALDH1</i>	Forward: 5'-TCC TGG TTA TGG GCC TAC AG-3'
	Reverse: 5'-CTG GCC CTG GTG GTA GAA TA-3'
<i>NANOG</i>	Forward: 5'-ATA ACC TTG GCT GCC GTC TC-3'



	Reverse: 5'-AGC CTC CCA ATC CCA AAC AA-3'
<i>OCT4</i>	Forward: 5'-CCT TCG CAA GCC CTC ATT TC-3'
	Reverse: 5'-GAA GCT TAG CCA GGT CCG AG-3'
<i>CCND1</i>	Forward: 5'-TTC GCT TTC TCC TGA CCG AC-3'
	Reverse: 5'-TGC TTC AAG CCA GGT CCG AG-3'
<i>MYC</i>	Forward: 5'-GCT TCT CTG AAA GGC TCT CCT-3'
	Reverse: 5'-CCA TTC CCG TTT TCC CTC TG-3'
<i>AXIN2</i>	Forward: 5'-CTG GCT TTG GTG AAC TGT TG-3'
	Reverse: 5'-AGT TGC TCA CAG CCA AGA CA-3'
<i>TCF4</i>	Forward: 5'-GAT GCT CTG GGG AAA GCA CT-3'
	Reverse: 5'-ATG GAG GAG AGC CAA CAG GA-3'
<i>DKK1</i>	Forward: 5'-TAG CAC CTT GGA TGG GTA TT-3'
	Reverse: 5'-ATC CTG AGG CAC AGT CTG AT-3'
<i>VEGF</i>	Forward: 5'-CTT TCT GCT GTC TTG GGT G-3'
	Reverse: 5'-ACT TCG TGA TGA TTC TGC C-3'
<i>FGF2</i>	Forward: 5'-AGG AGA GCG ACC CAC ACA TCA A-3'
	Reverse: 5'-AGC CAG CAG TCT TCC ATC TTC C-3'
<i>SDF1</i>	Forward: 5'-TCT GCT CTG GCG CTT TGT AA-3'
	Reverse: 5'-TAC CGT CAG GTT TGA GCA CC-3'
<i>MMP9</i>	Forward: 5'-ACA CCT CTG CCT CAC CAT-3'
	Reverse: 5'-TCG ACT CTC TCC ACG CAT CTC C-3'
<i>ACTIN</i>	Forward: 5'-ATC GTG CGT GAC ATT AAG AAG-3'
	Reverse: 5'-AGG AAG GAA GGC TGG AAG GTG-3'

### Protein Extraction and SDS-PAGE Preparation

The total proteins were isolated using lysis buffer containing proteases inhibitor cocktail (Merck Millipore) and then centrifuged at 14000 g for 20 minutes [8]. The supernatant was transferred into a new 1.5-mL microcentrifuge tube and stored in -20°C until further use. Total protein concentration was measured by a protein A280 method using NanoDrop One (Thermo Scientific, USA). Bovine serum albumin (BSA) was used as a protein concentration standard.

Sodium dodecyl sulfate polyacrylamide gel electrophoresis (SDS-PAGE) is used to separate proteins depend upon the isoelectric point, molecular weight and electric charge of each protein. The separating (lower) gels were prepared depend on the protein size of interested protein. For example, 10% gels were prepared by adding the following reagents;

1) Ultrapure water	5.76 mL
2) 40% acrylamide/bis-acrylamide (29:1)	3 mL
3) Tris base (1.5 M, pH 8.8)	3 mL
4) 10% sodium dodecyl sulfate (SDS)	0.12 mL
5) 10% ammonium persulfate (APS)	0.12 mL
6) Tetramethylethylenediamine (TEMED)	5 $\mu$ L
<u>Total volume</u>	<u>12 mL</u>

After adding TEMED, the solution was mixed in 15 mL tube and transferred to the casting chamber between the glass plates. Once lower gel has polymerized, stacking (5%) gel was prepared by adding the following reagents;

1) Ultrapure water	3.65 mL
2) 40% acrylamide/bis-acrylamide (29:1)	0.625 mL
3) Tris base (0.5 M, pH 6.8)	0.625 mL
4) 10% sodium dodecyl sulfate (SDS)	0.05 mL
5) 10% ammonium persulfate (APS)	0.05 mL
6) Tetramethylethylenediamine (TEMED)	5 $\mu$ L
<u>Total volume</u>	<u>5 mL</u>

Finally, upper layer was added by stacking gel and the comb was carefully inserted. The stacking gel was allowed to polymerize for 30 minutes. The gels were plastic wrapped and kept at 4-8°C until further use.

### Western Blot Analysis

Western blotting was performed to determine the inhibitory effect of PLB on protein expression involved in stem-like phenotypes, angiogenesis and EMT during metastasis. Equal amount of protein was loaded followed by transferring into nitrocellulose membrane, then blocked non-specific proteins with 5% non-fat dried milk

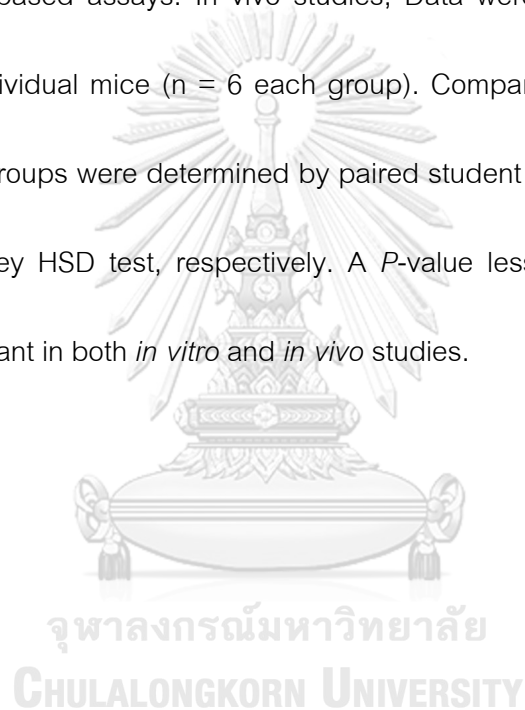
for 1 hour at room temperature (RT). Immunoblots were rinsed with tris-buffered saline supplemented with 0.1% Tween 20 (TBST) solution for 3 times and then incubated with primary antibody against anti-rabbit beta-Catenin (1:1000) (Cell Signaling, #8084), anti-rabbit phospho-AKT-Ser473 (1:1000) (Cell Signaling, #9271), anti-rabbit AKT-pan (1:1000) (Cell Signaling, #4691), anti-mouse FGF2 (1:1000) (Merck Millipore, #05118) at 4°C overnight. After washing with TBST, the blots were incubated with the horseradish peroxidase (HRP)-labeled anti-rabbit (1:2500) (Cell Signaling, #7074) or anti-mouse (1:3000) (Cell Signaling, #7076) secondary antibody for 1 hour at room temperature (25°C). The band density was detected using the Luminata Crescendo Western HRP chemiluminescent substrate (Merck Millipore) and then scanned by C-DiGit blot scanner (LI-COR Biosciences). Protein levels were analyzed using ImageStudio software (LI-COR) normalized to GAPDH as the internal control.

#### Ethical Statement

The *in vitro* study using human cell lines was exempted by the Institutional Review Board of the Faculty of Medicine, Chulalongkorn University (IRB Number: 371/2559 BE). Animal protocol was approved from ethics committee of Chulalongkorn University Animal Care and Use (License Number: 24/2560 BE). All experiments were carried out in accordance with the Guidelines for the Care and Use of Laboratory Animals [125].

### Statistical analysis

The IBM SPSS 24.0 software (Chicago, USA) was used to analyze the results. All graphs were created by GraphPad Prism for Windows, version 7 (GraphPad Software, San Diego, CA). Data were shown as the average  $\pm$  standard error of the mean (S.E.M) from three-independent experiments ( $n = 3$ ) and each experiment was performed in triplicates for cell-based assays. In vivo studies, Data were shown as the average  $\pm$  S.E.M from six individual mice ( $n = 6$  each group). Comparisons between two groups and more than 2 groups were determined by paired student t-test and one-way ANOVA with post-hoc Tukey HSD test, respectively. A *P*-value less than 0.05 was accepted statistically significant in both *in vitro* and *in vivo* studies.



## CHAPTER IV

### RESULTS

Characterization of cancer stem-like features in anti-hormonal resistant breast cancer cell lines.

It has been reported cancer stem-like features were observed in resistant breast cancer cells by increasing EMT phenotypes, mesenchymal expression and decreasing 4-OHT sensitivity [8, 43], resulted in increasing cell survival and tumorigenicity *in vivo* [43]. As shown in **Figure 5**, anti-hormonal resistant cells enriched cancer stem-like features by increasing mammosphere-forming capacity and amplifying cancer stem cell (CSC)-related genes such as *ALDH1*, *NANOG* and *OCT4*, respectively as showed in **Figure 6-8**. The results demonstrated that the mammosphere formation in serum-free medium (SFM) is suitable to show cancer stem-like features in anti-hormonal resistant breast cancer cells that express CSC-related genes. Therefore, these resistant cell lines could be used to evaluate the inhibitory effect and mechanism of plumbagin on cancer stem-like features.

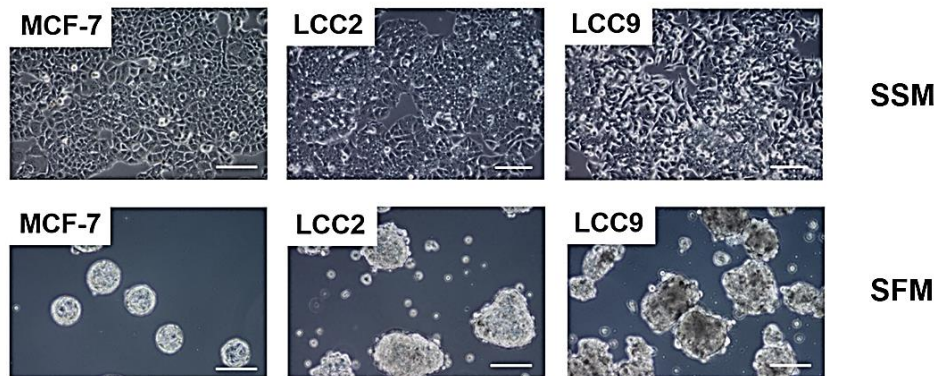


Figure 5. Characterization of cancer stem-like features in anti-hormonal resistant breast cancer cell lines. Morphology of MCF-7, LCC2 and LCC9 cells cultured in serum-supplement medium (SSM) and serum-free mammo-cult (SFM) conditions.

Scale bar = 100  $\mu$ m.

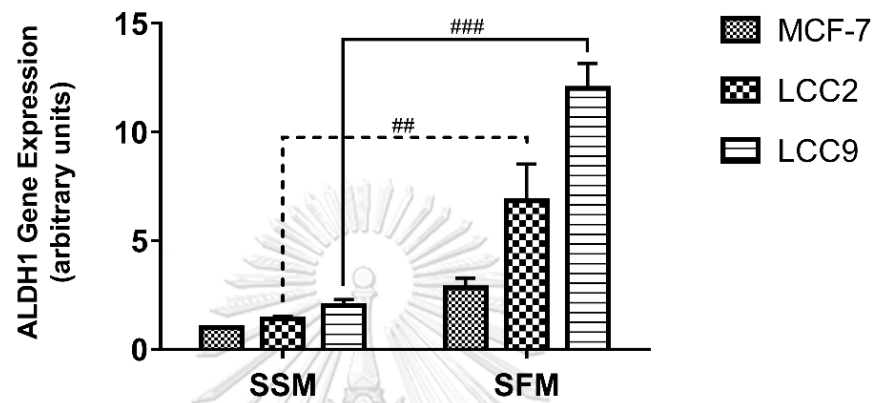


Figure 6. *ALDH1* mRNA expression of anti-hormonal resistant cells grown under adherent monolayer and mammosphere cultures. The bar graph showed relative mRNA expression of *ALDH1* normalized to GAPDH. Data were showed as the mean  $\pm$  S.E.M from three-independent experiment (n = 3). ## $p$ <0.01, ### $p$ <0.001 vs. SSM of each cell line.



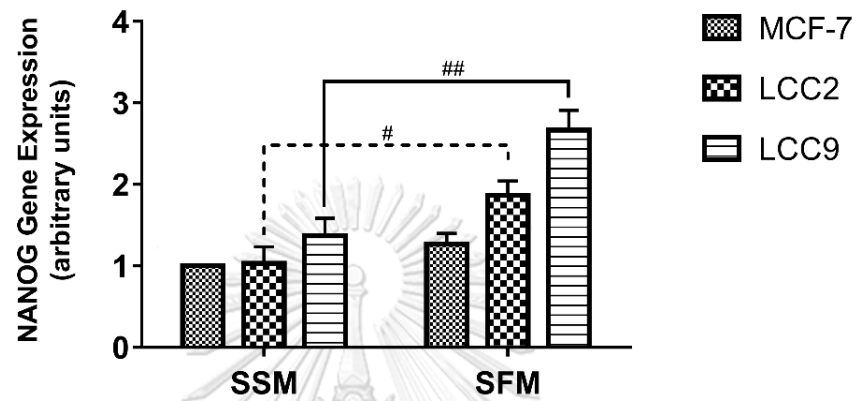


Figure 7. *NANOG* mRNA expression of anti-hormonal resistant cells grown under adherent monolayer and mammosphere cultures. The bar graph showed relative mRNA expression of *NANOG* normalized to GAPDH. Data were showed as the mean  $\pm$  S.E.M from three-independent experiment ( $n = 3$ ). #  $p < 0.05$ , ##  $p < 0.01$  vs. SSM of each cell line.

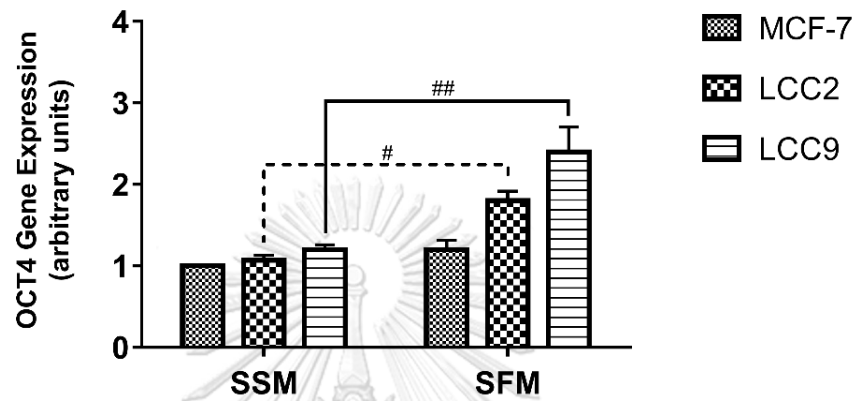


Figure 8. *OCT4* mRNA expression of anti-hormonal resistant cells grown under adherent monolayer and mammosphere cultures. The bar graph showed relative mRNA expression of *OCT4* normalized to GAPDH. Data were showed as the mean  $\pm$  S.E.M from three-independent experiment ( $n = 3$ ). #  $p < 0.05$ , ##  $p < 0.01$  vs. SSM of each cell line.

Aberrant activation of Wnt/beta-catenin signaling in anti-hormonal resistant breast cancer cell lines.

Snail is the transcriptional repressor of E-cadherin that can decrease E-cadherin expression. The decrease of E-cadherin activates Wnt/beta-catenin pathway [46]. The protein levels of beta-catenin expression in anti-hormonal resistant cells were increased approximately 2.8-fold higher than MCF-7 wild-type cells as showed in **Figure 9**. The expression levels of genes involved in canonical Wnt pathway including *CCND1*, *MYC*, *VEGF*, *AXIN2*, and *TCF4* were significantly increased (**Figure 10-11**). *DKK1* (negative regulator of Wnt pathway) was decreased in anti-hormonal resistant cell lines (**Figure 12**). Thus, both of resistant cell lines increased beta-catenin and expression of Wnt-targeted genes, suggesting the activation of Wnt/beta-catenin signaling.

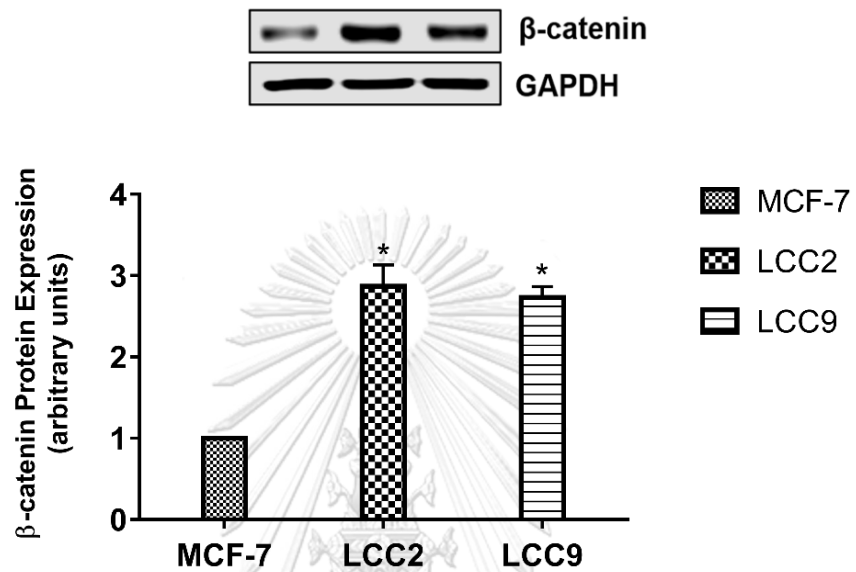


Figure 9. Protein expression of beta-catenin in breast cancer cell lines include MCF-7 (ER-positive cells) and LCC2 and LCC9 (anti-hormonal resistant cells). Data were showed as the mean  $\pm$  S.E.M from three-independent experiment (n = 3). \* $p$ <0.05 vs. MCF-7 cells.

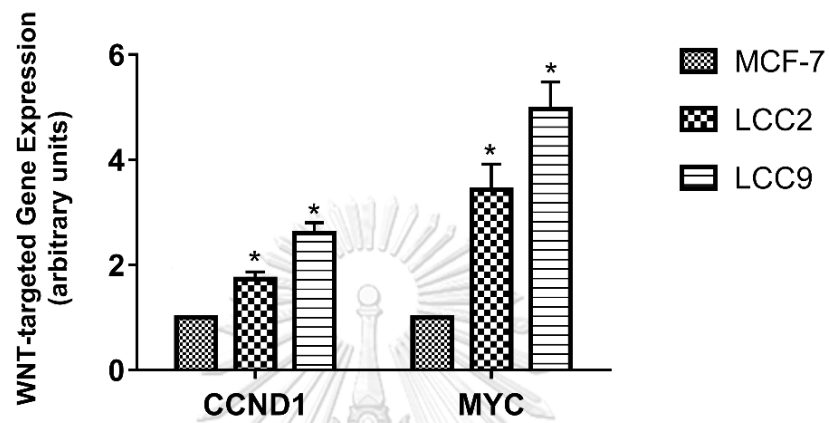


Figure 10. The canonical Wnt-targeted gene expression involved in cell proliferation (*CCND1* and, *MYC*) in anti-hormonal resistant cells. Data were showed as the mean  $\pm$  S.E.M from three-independent experiment (n = 3).

\* $p < 0.05$  vs. MCF-7 cells.

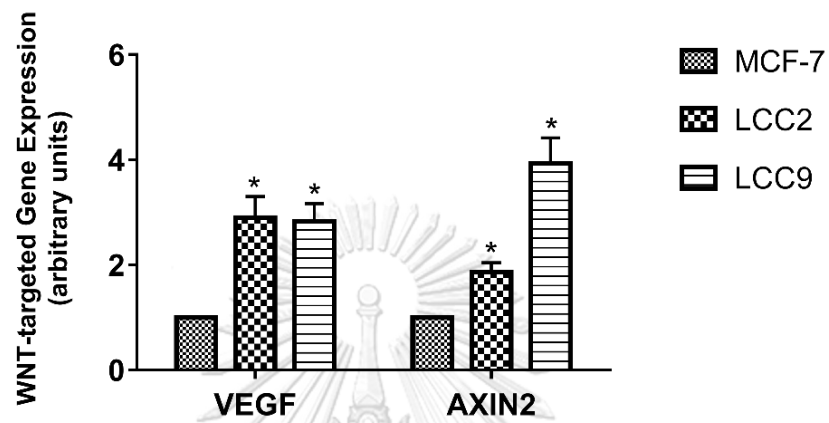


Figure 11. The canonical Wnt-targeted gene expression involved in angiogenesis and invasion (*VEGF* and *AXIN2*) in anti-hormonal resistant cells. Data were showed as the mean  $\pm$  S.E.M from three-independent experiment (n = 3). \* $p < 0.05$  vs. MCF-7 cells.

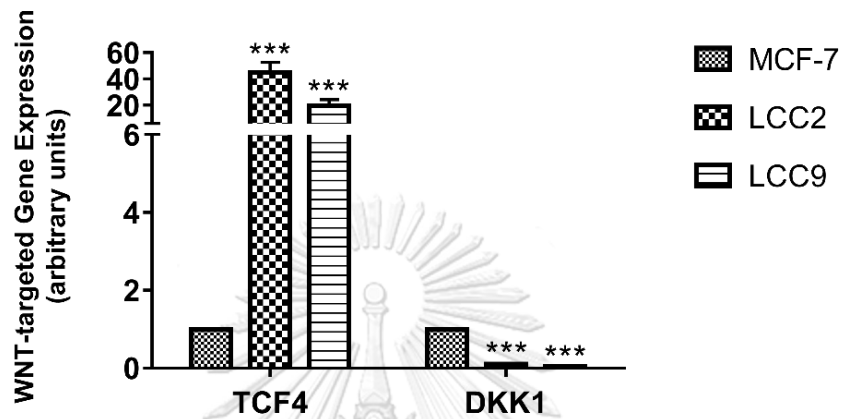


Figure 12. The canonical Wnt-targeted gene expression involved in EMT and metastasis (*TCF4* and *DKK1*) in anti-hormonal resistant cells. Data were showed as the mean  $\pm$  S.E.M from three-independent experiment ( $n = 3$ ). \*\*\* $p < 0.001$  vs. MCF-7 cells.

PLB inhibited cell proliferation and the expression of Wnt-targeted genes in anti-hormonal resistant breast cancer cell lines.

One of the major causes of tumor recurrence is the ability of resistant cells to proliferate. Wnt signaling pathway plays a role in regulating cell proliferation. Overexpression of Wnt-targeted genes was observed in anti-hormonal resistant breast cancer cells [136]. These findings demonstrated PLB decreased the clonogenicity in resistant cells as shown in **Figure 13**. PLB at the concentration of 0.75 and 1.0  $\mu\text{M}$  significantly repressed the colony formation with reduction ranging from 37% to 73% and 38% to 79% in both cell lines. However, the concentration below  $\text{IC}_{50}$  of PLB at 0.5  $\mu\text{M}$  slightly reduced colony forming by 13%-18% inhibition in anti-hormonal resistant cells (**Figure 13**).

Interestingly, PLB at the concentrations below  $\text{IC}_{50}$  of 0.5 and 1.0  $\mu\text{M}$  dramatically reduced Wnt-targeted genes include *AXIN-2*, *TCF4* levels and increased *DKK1* expression (**Figure 14-16**). PLB significantly downregulated the protein expression of beta-catenin in resistant LCC9 cells (**Figure 17**). FGF2, the important angiogenic factor, increased in anti-hormonal resistant breast cancer cells when compared to wild-type MCF-7 cells (**Figure 18**). In addition, PLB reduced gene and protein expression of FGF2 (**Figure 19**) and *VEGF* in both cell lines (**Figure 20**).



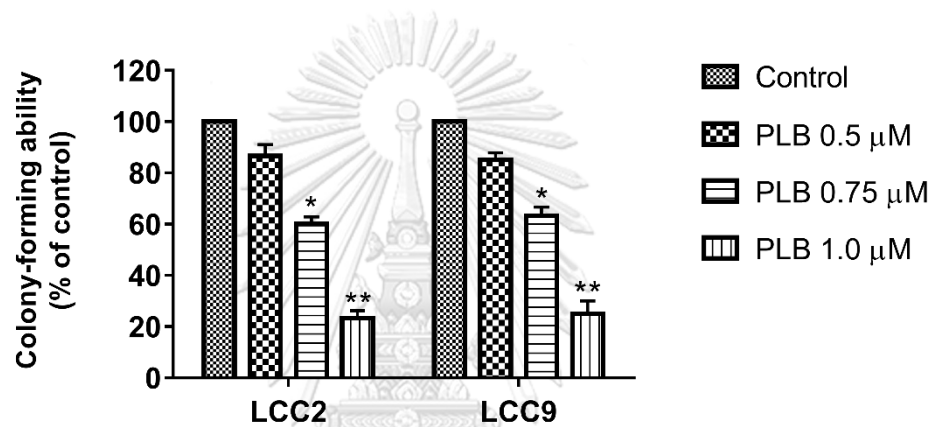
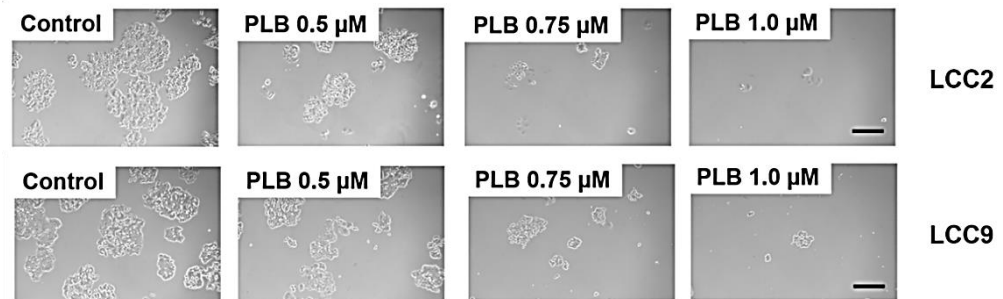


Figure 13. The inhibitory effect of PLB on colony formation of LCC2 and LCC9 cells after the treatment with 0.5, 0.75 and 1.0  $\mu\text{M}$  PLB for 7 days. Data were showed as the mean  $\pm$  S.E.M from three-independent experiments (n = 3).

\*p < 0.05, \*\*p < 0.01 vs. untreated control. Scale bar = 100  $\mu\text{m}$ .

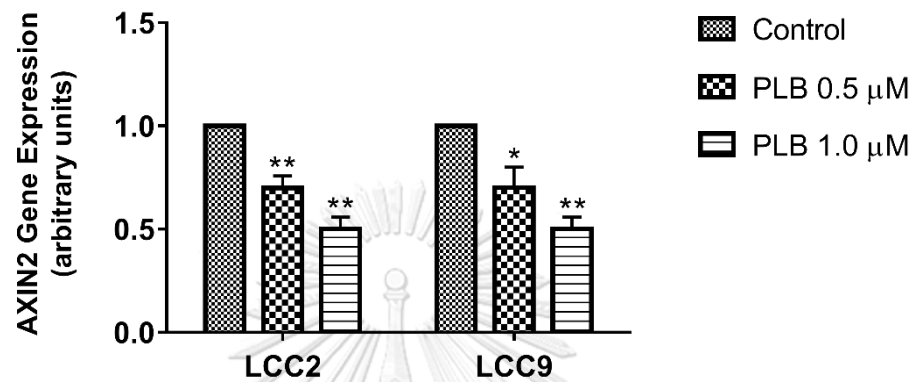


Figure 14. *AXIN2* mRNA expression in anti-hormonal resistant cells after the treatment with 0.5 and 1.0  $\mu$ M of PLB for 24 hours. Data were showed as the mean  $\pm$  S.E.M from three-independent experiments (n = 3). \* $p$ <0.05, \*\* $p$ <0.01 vs. untreated control.

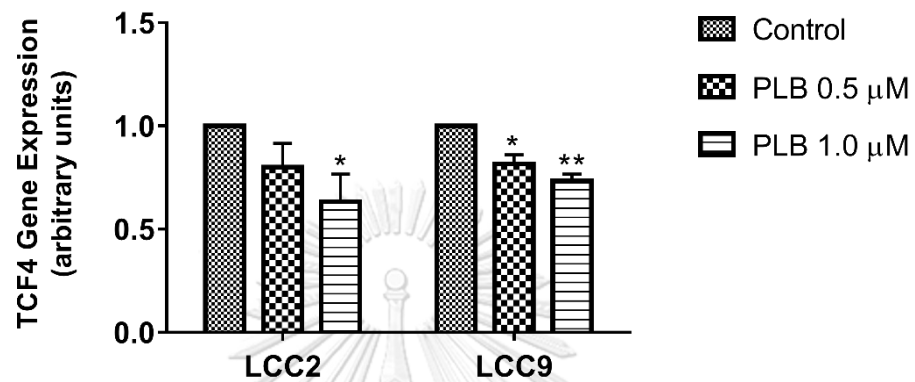


Figure 15. *TCF4* mRNA expression in anti-hormonal resistant cells after the treatment with 0.5 and 1.0  $\mu$ M of PLB for 24 hours. Data were showed as the mean  $\pm$  S.E.M from three-independent experiments (n = 3). \* $p$ <0.05, \*\* $p$ <0.01 vs. untreated control.

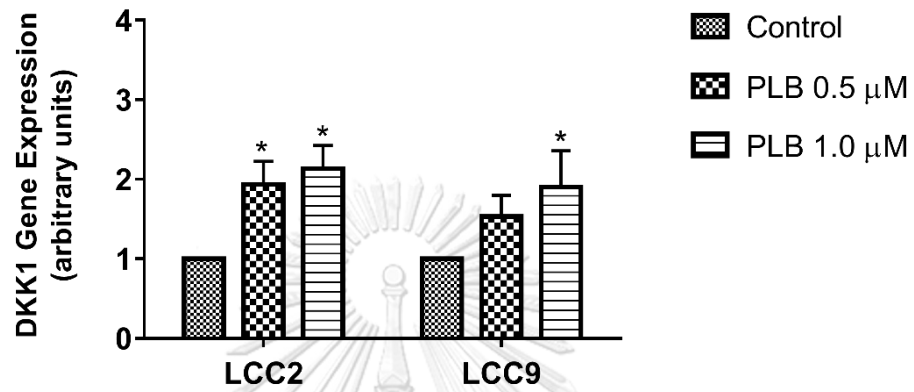


Figure 16. *DKK1* mRNA expression in anti-hormonal resistant cells after the treatment with 0.5 and 1.0  $\mu\text{M}$  of PLB for 24 hours. Data were showed as the mean  $\pm$  S.E.M from three-independent experiments ( $n = 3$ ). \* $p < 0.05$  vs. untreated control.

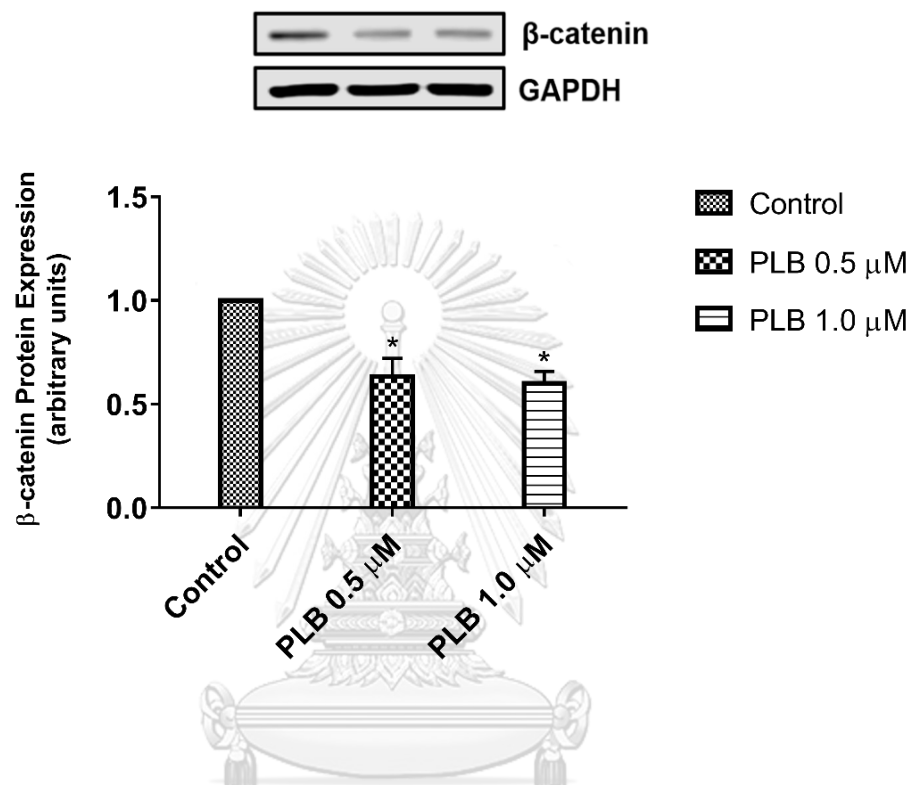


Figure 17. Protein expression of beta-catenin in anti-hormonal resistant LCC9 cells after the treatment with 0.5 and 1.0  $\mu$ M of PLB for 24 hours. Data were shown as the mean  $\pm$  S.E.M from three-independent experiments (n = 3).

\* $p < 0.05$  vs. untreated control.

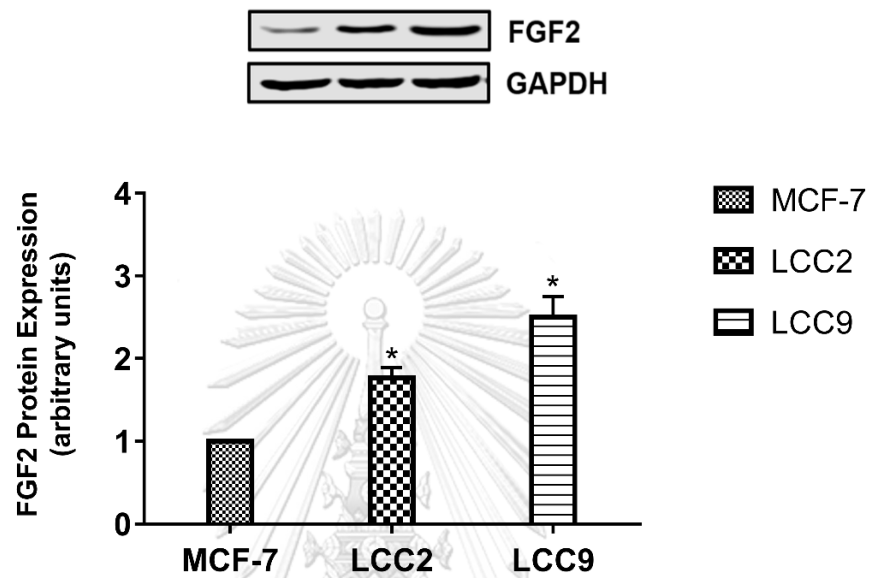


Figure 18. Protein expression of FGF2 in breast cancer cell lines include MCF-7 (ER-positive cells) and LCC2 and LCC9 (anti-hormonal resistant cells). Results were represented as the mean  $\pm$  S.E.M from three experiment (n = 3).

\* $p < 0.05$  vs. MCF-7 cells.

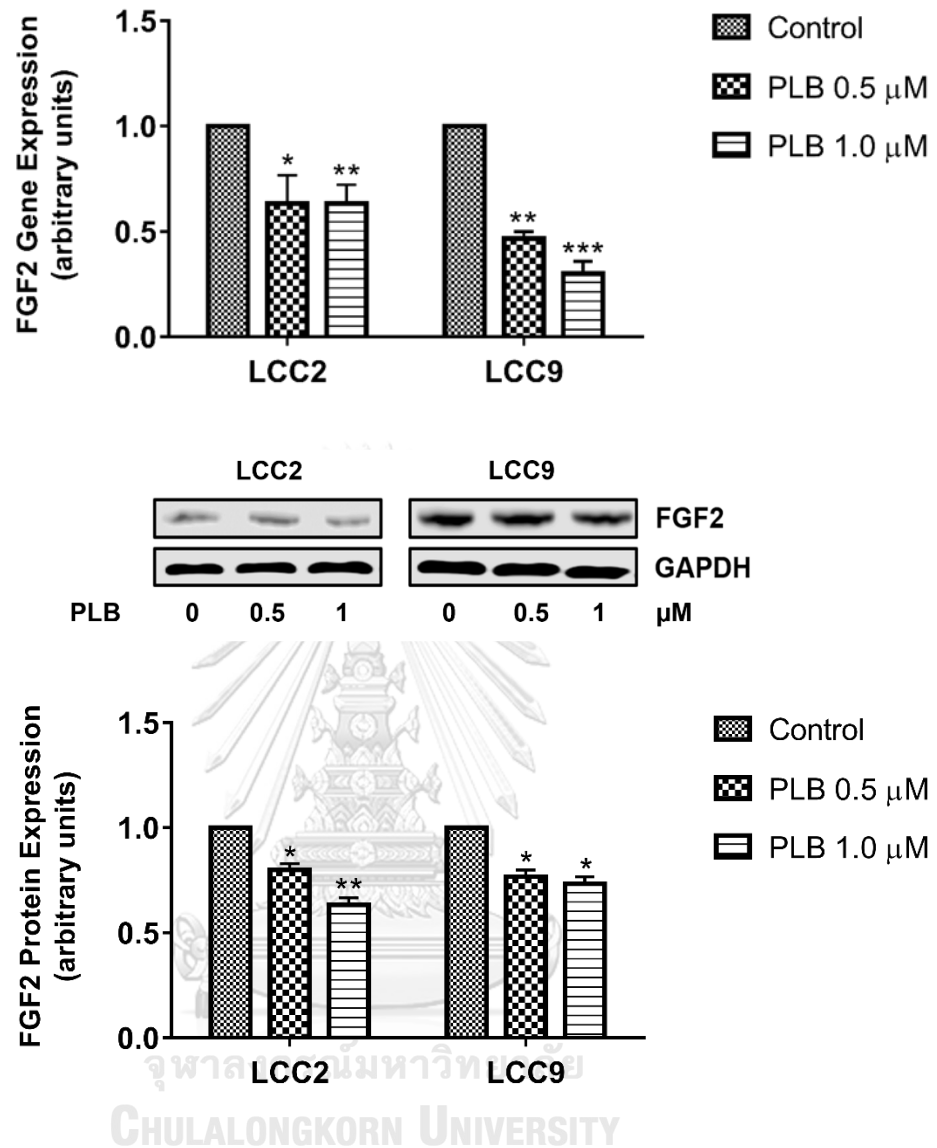


Figure 19. Protein and mRNA expression of FGF2 in anti-hormonal resistant cells after the treatment with 0.5 and 1.0  $\mu$ M PLB for 24 hours. Data were showed as the mean  $\pm$  S.E.M from three-independent experiments (n = 3). \* $p$ <0.05, \*\* $p$ <0.01, \*\*\* $p$ <0.001 vs. untreated control.

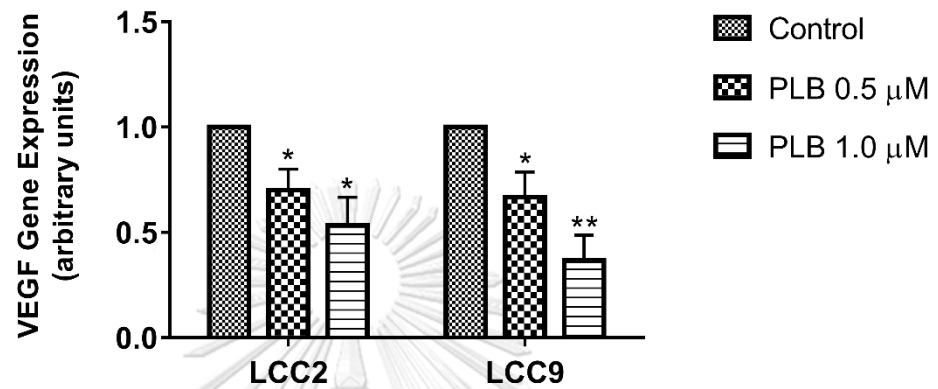


Figure 20. *VEGF* mRNA expression in anti-hormonal resistant cells after the treatment with 0.5 and 1.0 μM of PLB for 24 hours. Data were showed as the mean ± S.E.M from three-independent experiments (n = 3). \*p<0.05, \*\*p<0.01 vs. untreated control.



PLB decreased stem-like features and the expression of cancer stem cell genes in anti-hormonal resistant breast cancer cell lines.

Our previous study reported PLB inhibited cell invasion through the suppression of EMT in anti-hormonal resistant cells [8]. EMT process is a vital property of CSLCs. This study determined whether PLB inhibited stem-like features in anti-hormonal resistant cells by evaluating mammosphere-forming efficiency (MFE). As shown in **Figure 21**, PLB significantly reduced MFE in both LCC2 and LCC9 cell lines in the second passage of mammosphere formation by 47-52% and 78-83% inhibition at the concentration of 0.5 and 1.0  $\mu\text{M}$ , respectively. The same concentrations of PLB also reduced MFE in the third passage by 46-82% and 51-76% inhibition in both cell lines (**Figure 22**). In addition, PLB downregulated the mRNA expression of cancer stem cell markers including *ALDH1*, *NANOG* and *OCT4* in anti-hormonal resistant cells as shown in **Figure 23-25**. These results suggested that PLB diminished stem-like properties by the inhibition of CSC-related gene expression in anti-hormonal resistant cells.

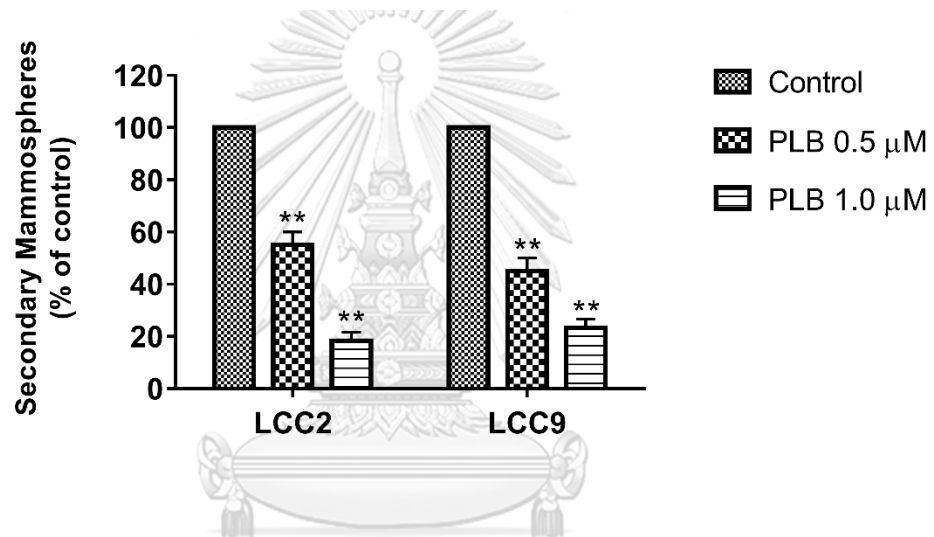
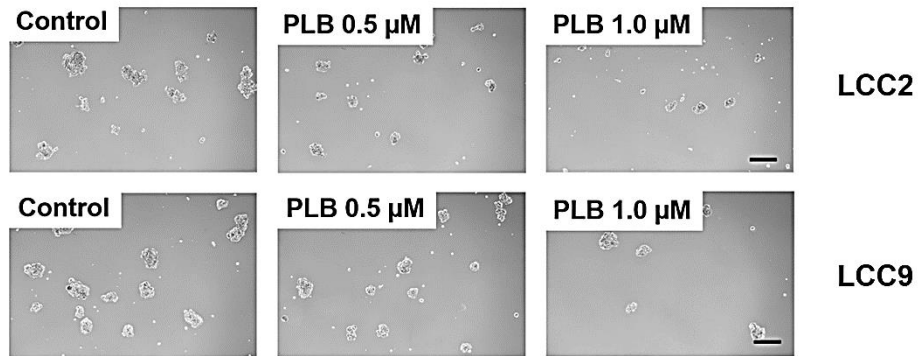


Figure 21. The inhibitory effect of PLB on the secondary mammospheres-forming efficiency (MFE) of LCC2 and LCC9 cells. Both cell lines were treated with 0.5 and 1.0 μM of PLB for 7-10 days. Results were represented as the mean  $\pm$  S.E.M from three experiment (n = 3). \*\*p<0.01 vs. untreated control. Scale bar = 100 μm.

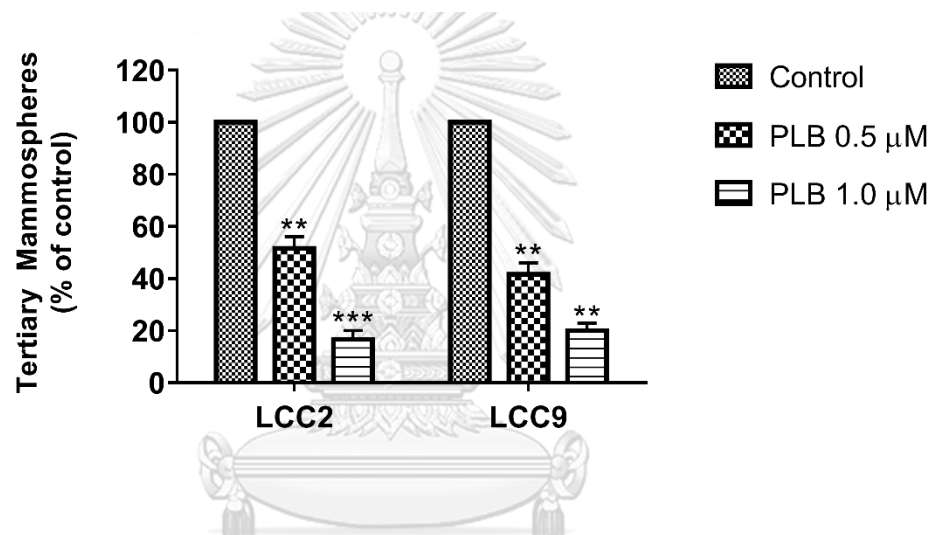
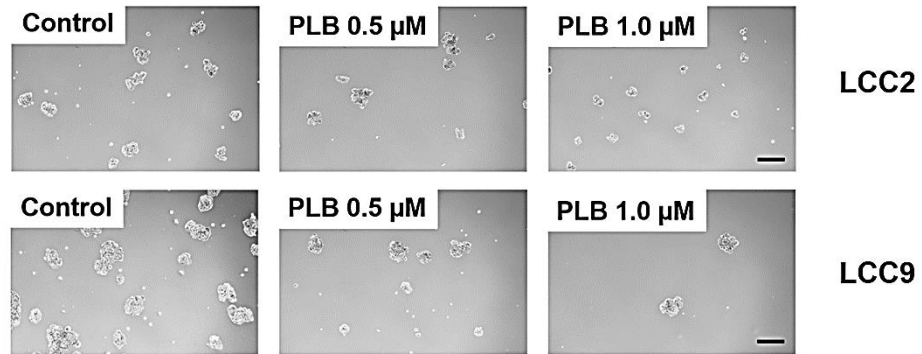


Figure 22. The inhibitory effect of PLB on the tertiary mammospheres-forming efficiency (MFE) of LCC2 and LCC9 cells. Both cell lines were treated with 0.5 and 1.0 μM of PLB for 7-10 days. Results were represented as the mean ± S.E.M from three experiment (n = 3). \*\*p<0.01, \*\*\*p<0.001 vs. untreated control. Scale bar = 100 μm.

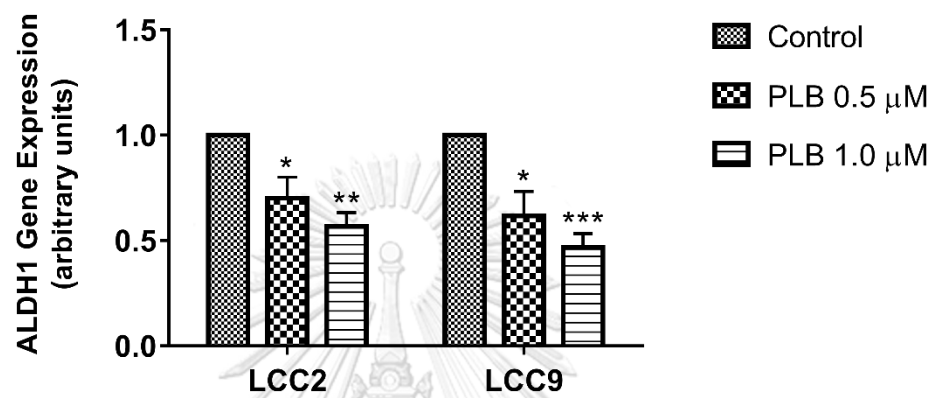


Figure 23. *ALDH1* mRNA expression in anti-hormonal resistant LCC2 and LCC9 cells after treatment with 0.5 and 1.0 μM PLB for 24 hours. Results were represented as the mean  $\pm$  S.E.M from three experiment (n = 3).

\* $p < 0.05$ , \*\* $p < 0.01$ , \*\*\* $p < 0.001$  vs. untreated control.

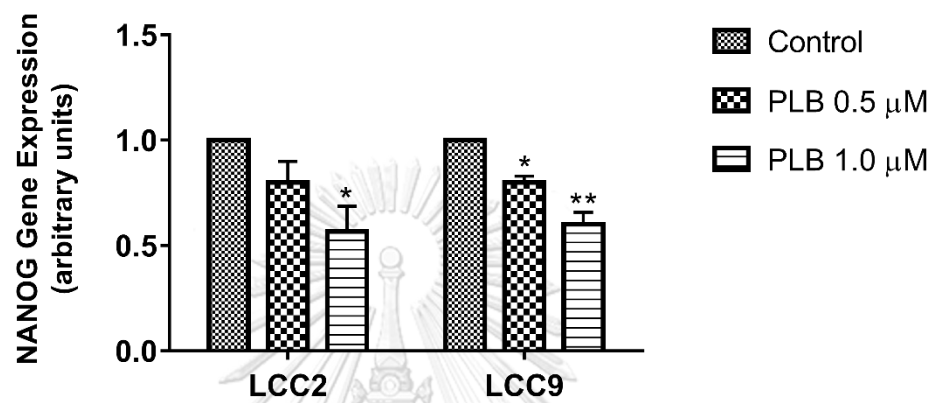


Figure 24. *NANOG* mRNA expression in anti-hormonal resistant LCC2 and LCC9 cells after treatment with 0.5 and 1.0  $\mu$ M PLB for 24 hours. Results were represented as the mean  $\pm$  S.E.M from three experiment (n = 3).

\* $p < 0.05$ , \*\* $p < 0.01$ , \*\*\* $p < 0.001$  vs. untreated control.

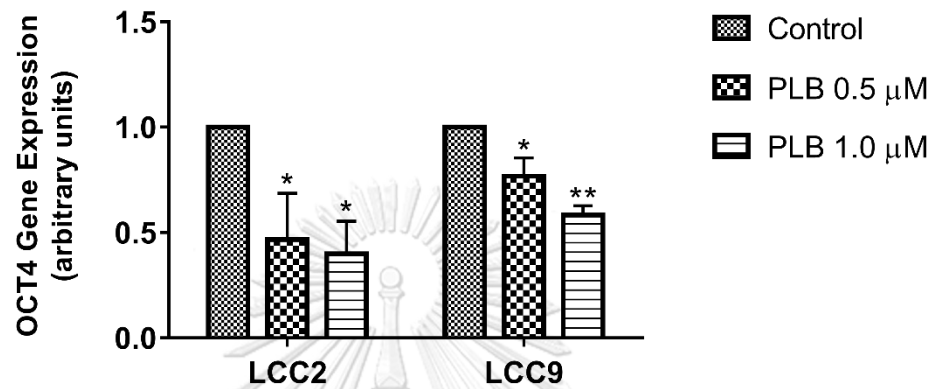


Figure 25. *OCT4* mRNA expression in anti-hormonal resistant LCC2 and LCC9 cells after treatment with 0.5 and 1.0  $\mu$ M PLB for 24 hours. Results were represented as the mean  $\pm$  S.E.M from three experiment (n = 3). \* $p < 0.05$ , \*\* $p < 0.01$ , \*\*\* $p < 0.001$  vs. untreated control.

PLB decreased Akt phosphorylation in anti-hormonal resistant breast cancer cell lines.

Our previous study showed that nuclear receptor coactivator 3 (NCOA3) protein level in anti-hormonal resistant cells was significantly higher than wild-type ER-positive breast cancer cell line [8]. Elevated NCOA3 expression can induce AKT signaling activation leading to promote cell proliferation, survival, and stem-like features resulted in antihormonal resistance in breast cancer [7, 28, 29]. This study determined whether PLB inhibited AKT signaling pathway in anti-hormonal resistant cells by using western blot analysis. As shown in **Figure 26**, AKT phosphorylation (p-AKT) increased 2.7-fold and 6.8-fold higher in the anti-hormonal resistant breast cancer LCC2 and LCC9 cell lines, respectively compared to wild-type MCF-7 cells. In addition, PLB at the concentration of 1  $\mu$ M significantly decreased p-AKT expression in both cell lines (**Figure 27-28**). This finding suggested that PLB was able to decrease AKT signaling pathway in anti-hormonal resistant breast cancer cells.

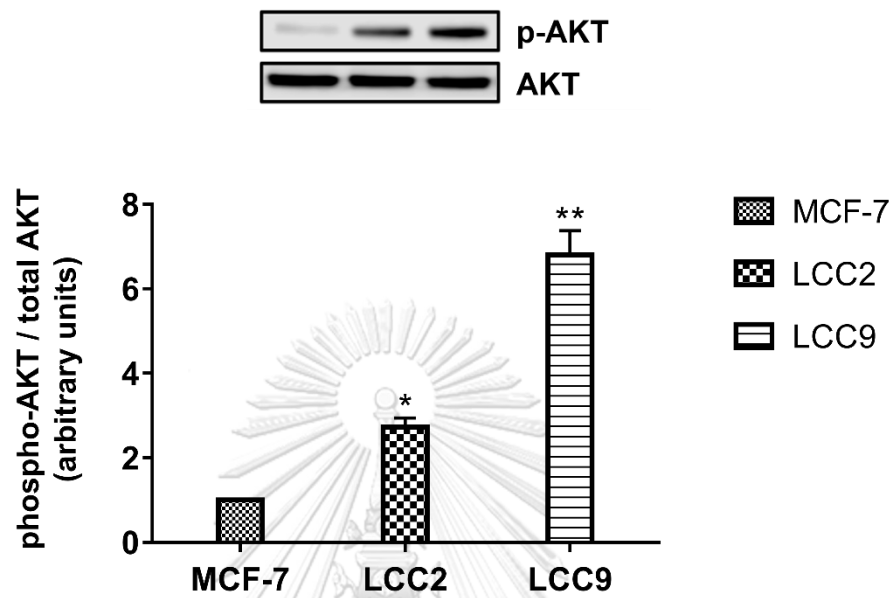


Figure 26. Protein expression of Akt phosphorylation at Ser473 in breast cancer cell lines include MCF-7 (ER-positive cells), LCC2 and LCC9 (anti-hormonal resistant cells). Results were represented as the mean  $\pm$  S.E.M from three experiment (n = 3). \* $p < 0.05$  vs. MCF-7 cells.



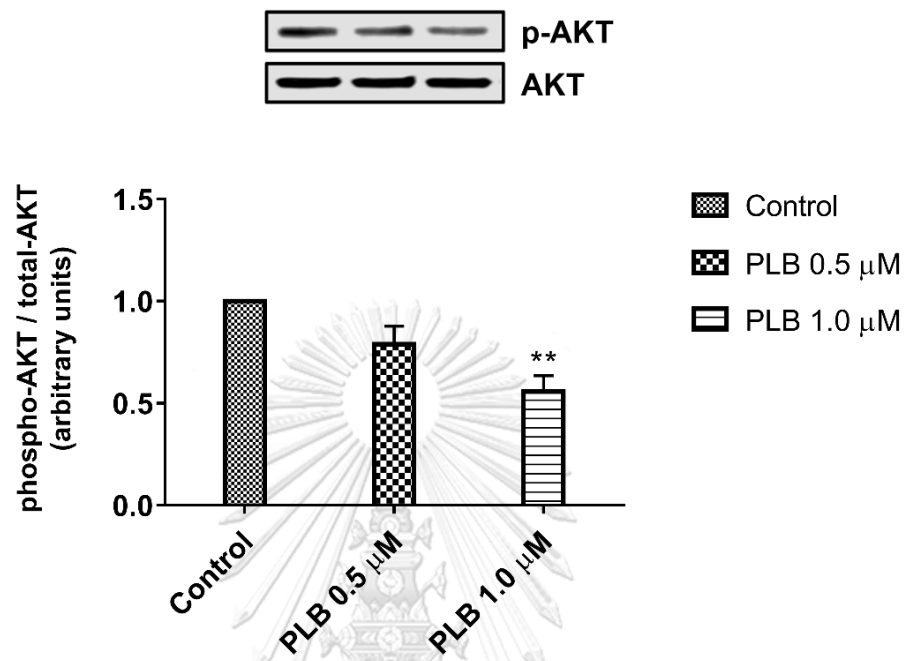


Figure 27. Protein expression of phosphorylated Akt in anti-hormonal resistant LCC2 cells after treatment with 0.5 and 1.0  $\mu$ M of PLB for 24 hours. Data were showed as the mean  $\pm$  S.E.M from three-independent experiments (n = 3).

\*\*p<0.01 vs. untreated control.

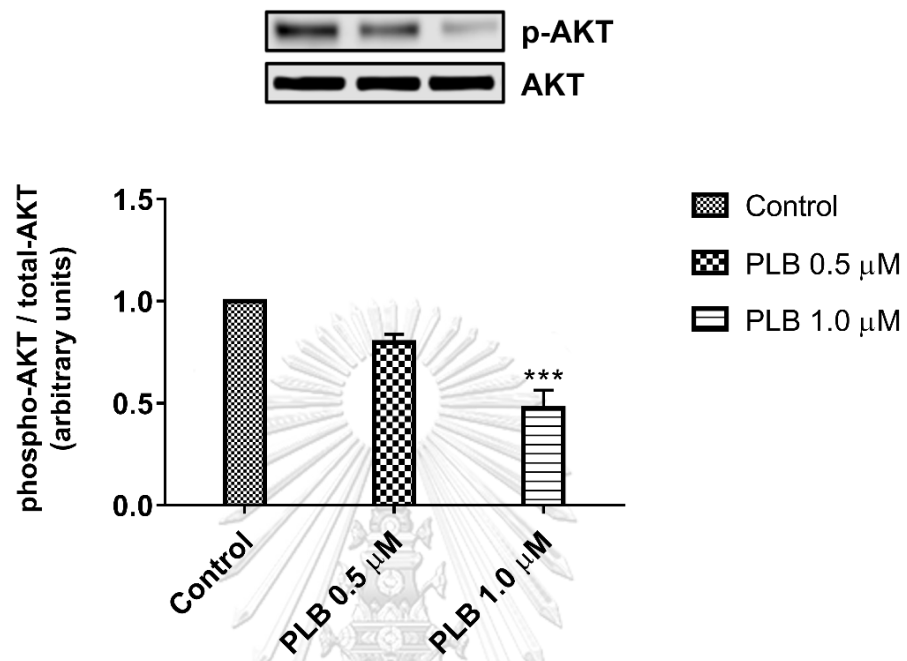


Figure 28. Protein expression of phosphorylated Akt in anti-hormonal resistant LCC9 cells after the treatment with 0.5 and 1.0  $\mu$ M of PLB for 24 hours. Data were showed as the mean  $\pm$  S.E.M from three-independent experiments (n = 3). \*\*\*p<0.001 vs. untreated control.

PLB abrogated Wnt-mediated proliferation and invasion via the modulation of *CCND1* and *MYC* in anti-hormonal resistant cell lines.

Wnt signaling was implicated in part of the cell proliferation and invasion of aggressive breast cancer cells in several studies [137, 138]. To determine whether the effect of PLB was mediated by Wnt signaling in anti-hormonal resistant cells, human Wnt1 recombinant and Wnt inhibitor (IWP2) were used. Wnt1 ligands dramatically increased cell proliferation approximately 1.4-fold in anti-hormonal resistant cells. Moreover, PLB treatment significantly decreased Wnt1-induced cell proliferation (Figure 29). In contrast, the growth inhibitory effect of PLB was attenuated in both cell lines when pre-treated with 10  $\mu$ M IWP2. However, pre-treated cells with IWP2 alone did not change cell viability from untreated controls in these resistant cells as showed in Figure 30.

Cyclin D1 and c-MYC are the direct targets of canonical Wnt pathway and play important roles in cell proliferation [137, 139]. PLB decreased the levels of *CCND1* and *MYC* in both cell lines. However, the inhibitory effect of PLB was abrogated in cells pre-treated with IWP2 whereas pre-treatment with IWP2 alone did not alter mRNA expression of *CCND1* and *MYC* (Figure 31-32). To determine whether Wnt signaling mediated anti-invasive effect of PLB in anti-hormonal resistant cells, IWP2 inhibitor was used to pre-treat the cells in Matrigel invasion assay. The pre-treatment of 5  $\mu$ M IWP2 and PLB significantly decreased cell invasion by 11.7% inhibition in LCC2 cells and 11.2% inhibition in LCC9 cells when compared with PLB alone (Figure 33-34). While pre-

treated cells with IWP2 alone did not affect invasive ability in resistant cell lines as shown in Figure 35-36. These results suggested that the inhibitory effects of PLB on cell proliferation and invasion were mediated in-part by canonical Wnt signaling in anti-hormonal resistant cells.



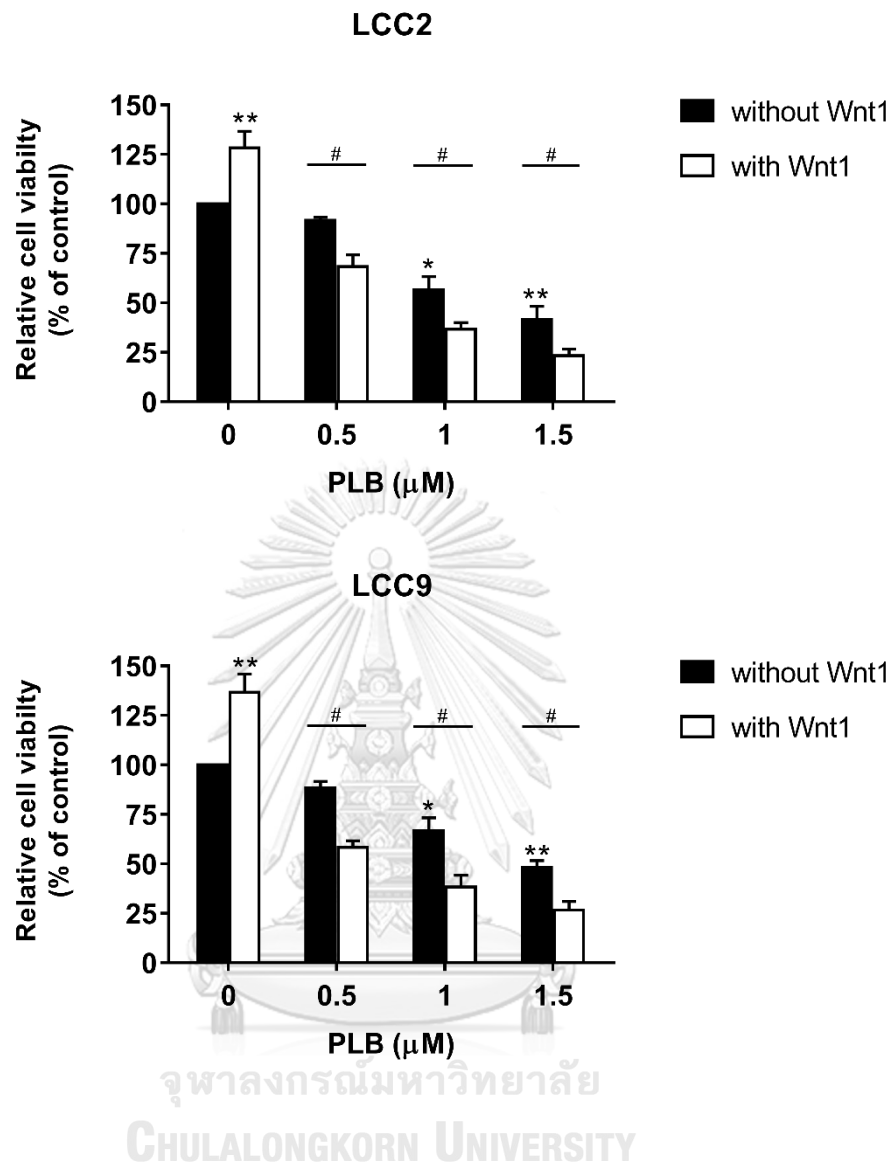


Figure 29. Cell viability of LCC2 and LCC9 treated with 0.5, 1.0, and 1.5  $\mu\text{M}$  of PLB for 24 hours with or without the pre-treatment with 100 ng/mL Wnt1 ligand. Results were represented as the mean  $\pm$  S.E.M from three experiment (n = 3). \* $p < 0.05$ , \*\* $p < 0.01$  vs. untreated control; # $p < 0.05$ , vs. PLB alone (without Wnt1).

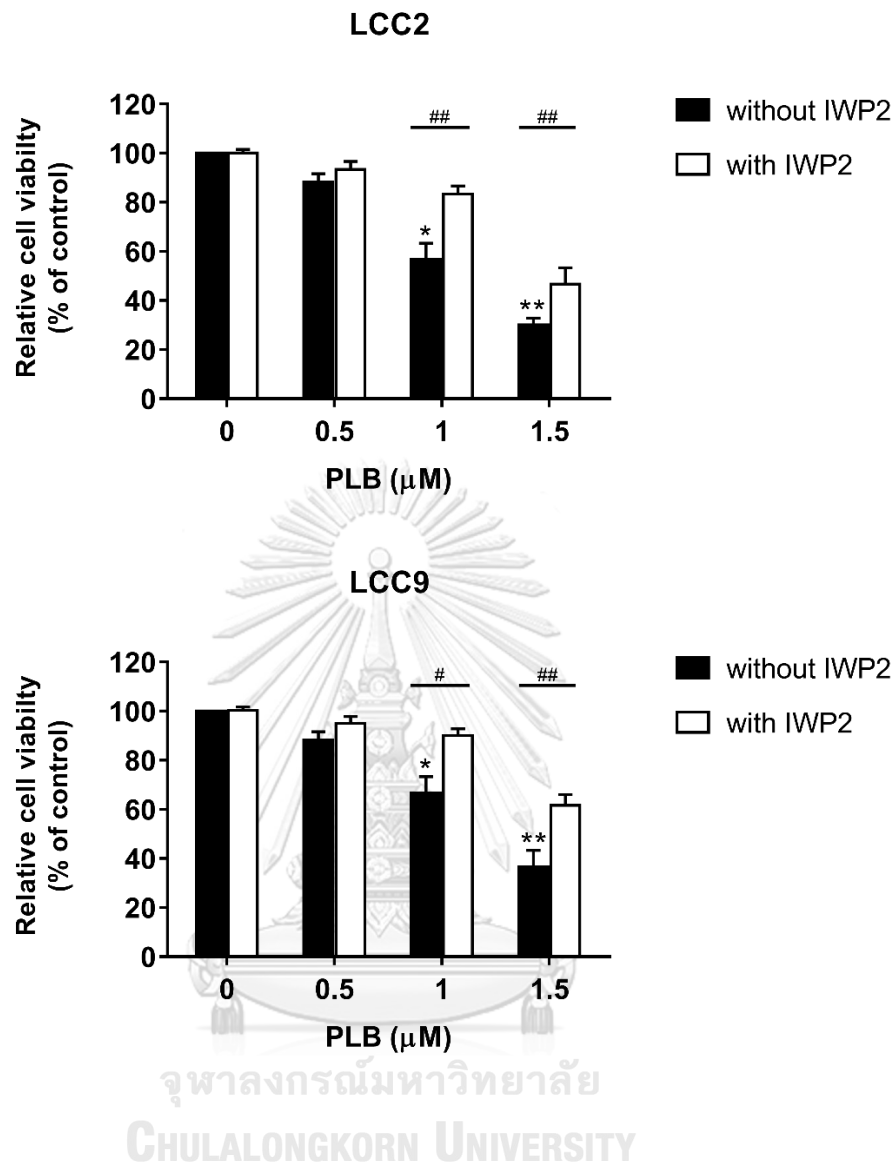


Figure 30. Cell viability of LCC2 and LCC9 treated with 0.5, 1.0, and 1.5  $\mu\text{M}$  of PLB for 24 hours with or without the 5  $\mu\text{M}$  IWP2 (Wnt inhibitor). Results were represented as the mean  $\pm$  S.E.M from three experiment ( $n = 3$ ). \* $p < 0.05$ , \*\* $p < 0.01$  vs. untreated control; # $p < 0.05$ , ## $p < 0.01$  vs. PLB alone (without IWP2).

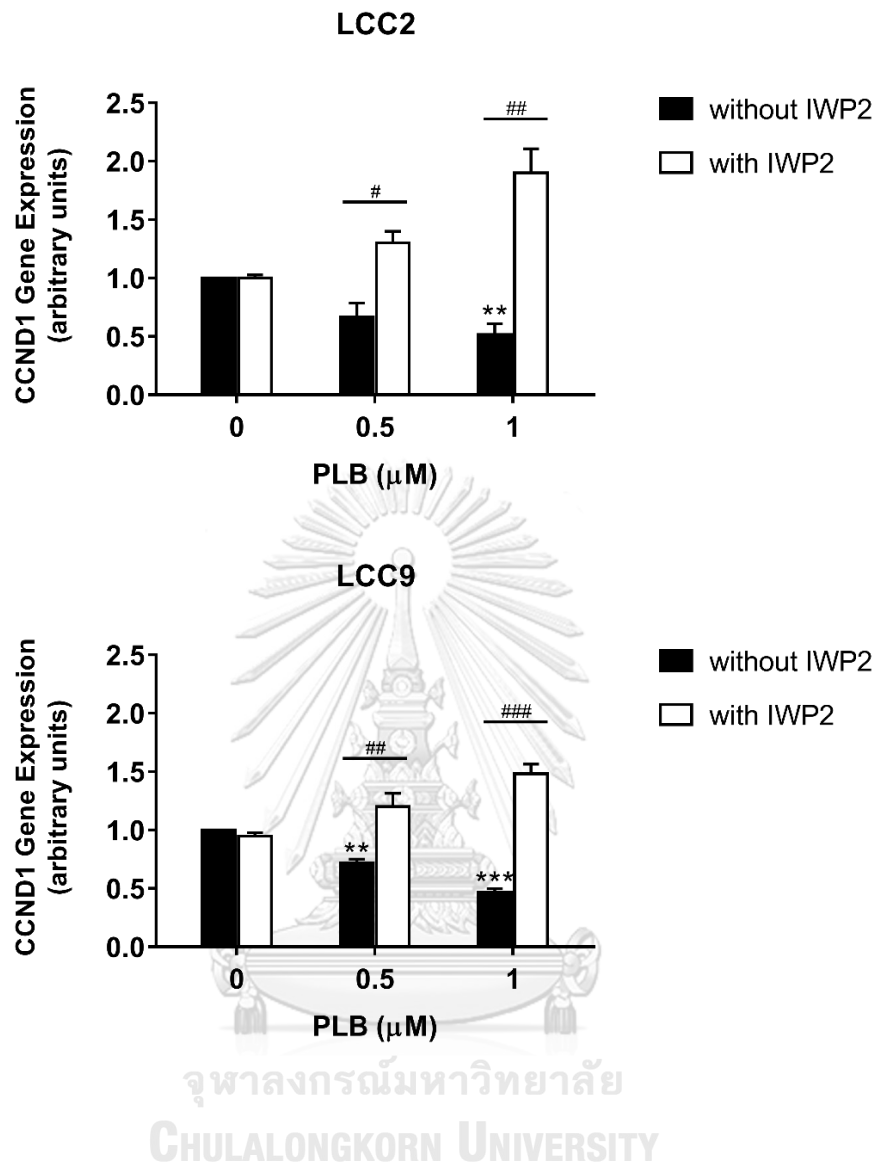


Figure 31. *CCND1* mRNA expression after the treatment with 0.5 and 1.0  $\mu\text{M}$  of PLB with or without pre-treatment with 5  $\mu\text{M}$  IWP2 (Wnt inhibitor) for 24 hours. Results were represented as the mean  $\pm$  S.E.M from three experiment ( $n = 3$ ). \*\* $p < 0.01$ , \*\*\* $p < 0.001$  vs. untreated control; # $p < 0.05$ , ## $p < 0.01$ , ### $p < 0.001$  vs. PLB alone (without IWP2).

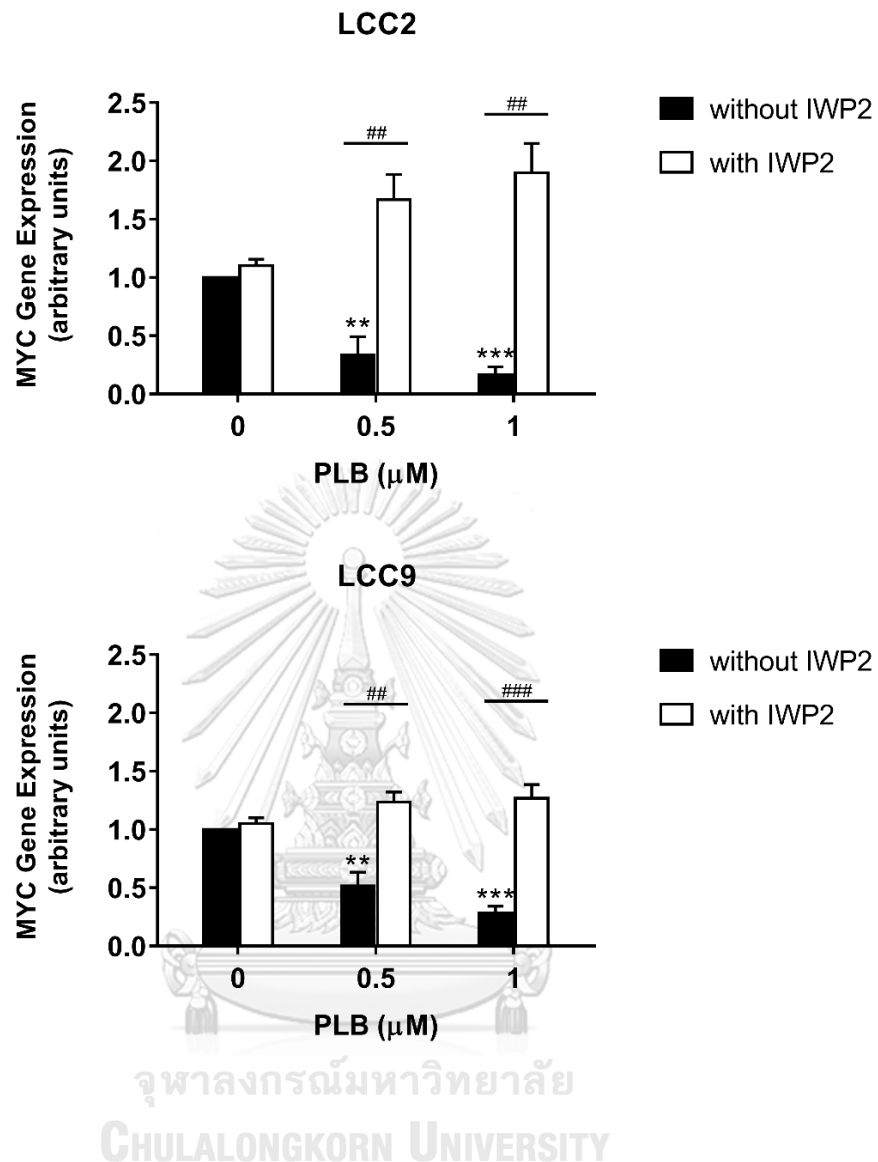


Figure 32. MYC mRNA expression after the treatment with 0.5 and 1.0  $\mu\text{M}$  of PLB with or without pre-treatment with 5  $\mu\text{M}$  IWP2 (Wnt inhibitor) for 24 hours. Results were represented as the mean  $\pm$  S.E.M from three experiment (n = 3). \*\*p<0.01, \*\*\*p<0.001 vs. untreated control; #p<0.05, ##p<0.01, ###p<0.001 vs. PLB alone (without IWP2).



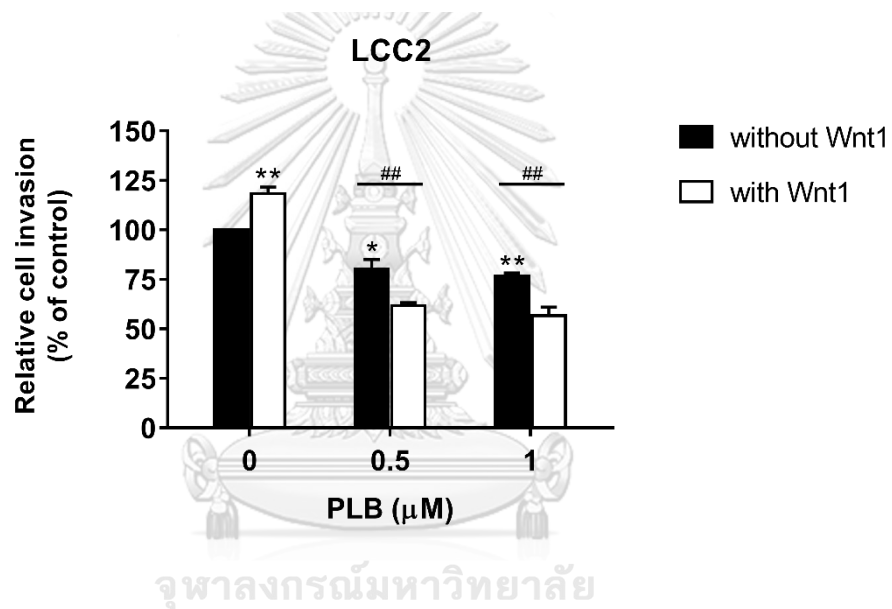
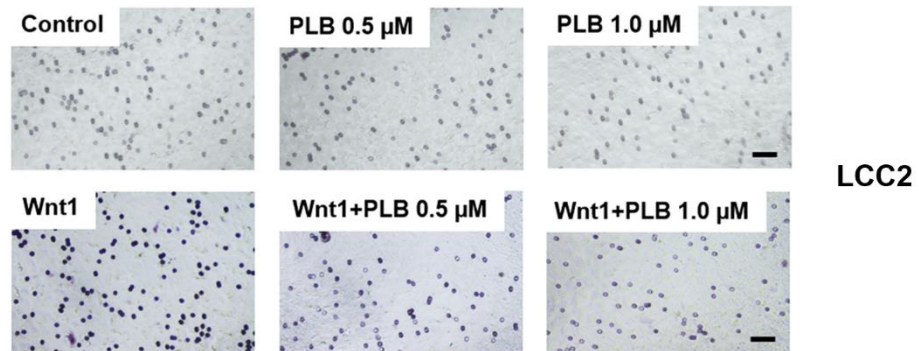


Figure 33. Cell invasion of LCC2 treated with 0.5 and 1.0  $\mu\text{M}$  of PLB for 48 hours with or without the pre-treatment with 100 ng/mL Wnt1 ligand. Results were represented as the mean  $\pm$  S.E.M from three experiment (n = 3). \* $p < 0.05$ , \*\* $p < 0.01$  vs. untreated control; # $p < 0.05$ , ## $p < 0.01$  vs. PLB alone (without Wnt1).

Scale bar = 100  $\mu\text{m}$ .

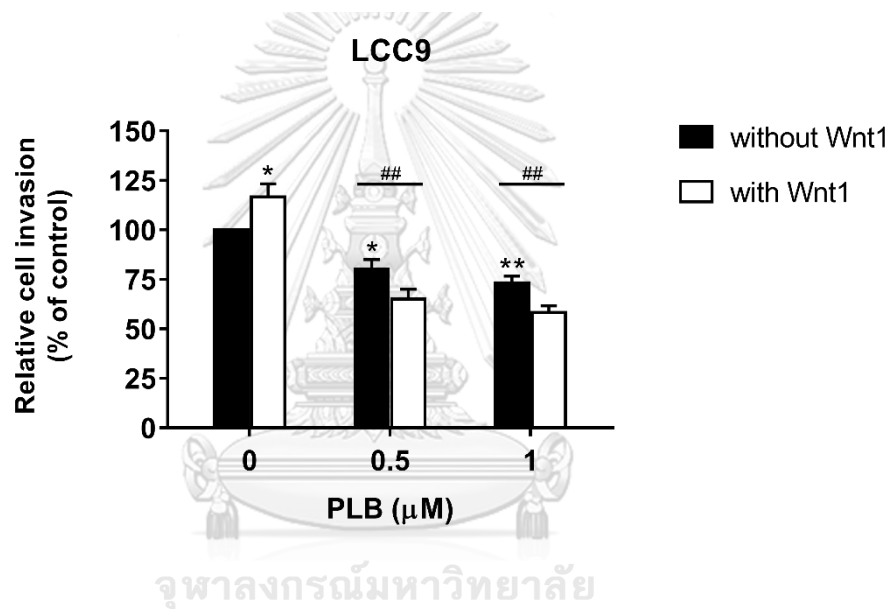
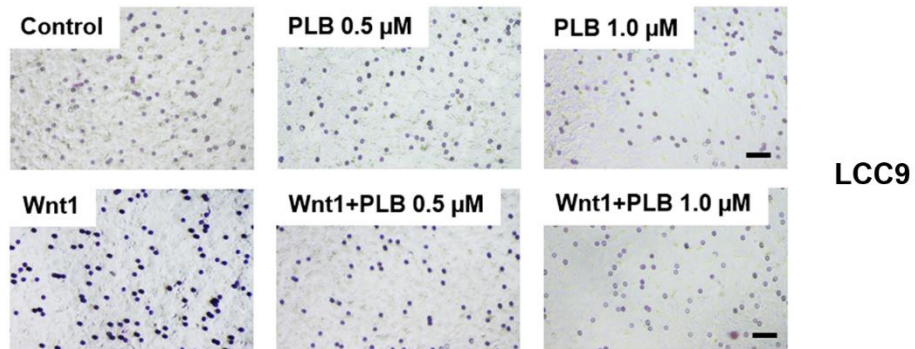


Figure 34. Cell invasion of LCC9 treated with 0.5 and 1.0  $\mu\text{M}$  of PLB for 48 hours with or without the pre-treatment with 100 ng/mL Wnt1 ligand. Results were represented as the mean  $\pm$  S.E.M from three experiment ( $n = 3$ ). \* $p < 0.05$ , \*\* $p < 0.01$  vs. untreated control; # $p < 0.05$ , ## $p < 0.01$  vs. PLB alone (without Wnt1). Scale bar = 100  $\mu\text{m}$ .

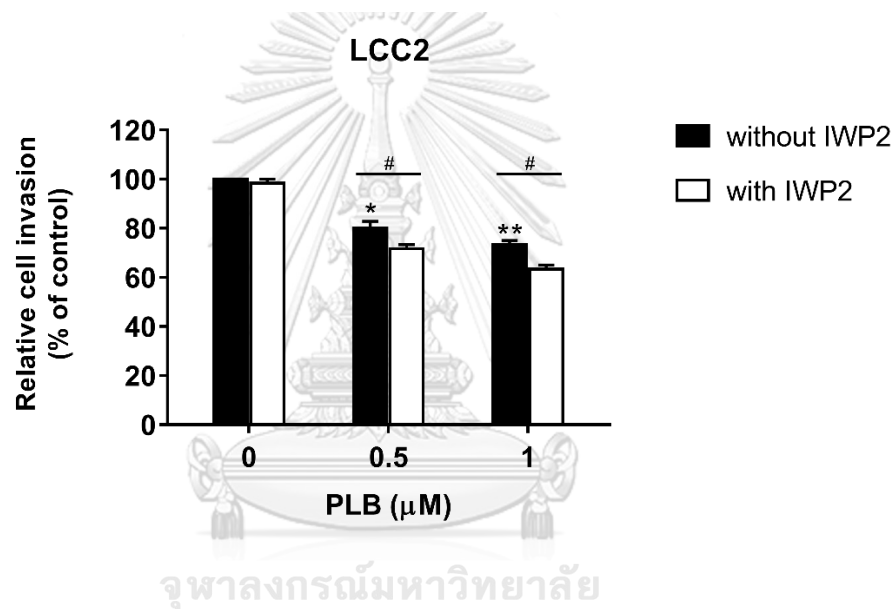
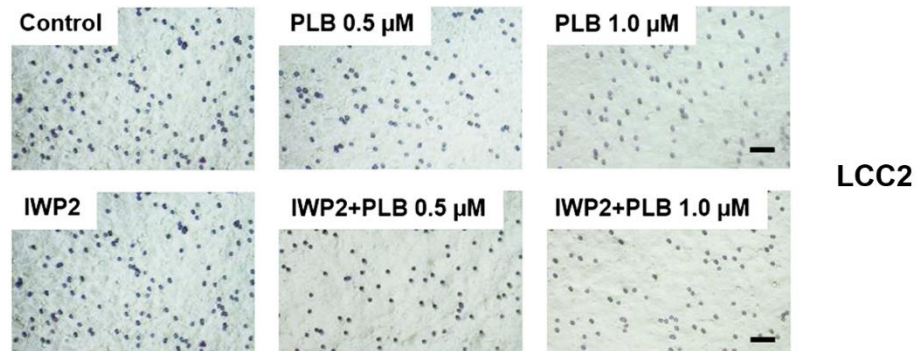


Figure 35. Cell invasion of LCC2 treated with 0.5 and 1.0  $\mu\text{M}$  of PLB for 48 hours with or without the pre-treatment with 5  $\mu\text{M}$  IWP2 (Wnt inhibitor). Results were represented as the mean  $\pm$  S.E.M from three experiment ( $n = 3$ ). \* $p < 0.05$ , \*\* $p < 0.01$  vs. untreated control; # $p < 0.05$  vs. PLB alone (without IWP2). Scale bar = 100  $\mu\text{m}$ .

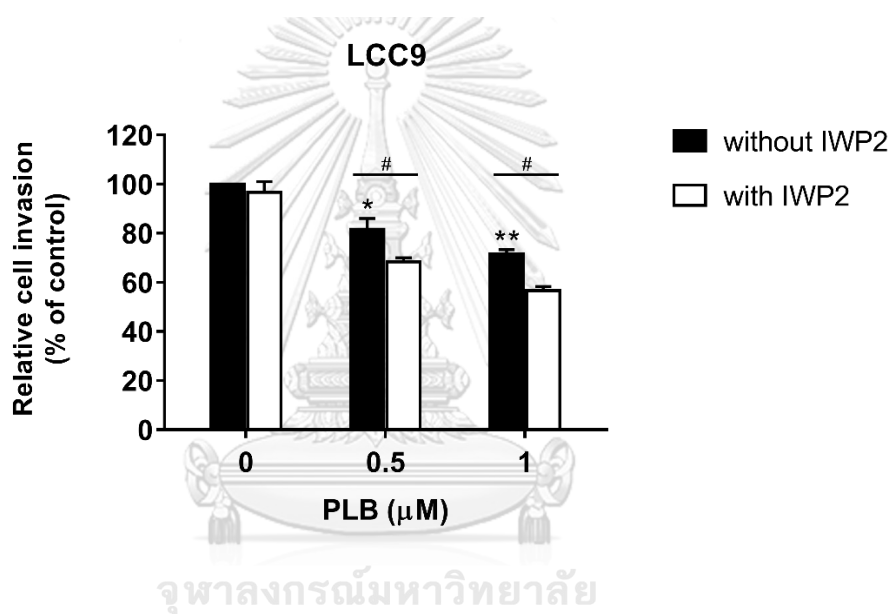
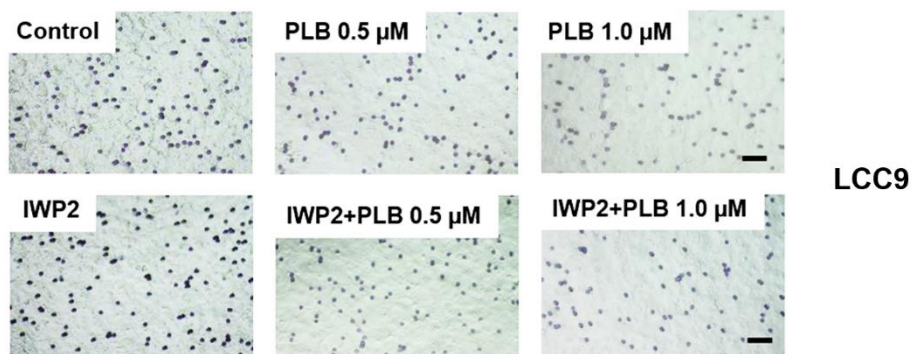


Figure 36. Cell invasion of LCC9 treated with 0.5 and 1.0  $\mu\text{M}$  of PLB for 48 hours with or without the pre-treatment with 5  $\mu\text{M}$  IWP2 (Wnt inhibitor). Results were represented as the mean  $\pm$  S.E.M from three experiment ( $n = 3$ ). \* $p < 0.05$ , \*\* $p < 0.01$  vs. untreated control; # $p < 0.05$  vs. PLB alone (without IWP2). Scale bar = 100  $\mu\text{m}$ .

PLB significantly inhibited tumor growth without serious adverse effects in anti-hormonal resistant breast cancer orthotopic xenografts in mice.

Colonies were highly formed in anti-hormonal resistant breast cancer LCC9 cells than MCF-7 and LCC2 cell lines (unpublished data), suggested that LCC9 cells exhibited the clonogenicity *in vitro* and tumorigenesis *in vivo*. To determine whether PLB inhibited tumor growth in orthotopic xenograft mouse model, LCC9 cells were inoculated into the mammary fat pads of female nude mice. The palpable tumors were observed in every mouse inoculating with anti-hormonal resistant breast cancer LCC9 cells at least 7 days. In comparison to the control group, PLB treatment at low-dose (2 mg/kg/day) and high-dose (4 mg/kg/day) significantly reduced the tumor growth. The average of tumor volume was about 50-60 mm<sup>3</sup> after 2.5 weeks of cell inoculation (Figure 37). The intraperitoneal administration of PLB did not affect the body weight and behaviors of animals throughout the treatment (Figure 38). The tumor weights in mice treated with PLB at 2 mg/kg/day (low-dose) and 4 mg/kg/day (high-dose) declined by 49% and 76% when compared to control group (Figure 39). Moreover, prothrombin time (PT) did not significantly different in each group (Figure 40). These results suggested that PLB inhibited tumorigenesis without effects on body weight and blood coagulation in orthotopic xenografts of anti-hormonal resistant breast cancer.

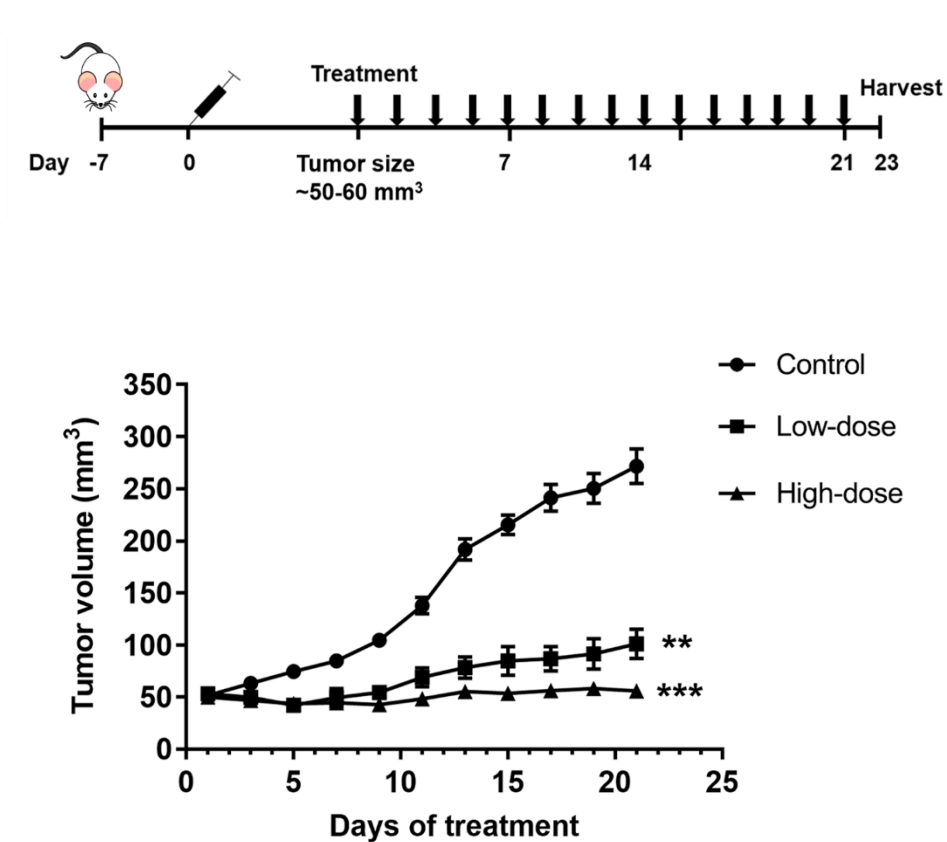


Figure 37. Time schedule of treatments and tumor volume in mice treated with 0.1% DMSO in normal saline (control), 2 mg/kg/day PLB (low-dose) and 4 mg/kg/day PLB (high-dose), intraperitoneal injection, 5 times/week for 3 weeks. Results were showed as the mean  $\pm$  S.E.M from six individual mice (n = 6 each group). \*\*p<0.01, \*\*\*p<0.001 vs. control group.

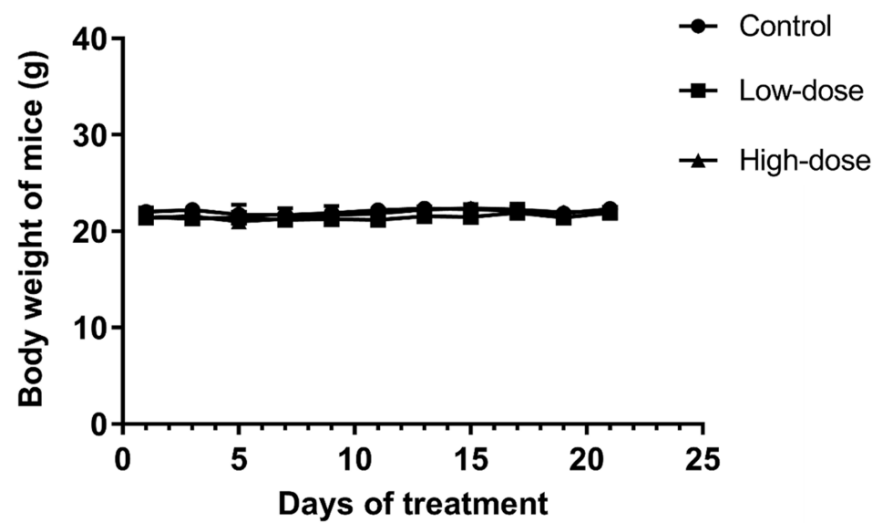


Figure 38. The body weight in grams of mice treated with 0.1% DMSO in normal saline (control), 2 mg/kg/day PLB (low-dose) and 4 mg/kg/day PLB (high-dose) was monitored every other day throughout the treatment. Results were showed as the mean  $\pm$  S.E.M from six individual mice (n = 6 each group).

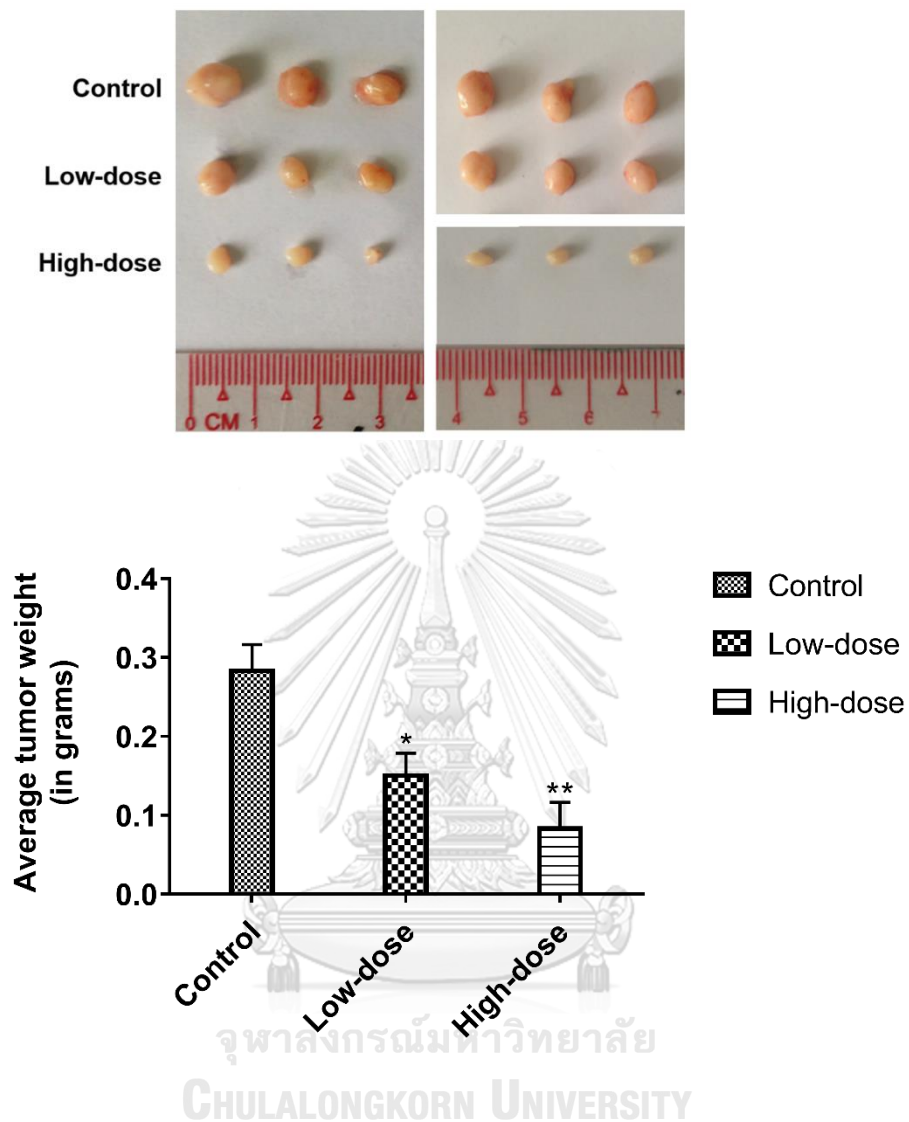


Figure 39. The average of tumor weight in mice treated with 0.1% DMSO in normal saline (control), 2 mg/kg/day PLB (low-dose) and 4 mg/kg/day PLB (high-dose), intraperitoneal injection, 5 times/week for 3 weeks. The tumor was measured when resected the tumors after the first treatment for 23 days. Results were showed as the mean  $\pm$  S.E.M from six individual mice (n = 6 each group). \* $p < 0.05$ , \*\* $p < 0.01$  vs. control group.



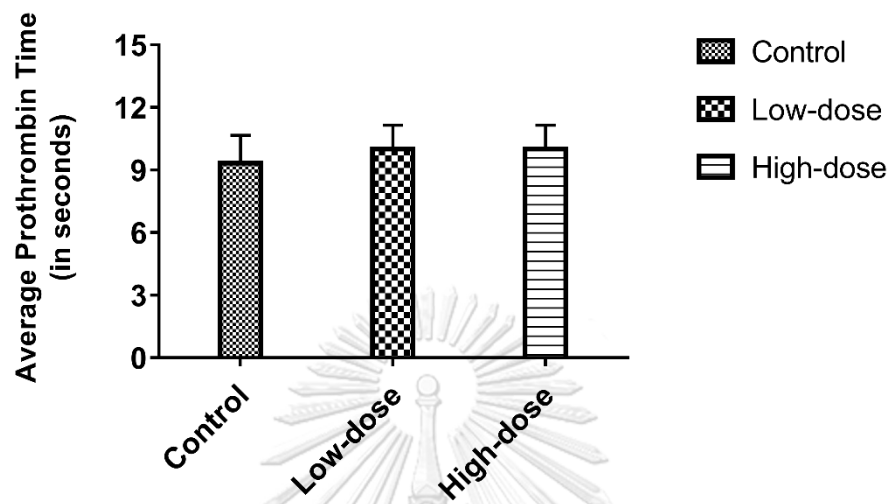


Figure 40. The prothrombin time (PT) in seconds in blood sample collected from mice treated with PLB on the sacrificed day (after the first treatment for 23 days). The data were recorded from the automated machine. The mean  $\pm$  S.E.M of PT is  $11.9 \pm 0.30$  seconds in mice (Normal range = 10.0-15.2 seconds) [134, 135]. Results were showed as the mean  $\pm$  S.E.M from six individual mice ( $n = 6$  each group).

PLB inhibited tumor angiogenesis and metastasis in anti-hormonal resistant breast cancer orthotopic xenograft mice.

The injection of cancer cells into mammary fat pads (orthotopic xenografts) represented more clinical relevance than the injection of cancer cells to tail veins of mice. Orthotopic xenografts provide the microenvironment in supporting tumor growth, EMT and metastatic process. In addition, these resistant ER-positive breast cancer cell type often metastasized to the lungs similar to breast cancer patients [140]. Lung metastases of LCC9 tumor-bearing mice were observed in the control group after cell inoculation for 38-41 days (**Figure 41**). The number of mice with lung metastasis was reduced in PLB treated groups compared to control group (**Figure 41**) which did not change the weight of lung in each group of mice (**Figure 42**). The expression levels of genes involved in metastasis were also diminished in mice treated with 4 mg/kg/day of PLB for *SDF-1* expression (**Figure 43**) and PLB significantly reduced *MMP9* mRNA level in mice treated with 2 mg/kg/day (low-dose group) and 4 mg/kg/day (high-dose group) when compared to control group (**Figure 44**).

Results from IHC analysis of endothelial marker (PECAM/CD31) was markedly lower in mice treated with PLB than the control group as showed in **Figure 45**. Moreover, tumor-associated neovascularization as indicated by the PECAM/CD31 staining was quantified. The brown spots of PECAM/CD31 was markedly lower in mice treated with both low dose and high dose of PLB groups than the control group by 48% to 86%

(Figure 45). PLB also significantly downregulated angiogenesis-related genes including *VEGF* and *FGF2* in mice treated with PLB 4 mg/kg/day (high-dose group) compared to control group (Figure 46-47). These results indicated that PLB was able to inhibit lung metastasis and angiogenesis *in vivo*.



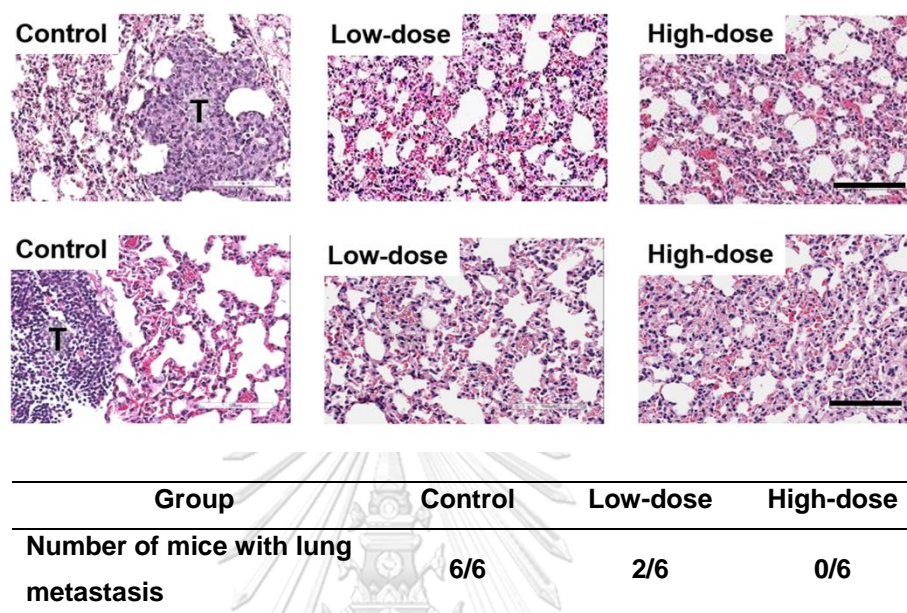


Figure 41. The micrometastasis and the incidence of lung metastasis in mice treated with 0.1% DMSO in normal saline (control), 2 mg/kg/day PLB (low-dose) and 4 mg/kg/day PLB (high-dose) intraperitoneal injection, 5 times/week for 3 weeks. Data were showed as number of mice from six individual animals counted from H&E staining (n = 6 each group).

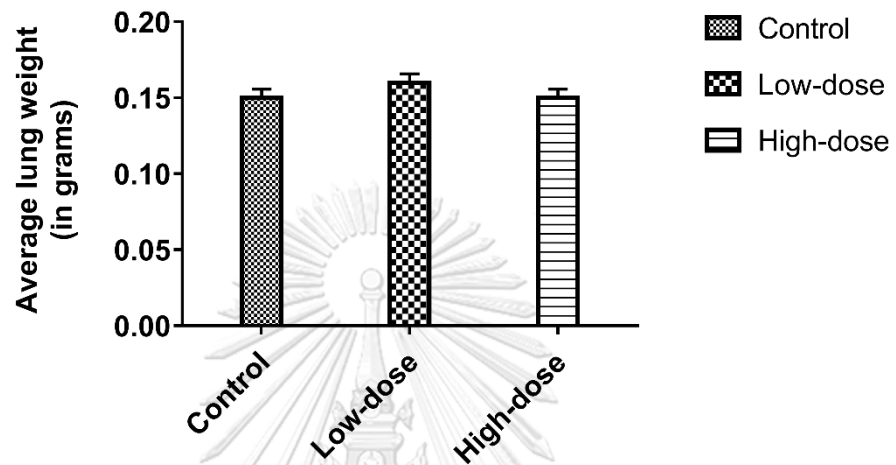


Figure 42. The mean lung weight in grams of mice treated with 0.1% DMSO in normal saline (control), 2 mg/kg/day PLB (low-dose) and 4 mg/kg/day PLB (high-dose). Data were showed as the mean  $\pm$  S.E.M from six individual animals (n = 6 each group).

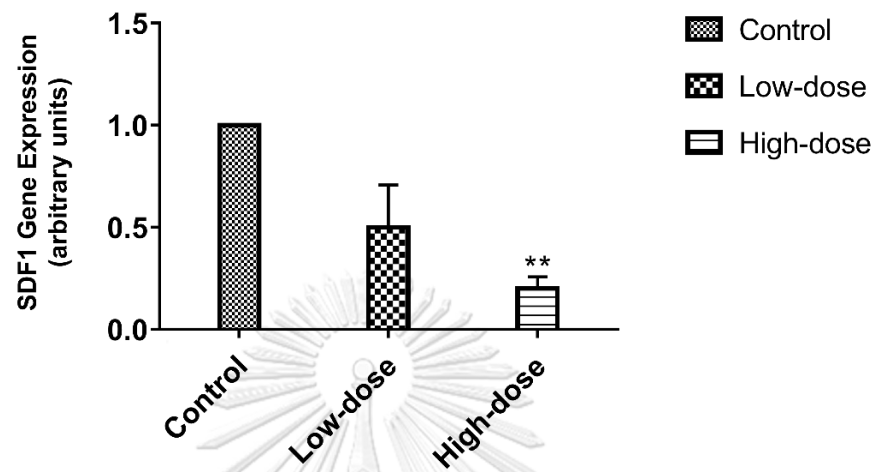


Figure 43. *SDF1* mRNA expression levels in lung tissues of mice after treatment with 0.1% DMSO in normal saline (control), 2 mg/kg/day PLB (low-dose) and 4 mg/kg/day PLB (high-dose) intraperitoneal injection, 5 times/week for 3 weeks. Data were showed as the mean  $\pm$  S.E.M from six individual animals ( $n = 6$  each group). \*\* $p < 0.01$  vs. control group.

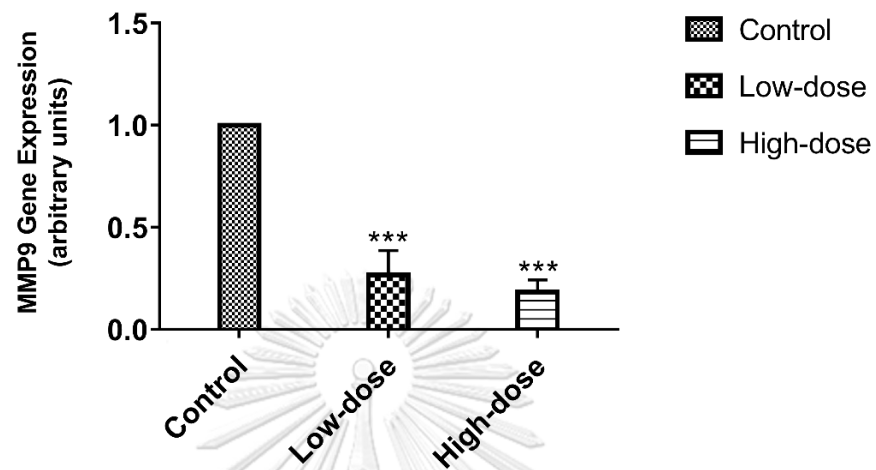


Figure 44. *MMP9* mRNA expression levels in lung tissues of mice after treatment with 0.1% DMSO in normal saline (control), 2 mg/kg/day PLB (low-dose) and 4 mg/kg/day PLB (high-dose) intraperitoneal injection, 5 times/week for 3 weeks. Data were showed as the mean  $\pm$  S.E.M from six individual animals ( $n = 6$  each group). \*\*\* $p < 0.001$  vs. control group.

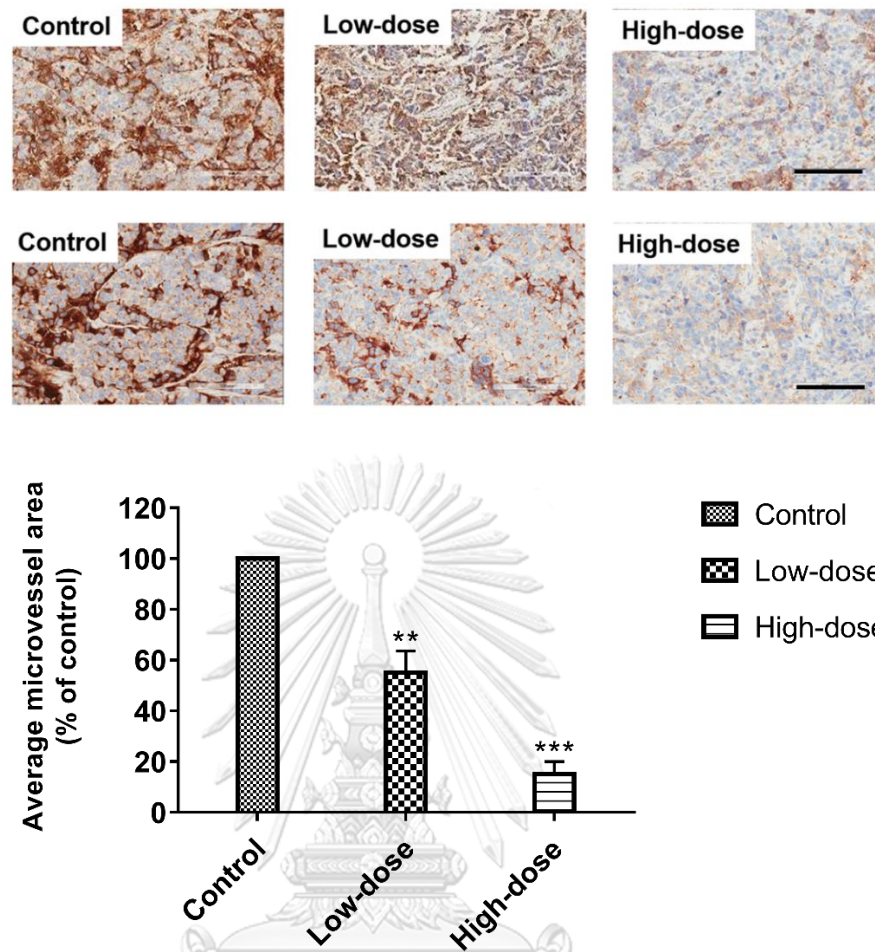


Figure 45. PECAM staining showed the relative microvessel area of PECAM/CD31 in tumor tissues. Mice were treated with 0.1% DMSO in normal saline (control), 2 mg/kg/day PLB (low-dose) and 4 mg/kg/day PLB (high-dose) intraperitoneal injection, 5 times/week for 3 weeks. Brown stainings were chosen at least 5 random fields per slide and analyzed using the Microvessel algorithm. Data were showed as the mean  $\pm$  S.E.M from six individual animals (n = 6 each group). \*\*p<0.01, \*\*\*p<0.001 vs. control group.



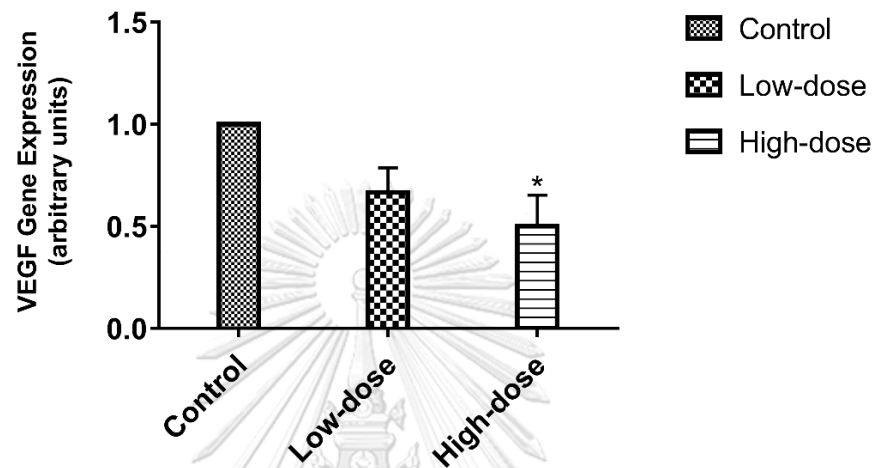


Figure 46. VEGF mRNA expression levels in lung tissues of mice after treatment with 0.1% DMSO in normal saline (control), 2 mg/kg/day PLB (low-dose) and 4 mg/kg/day PLB (high-dose) intraperitoneal injection, 5 times/week for 3 weeks. Data were showed as the mean  $\pm$  S.E.M from six individual animals (n = 6 each group). \*p<0.05 vs. control group.

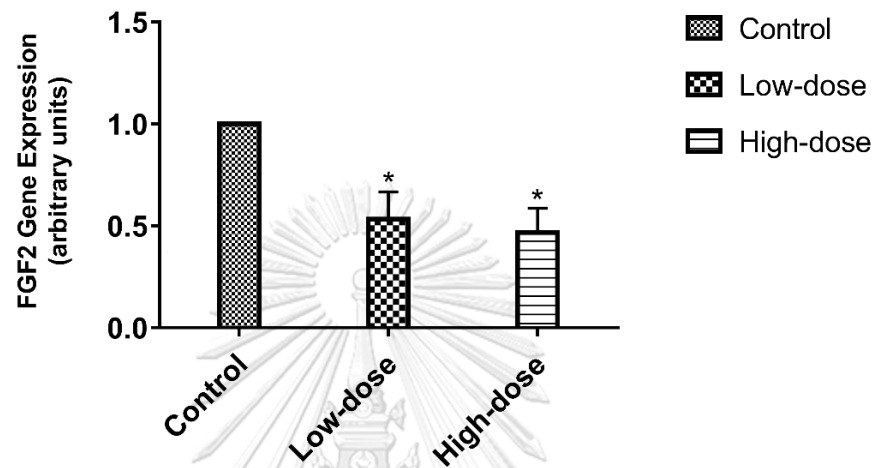


Figure 47. *FGF2* mRNA expression levels in lung tissues of mice after treatment with 0.1% DMSO in normal saline (control), 2 mg/kg/day PLB (low-dose) and 4 mg/kg/day PLB (high-dose) intraperitoneal injection, 5 times/week for 3 weeks. Data were shown as the mean  $\pm$  S.E.M from six individual animals (n = 6 each group). \* $p < 0.05$  vs. control group.

## CHAPTER V

### DISCUSSION AND CONCLUSION

Tamoxifen has been used as a first-line drug in anti-hormonal therapy for ER-positive breast cancer patients [26, 141]. Although tamoxifen is very effective, the long-term exposure of tamoxifen finally causes resistance, tumor recurrence and metastasis [26]. Recent studies showed mechanisms of acquired resistance to tamoxifen can cause by cancer stem-like characteristics (CSLCs) in bulk tumor which induce epithelial-to-mesenchymal transition (EMT), enhanced cancer stem cells (CSC) markers, and tumorigenicity *in vivo* [32, 43, 136]. Our findings are consistent with previous studies [18, 43] that the properties of cancer stem-like cells enriched in anti-hormonal resistant cells with increased markers of CSC, overexpression beta-catenin and Wnt-targeted genes. Our previous study reported that PLB inhibited EMT process by the reduction of Snail transcription factor and re-expression of epithelial marker E-cadherin in resistant cells [8]. This recent study observed 0.75  $\mu\text{M}$  and 1  $\mu\text{M}$  of PLB were able to inhibit colony formation in anti-hormonal resistant breast cancer cells, but the minimal concentration of PLB (0.5  $\mu\text{M}$ ) was not statistically significant in inhibiting colony-forming ability when compared to untreated control ( $p > 0.05$ ). However, 0.5  $\mu\text{M}$  of PLB significantly inhibited mammosphere formation. Thus, the concentrations of 0.5 and 1  $\mu\text{M}$  of PLB were chosen for determining the inhibitory effect of PLB for the rest of

experiments. In transcriptional level, 0.5  $\mu\text{M}$  and 1  $\mu\text{M}$  of PLB significantly downregulated the expression of Wnt responsive genes. Additionally, PLB dramatically reduced the secondary and tertiary mammosphere formation cells and downregulated expression of cancer stem-like genes in both anti-hormonal resistant breast cancer LCC2 and LCC9. However, the inhibitory mechanism of PLB on cancer stem-like characteristics has not been fully understood in this study and required further investigation.

The important mechanisms involved in anti-hormone resistant are the crosstalk between estrogen receptor (ER) and human epidermal growth factor receptor 2 (HER2) and increased expression of NCOA3 [25]. NCOA3 acts as a key transcription factor to drive transcription of ER-targeted genes resulted in breast cancer cell survival from adjuvant hormonal therapy [25, 28]. NCOA3 has been demonstrated to be activate AKT signaling pathway in advanced breast cancer led to increase cell proliferation and avoiding apoptosis [7, 29, 123]. This study indicated that AKT phosphorylation was increased in anti-hormonal resistant breast cancer cell lines. Moreover, PLB inhibited AKT signaling in both cell lines.

Furthermore, PLB treatment decreased cell proliferation and invasion in both cell lines of anti-hormonal resistant cancer *in vitro*. The inhibitory effects of PLB on cell proliferation and invasion was further determined whether they were partly mediated by Wnt signaling pathway in anti-hormonal resistant cells. This study exhibited that PLB

significantly inhibited Wnt-mediated proliferation and invasion in anti-hormonal resistant cancer cells by using Wnt1 ligand and Wnt inhibitor IWP2. PLB treatment significantly decreased Wnt1-induced cell proliferation and invasion in both cell lines. On the other hand, Wnt inhibitor IWP2 abrogated the inhibitory effect of PLB on cancer cell invasion in anti-hormonal resistant cells. This finding suggested Wnt signaling pathway might be involved in the inhibitory mechanism of PLB.

Since the beta-catenin can modulate Wnt-targeted genes including *c-MYC* and *Cyclin D1* which associated with the progression of breast cancer [142, 143]. In molecular level, the inhibitory effect of PLB on *MYC* and *CCND1* mRNA expression was decreased when treated cells with Wnt inhibitor in anti-hormonal resistant cell lines. These findings demonstrated that the inhibitory mechanisms of PLB on cell growth and invasion were mediated in part through Wnt/beta-catenin pathway in anti-hormonal resistant breast cancer cells which were consisted with previous studies [138, 143, 144]. Importantly, Wnt inhibitor IWP2 (5  $\mu\text{M}$  and 10  $\mu\text{M}$ ) used in this study was not statistically significant in inhibiting cell viability compared to untreated control.

As mentioned above, beta-catenin plays critical roles in Wnt signaling, cell fate specification and EMT process in metastatic phenotypes [145]. Elevated beta-catenin expression also correlated with drug resistance and tumor recurrence in breast cancer patients [18, 146]. This study demonstrated that PLB could significantly reduce the protein levels of beta-catenin-dependent canonical Wnt signaling in anti-hormonal

resistant cells. We also investigated whether PLB regulates *AXIN-2*, *TCF4*, and negative regulator dickkopf-1 (*DKK1*) expression involving in canonical Wnt pathway which might regulate cell invasion and angiogenesis. The results indicated that PLB markedly downregulated *AXIN-2*, *TCF4* and upregulated *DKK1* expression levels in both resistant cell lines. Our result confirmed that PLB plays a critical role in regulating downstream targets of Wnt-signaling involved in cell proliferation and EMT process in anti-hormonal resistant cells.

Up to 90% of deaths from breast cancer cause by distant metastasis to vital organs such as bone, lung, brain and liver [26]. Tumor metastasis is a multi-step process starting from EMT process to enhance cell migration and invasion. Matrix metalloproteases (MMPs), especially *MMP9* function in promoting angiogenesis, invasion, migration, and colonization [147]. The colonization of breast cancer cells at the metastatic sites relies on the growth-promoting chemokine CXCL12/SDF1 level which is secreted at the metastatic sites and acts as a chemoattractant for its cognate receptor (CXCR4) on cancer cells and could potentially enable cancer cells to homing to lung tissues [148]. Therefore, invasive ability of cancer cells is an important factor of metastasis. The chemoattractant in microenvironment niches may be the effective target for the inhibition of tumor metastasis. Our result showed that PLB inhibited lung metastasis *in vivo* and did not change the weight of lung tissues by the downregulation of *SDF1* and *MMP9* mRNA expression.

Angiogenesis is another important hallmark of cancer which assist tumor growth and metastasis [149]. A novel anti-angiogenic candidate will be benefited to treat metastatic phenotype of anti-hormonal resistant breast cancer since the indication of anti-VEGF has been removed for the treatment of breast cancer due to inducing of tumor progression and metastasis [149, 150]. Because our result demonstrated PLB inhibited Wnt signaling which involved in angiogenesis in resistant cell lines, we further studied the inhibitory effect of PLB on angiogenesis in xenograft model. PECAM/CD31 is the endothelial marker of tumor angiogenesis [40]. Our result demonstrated that PLB significantly reduced the area of PECAM/CD31 positive staining. PLB also suppressed tumor growth in orthotopic xenograft mice. The depletion of angiogenesis may be one of the mechanisms of the reduction of tumor growth. This finding are consistent with the previous study reported that PLB could inhibit angiogenesis by decreasing VEGF/VEGFR2 through the suppression of RAS/MEK signaling pathways in endothelial and cancer cells [120].

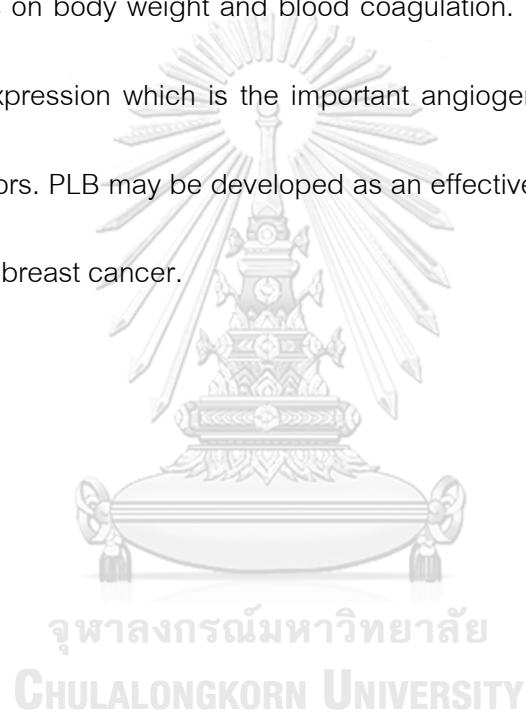
Basic fibroblast growth factor (FGF2) overexpression was observed in aggressive cancer and correlated with anti-hormonal resistance and poor prognosis in breast cancer [151, 152]. A report demonstrated that FGF2 had a synergistic effect in inducing tumor angiogenesis with the combination with VEGF [153]. In addition, FGF2 interacts with Wnt/beta-catenin in angiogenesis process in tumors [154]. FGF2 is a potent vascular growth factor in activating angiogenic events, whereas Wnt signaling

assists guiding cell fate determination that appropriately shapes the new blood vessels [136]. These findings suggested that Wnt/beta-catenin and FGF2 are good therapeutic targets in advance- stage breast cancer [149, 154, 155]. A possible mechanism involved in anti-VEGF resistance is alternative signaling pathways, such as FGF2, resulting in increased endothelial cell proliferation and tumor angiogenesis [149, 153]. Interestingly, we found that the level of *FGF2* significantly upregulated in both anti-hormonal resistant cell lines. PLB reduced the mRNA expression of *FGF2* level in tumor-bearing mouse tissues. This finding in mice is similar with the effect of PLB in both resistant cell lines. These results suggested that PLB can significantly inhibit tumor angiogenesis and metastasis. The dose of PLB used in this animal study based on the median lethal dose ( $LD_{50}$ ) of PLB in rodents at 65 mg/kg [125]. From our pilot study, we observed PLB at 2 mg/kg and 4 mg/kg were able to decrease tumor size. Therefore, our findings showed PLB effectively inhibited tumor growth in anti-hormonal resistant breast cancer *in vivo* without any serious adverse effects such as body weight, daily activities, food intake and blood clot formation. These findings are similar to other studies demonstrated that PLB administration exhibited a potent anti-cancer effect [70] and safety in rodents [125].

In conclusion, the recent study exhibited the anti-cancer effects of PLB on the elimination of CSLCs, inhibition of tumor growth, angiogenesis and metastasis. Our



previous study reported PLB inhibited cell invasion through EMT marker which was able to modulate Wnt signaling pathway. This study further confirmed that the mechanism of PLB on cell proliferation and invasion was mediated by Wnt/beta-catenin in anti-hormonal resistant breast cancer cells. This study also showed the potent inhibitory effect of PLB on tumor growth and angiogenesis in orthotopic xenograft mouse model without any effects on body weight and blood coagulation. Furthermore, PLB was able to inhibit FGF-2 expression which is the important angiogenic factor in both cell lines and xenograft tumors. PLB may be developed as an effective anti-cancer agent for anti-hormonal resistant breast cancer.



### Future Perspective

This study demonstrated the Wnt-mediated inhibitory mechanisms of PLB on cell proliferation and invasion in anti-hormonal resistant breast cancer cell lines. However, the inhibitory mechanisms of PLB *in vivo* have not been clearly understood. To provide more information on this mechanism, (i) Wnt1 siRNA knockdown cells will be determine in anti-hormonal resistant breast cancer cells and (ii) pre-treatment with Wnt inhibitor will be performed in orthotopic xenograft mouse model. These further experiments will confirm the role of Wnt signaling in anti-cancer mechanism of PLB.



## REFERENCES

1. Siegel RL, Miller KD, Jemal A. **Cancer statistics, 2019.** *CA Cancer J Clin* 2019, 69:7-34.
2. Sripaiboonkij N, Thinkamrop B, Promthet S, Kannawat C, Tangcharoensathien V, Ansusing T, Rattanamongkolgul S. **Breast Cancer Detection Rate, Incidence, Prevalence and Interval Cancer-related Mammography Screening Times among Thai Women.** *Asian Pac J Cancer Prev* 2016, 17:4137-4141.
3. Dai X, Li T, Bai Z, Yang Y, Liu X, Zhan J, Shi B. **Breast cancer intrinsic subtype classification, clinical use and future trends.** *Am J Cancer Res* 2015, 5:2929-2943.
4. Larionov AA, Miller WR. **Challenges in defining predictive markers for response to endocrine therapy in breast cancer.** *Future Oncol* 2009, 5:1415-1428.
5. Musgrove EA, Sutherland RL. **Biological determinants of endocrine resistance in breast cancer.** *Nat Rev Cancer* 2009, 9:631-643.
6. O'Sullivan CC. **Overcoming Endocrine Resistance in Hormone-Receptor Positive Advanced Breast Cancer-The Emerging Role of CDK4/6 Inhibitors.** *Int J Cancer Clin Res* 2015, 2:29-56.
7. Ao X, Nie P, Wu B, Xu W, Zhang T, Wang S, Chang H, Zou Z. **Decreased expression of microRNA-17 and microRNA-20b promotes breast cancer resistance to taxol therapy by upregulation of NCOA3.** *Cell Death Dis* 2016, 7:e2463.

8. Sakunrangsit N, Kalpongukul N, Pisitkun T, Ketchart W. Plumbagin Enhances Tamoxifen Sensitivity and Inhibits Tumor Invasion in Endocrine Resistant Breast Cancer through EMT Regulation. *Phytother Res* 2016, 30:1968-1977.
9. Kim MR, Choi HS, Yang JW, Park BC, Kim JA, Kang KW. Enhancement of vascular endothelial growth factor-mediated angiogenesis in tamoxifen-resistant breast cancer cells: role of Pin1 overexpression. *Mol Cancer Ther* 2009, 8:2163-2171.
10. Wanami LS, Chen HY, Peiro S, Garcia de Herreros A, Bachelder RE. Vascular endothelial growth factor-A stimulates Snail expression in breast tumor cells: implications for tumor progression. *Exp Cell Res* 2008, 314:2448-2453.
11. Guo W. Concise review: breast cancer stem cells: regulatory networks, stem cell niches, and disease relevance. *Stem Cells Transl Med* 2014, 3:942-948.
12. Smith BN, Burton LJ, Henderson V, Randle DD, Morton DJ, Smith BA, Taliaferro-Smith L, Nagappan P, Yates C, Zayzafoon M, et al. Snail promotes epithelial mesenchymal transition in breast cancer cells in part via activation of nuclear ERK2. *PLoS One* 2014, 9:e104987.
13. Mezencev R, Matyunina LV, Jabbari N, McDonald JF. Snail-induced epithelial-to-mesenchymal transition of MCF-7 breast cancer cells: systems analysis of molecular changes and their effect on radiation and drug sensitivity. *BMC Cancer* 2016, 16:236.
14. Ota I, Masui T, Kurihara M, Yook JI, Mikami S, Kimura T, Shimada K, Konishi N,

- Yane K, Yamanaka T, Kitahara T. Snail-induced EMT promotes cancer stem cell-like properties in head and neck cancer cells. *Oncol Rep* 2016, 35:261-266.
15. Zhou W, Lv R, Qi W, Wu D, Xu Y, Liu W, Mou Y, Wang L. Snail contributes to the maintenance of stem cell-like phenotype cells in human pancreatic cancer. *PLoS One* 2014, 9:e87409.
16. Ye X, Tam WL, Shibue T, Kaygusuz Y, Reinhardt F, Ng Eaton E, Weinberg RA. Distinct EMT programs control normal mammary stem cells and tumour-initiating cells. *Nature* 2015, 525:256-260.
17. Lamouille S, Xu J, Derynck R. Molecular mechanisms of epithelial-mesenchymal transition. *Nat Rev Mol Cell Biol* 2014, 15:178-196.
18. Loh YN, Hedditch EL, Baker LA, Jary E, Ward RL, Ford CE. The Wnt signalling pathway is upregulated in an in vitro model of acquired tamoxifen resistant breast cancer. *BMC Cancer* 2013, 13:174.
19. DeSantis CE, Ma J, Goding Sauer A, Newman LA, Jemal A. Breast cancer statistics, 2017, racial disparity in mortality by state. *CA Cancer J Clin* 2017, 67:439-448.
20. Phanphaisarn A, Patumanond J, Settakorn J, Chaiyawat P, Klangjorhor J, Pruksakorn D. Prevalence and Survival Patterns of Patients with Bone Metastasis from Common Cancers in Thailand. *Asian Pac J Cancer Prev* 2016, 17:4335-4340.

21. Waks AG, Winer EP. **Breast Cancer Treatment: A Review.** *Jama* 2019, **321**:288-300.
22. Neven P, Jongen L, Lintermans A, Van Asten K, Blomme C, Lambrechts D, Poppe A, Wildiers H, Dieudonne AS, Brouckaert O, et al. **Tamoxifen Metabolism and Efficacy in Breast Cancer: A Prospective Multicenter Trial.** *Clin Cancer Res* 2018, **24**:2312-2318.
23. Yeh WL, Shioda K, Coser KR, Rivizzigno D, McSweeney KR, Shioda T. **Fulvestrant-induced cell death and proteasomal degradation of estrogen receptor alpha protein in MCF-7 cells require the CSK c-Src tyrosine kinase.** *PLoS One* 2013, **8**:e60889.
24. Lumachi F, Luisetto G, Basso SM, Basso U, Brunello A, Camozzi V. **Endocrine therapy of breast cancer.** *Curr Med Chem* 2011, **18**:513-522.
25. Osborne CK, Schiff R. **Mechanisms of endocrine resistance in breast cancer.** *Annu Rev Med* 2011, **62**:233-247.
26. Murphy CG, Dickler MN. **Endocrine resistance in hormone-responsive breast cancer: mechanisms and therapeutic strategies.** *Endocr Relat Cancer* 2016, **23**:R337-352.
27. Ochnik AM, Peterson MS, Avdulov SV, Oh AS, Bitterman PB, Yee D. **Amplified in Breast Cancer Regulates Transcription and Translation in Breast Cancer Cells.** *Neoplasia* 2016, **18**:100-110.

28. Yan J, Yu CT, Ozen M, Ittmann M, Tsai SY, Tsai MJ. Steroid receptor coactivator-3 and activator protein-1 coordinately regulate the transcription of components of the insulin-like growth factor/AKT signaling pathway. *Cancer Res* 2006, 66:11039-11046.
29. Truong TH, Hu H, Temiz NA, Hagen KM, Girard BJ, Brady NJ, Schwertfeger KL, Lange CA, Ostrander JH. Cancer Stem Cell Phenotypes in ER(+) Breast Cancer Models Are Promoted by PELP1/AIB1 Complexes. *Mol Cancer Res* 2018, 16:707-719.
30. De Craene B, Berx G. Regulatory networks defining EMT during cancer initiation and progression. *Nat Rev Cancer* 2013, 13:97-110.
31. Shih JY, Yang PC. The EMT regulator slug and lung carcinogenesis. *Carcinogenesis* 2011, 32:1299-1304.
32. Yuan J, Liu M, Yang L, Tu G, Zhu Q, Chen M, Cheng H, Luo H, Fu W, Li Z, Yang G. Acquisition of epithelial-mesenchymal transition phenotype in the tamoxifen-resistant breast cancer cell: a new role for G protein-coupled estrogen receptor in mediating tamoxifen resistance through cancer-associated fibroblast-derived fibronectin and beta1-integrin signaling pathway in tumor cells. *Breast Cancer Res* 2015, 17:69.
33. Chen K, Huang YH, Chen JL. Understanding and targeting cancer stem cells: therapeutic implications and challenges. *Acta Pharmacol Sin* 2013, 34:732-740.

34. Somasundaram V, Hemalatha SK, Pal K, Sinha S, Nair AS, Mukhopadhyay D, Srinivas P. Selective mode of action of plumbagin through BRCA1 deficient breast cancer stem cells. *BMC Cancer* 2016, 16:336.
35. Hiscox S, Jiang WG, Obermeier K, Taylor K, Morgan L, Burmi R, Barrow D, Nicholson RI. Tamoxifen resistance in MCF7 cells promotes EMT-like behaviour and involves modulation of beta-catenin phosphorylation. *Int J Cancer* 2006, 118:290-301.
36. Pohl SG, Brook N, Agostino M, Arfuso F, Kumar AP, Dharmarajan A. Wnt signaling in triple-negative breast cancer. *Oncogenesis* 2017, 6:e310.
37. McNeill H, Woodgett JR. When pathways collide: collaboration and connivance among signalling proteins in development. *Nat Rev Mol Cell Biol* 2010, 11:404-413.
38. Schlange T, Matsuda Y, Lienhard S, Huber A, Hynes NE. Autocrine WNT signaling contributes to breast cancer cell proliferation via the canonical WNT pathway and EGFR transactivation. *Breast Cancer Res* 2007, 9:R63.
39. Guo P, Fang Q, Tao HQ, Schafer CA, Fenton BM, Ding I, Hu B, Cheng SY. Overexpression of vascular endothelial growth factor by MCF-7 breast cancer cells promotes estrogen-independent tumor growth in vivo. *Cancer Res* 2003, 63:4684-4691.
40. Clapp C, Thebault S, Jeziorski MC, Martinez De La Escalera G. Peptide hormone



regulation of angiogenesis. *Physiol Rev* 2009, **89**:1177-1215.

41. Sharpe R, Pearson A, Herrera-Abreu MT, Johnson D, Mackay A, Welti JC, Natrajan R, Reynolds AR, Reis-Filho JS, Ashworth A, Turner NC. FGFR signaling promotes the growth of triple-negative and basal-like breast cancer cell lines both in vitro and in vivo. *Clin Cancer Res* 2011, **17**:5275-5286.
42. Butler SJ, Richardson L, Farias N, Morrison J, Coomber BL. Characterization of cancer stem cell drug resistance in the human colorectal cancer cell lines HCT116 and SW480. *Biochem Biophys Res Commun* 2017, **490**:29-35.
43. Liu H, Zhang HW, Sun XF, Guo XH, He YN, Cui SD, Fan QX. Tamoxifen-resistant breast cancer cells possess cancer stem-like cell properties. *Chin Med J (Engl)* 2013, **126**:3030-3034.
44. Kanwal R, Shukla S, Walker E, Gupta S. Acquisition of tumorigenic potential and therapeutic resistance in CD133+ subpopulation of prostate cancer cells exhibiting stem-cell like characteristics. *Cancer Lett* 2018, **430**:25-33.
45. Xu L, Zhang L, Hu C, Liang S, Fei X, Yan N, Zhang Y, Zhang F. WNT pathway inhibitor pyrvinium pamoate inhibits the self-renewal and metastasis of breast cancer stem cells. *Int J Oncol* 2016, **48**:1175-1186.
46. Mani SA, Guo W, Liao MJ, Eaton EN, Ayyanan A, Zhou AY, Brooks M, Reinhard F, Zhang CC, Shipitsin M, et al. The epithelial-mesenchymal transition generates cells with properties of stem cells. *Cell* 2008, **133**:704-715.

47. Shukla S, Wu CP, Nandigama K, Ambudkar SV. The naphthoquinones, vitamin K3 and its structural analogue plumbagin, are substrates of the multidrug resistance linked ATP binding cassette drug transporter ABCG2. *Mol Cancer Ther* 2007, 6:3279-3286.
48. Omosa LK, Midiwo JO, Mbaveng AT, Tankeo SB, Seukep JA, Voukeng IK, Dzutam JK, Isemeki J, Derese S, Omolle RA, et al. Antibacterial activities and structure-activity relationships of a panel of 48 compounds from Kenyan plants against multidrug resistant phenotypes. *Springerplus* 2016, 5:901.
49. Dhaked HP, Bhattacharya A, Yadav S, Dantu SC, Kumar A, Panda D. Mutation of Arg191 in FtsZ Impairs Cytokinetic Abscission of *Bacillus subtilis* Cells. *Biochemistry* 2016, 55:5754-5763.
50. Ohene-Agyei T, Mowla R, Rahman T, Venter H. Phytochemicals increase the antibacterial activity of antibiotics by acting on a drug efflux pump. *Microbiologyopen* 2014, 3:885-896.
51. Kaewbumrung S, Panichayupakaranant P. Isolation of three antibacterial naphthoquinones from *Plumbago indica* roots and development of a validated quantitative HPLC analytical method. *Nat Prod Res* 2012, 26:2020-2023.
52. Kuete V, Alibert-Franco S, Eyong KO, Ngameni B, Folefoc GN, Nguemeving JR, Tangmouo JG, Fotso GW, Komguem J, Ouahouo BM, et al. Antibacterial activity of some natural products against bacteria expressing a multidrug-resistant

- phenotype. *Int J Antimicrob Agents* 2011, **37**:156-161.
53. Hassan ST, Berchova-Bimova K, Petras J. Plumbagin, a Plant-Derived Compound, Exhibits Antifungal Combinatory Effect with Amphotericin B against *Candida albicans* Clinical Isolates and Anti-hepatitis C Virus Activity. *Phytother Res* 2016, **30**:1487-1492.
54. Tian J, Chen Y, Ma B, He J, Tong J, Wang Y. *Drosera peltata* Smith var. *lunata* (Buch.-Ham.) C. B. Clarke as a feasible source of plumbagin: phytochemical analysis and antifungal activity assay. *World J Microbiol Biotechnol* 2014, **30**:737-745.
55. Gwee PS, Khoo KS, Ong HC, Sit NW. Bioactivity-guided isolation and structural characterization of the antifungal compound, plumbagin, from *Nepenthes gracilis*. *Pharm Biol* 2014, **52**:1526-1531.
56. Sumsakul W, Chaijaroenkul W, Na-Bangchang K. In vitro inhibitory effects of plumbagin, the promising antimalarial candidate, on human cytochrome P450 enzymes. *Asian Pac J Trop Med* 2015, **8**:914-918.
57. Pradeepa V, Sathish-Narayanan S, Kirubakaran SA, Senthil-Nathan S. Antimalarial efficacy of dynamic compound of plumbagin chemical constituent from *Plumbago zeylanica* Linn (Plumbaginaceae) against the malarial vector *Anopheles stephensi* Liston (Diptera: Culicidae). *Parasitol Res* 2014, **113**:3105-3109.
58. Wang SX, Wang J, Shao JB, Tang WN, Zhong JQ. Plumbagin Mediates

Cardioprotection Against Myocardial Ischemia/Reperfusion Injury Through Nrf-2 Signaling. *Med Sci Monit* 2016, 22:1250-1257.

59. Chu H, Yu H, Ren D, Zhu K, Huang H. Plumbagin exerts protective effects in nucleus pulposus cells by attenuating hydrogen peroxide-induced oxidative stress, inflammation and apoptosis through NF-kappaB and Nrf-2. *Int J Mol Med* 2016, 37:1669-1676.
60. Son TG, Kawamoto EM, Yu QS, Greig NH, Mattson MP, Camandola S. Naphthazarin protects against glutamate-induced neuronal death via activation of the Nrf2/ARE pathway. *Biochem Biophys Res Commun* 2013, 433:602-606.
61. Yong R, Chen XM, Shen S, Vijayaraj S, Ma Q, Pollock CA, Saad S. Plumbagin ameliorates diabetic nephropathy via interruption of pathways that include NOX4 signalling. *PLoS One* 2013, 8:e73428.
62. Sunil C, Duraipandiyan V, Agastian P, Ignacimuthu S. Antidiabetic effect of plumbagin isolated from *Plumbago zeylanica* L. root and its effect on GLUT4 translocation in streptozotocin-induced diabetic rats. *Food Chem Toxicol* 2012, 50:4356-4363.
63. Zhang W, Cheng L, Hou Y, Si M, Zhao YP, Nie L. Plumbagin Protects Against Spinal Cord Injury-induced Oxidative Stress and Inflammation in Wistar Rats through Nrf-2 Upregulation. *Drug Res (Stuttg)* 2015, 65:495-499.
64. Kumar S, Gautam S, Sharma A. Antimutagenic and antioxidant properties of

- plumbagin and other naphthoquinones. *Mutat Res* 2013, 755:30-41.
65. Wang T, Wu F, Jin Z, Zhai Z, Wang Y, Tu B, Yan W, Tang T. Plumbagin inhibits LPS-induced inflammation through the inactivation of the nuclear factor-kappa B and mitogen activated protein kinase signaling pathways in RAW 264.7 cells. *Food Chem Toxicol* 2014, 64:177-183.
66. Checker R, Patwardhan RS, Sharma D, Menon J, Thoh M, Sandur SK, Sainis KB, Poduval TB. Plumbagin, a vitamin K3 analogue, abrogates lipopolysaccharide-induced oxidative stress, inflammation and endotoxic shock via NF-kappaB suppression. *Inflammation* 2014, 37:542-554.
67. Checker R, Sharma D, Sandur SK, Khanam S, Poduval TB. Anti-inflammatory effects of plumbagin are mediated by inhibition of NF-kappaB activation in lymphocytes. *Int Immunopharmacol* 2009, 9:949-958.
68. Kawiak A, Domachowska A. Plumbagin Suppresses the Invasion of HER2-Overexpressing Breast Cancer Cells through Inhibition of IKKalpha-Mediated NF-kappaB Activation. *PLoS One* 2016, 11:e0164064.
69. Manu KA, Shanmugam MK, Rajendran P, Li F, Ramachandran L, Hay HS, Kannaiyan R, Swamy SN, Vali S, Kapoor S, et al. Plumbagin inhibits invasion and migration of breast and gastric cancer cells by downregulating the expression of chemokine receptor CXCR4. *Mol Cancer* 2011, 10:107.
70. Hafeez BB, Zhong W, Fischer JW, Mustafa A, Shi X, Meske L, Hong H, Cai W,

- Havighurst T, Kim K, Verma AK. Plumbagin, a medicinal plant (*Plumbago zeylanica*)-derived 1,4-naphthoquinone, inhibits growth and metastasis of human prostate cancer PC-3M-luciferase cells in an orthotopic xenograft mouse model. *Mol Oncol* 2013, 7:428-439.
71. Sung B, Oyajobi B, Aggarwal BB. Plumbagin inhibits osteoclastogenesis and reduces human breast cancer-induced osteolytic bone metastasis in mice through suppression of RANKL signaling. *Mol Cancer Ther* 2012, 11:350-359.
72. Li Z, Xiao J, Wu X, Li W, Yang Z, Xie J, Xu L, Cai X, Lin Z, Guo W, et al. Plumbagin inhibits breast tumor bone metastasis and osteolysis by modulating the tumor-bone microenvironment. *Curr Mol Med* 2012, 12:967-981.
73. Xue YL, Meng XQ, Ma LJ, Yuan Z. Plumbagin exhibits an anti-proliferative effect in human osteosarcoma cells by downregulating FHL2 and interfering with Wnt/beta-catenin signalling. *Oncol Lett* 2016, 12:1095-1100.
74. Anuf AR, Ramachandran R, Krishnasamy R, Gandhi PS, Periyasamy S. Antiproliferative effects of *Plumbago rosea* and its purified constituent plumbagin on SK-MEL 28 melanoma cell lines. *Pharmacognosy Res* 2014, 6:312-319.
75. Niu M, Cai W, Liu H, Chong Y, Hu W, Gao S, Shi Q, Zhou X, Liu X, Yu R. Plumbagin inhibits growth of gliomas in vivo via suppression of FOXM1 expression. *J Pharmacol Sci* 2015, 128:131-136.
76. Liu X, Cai W, Niu M, Chong Y, Liu H, Hu W, Wang D, Gao S, Shi Q, Hu J, et al.

- Plumbagin induces growth inhibition of human glioma cells by downregulating the expression and activity of FOXM1. *J Neurooncol* 2015, 121:469-477.
77. Khaw AK, Sameni S, Venkatesan S, Kalthur G, Hande MP. Plumbagin alters telomere dynamics, induces DNA damage and cell death in human brain tumour cells. *Mutat Res Genet Toxicol Environ Mutagen* 2015, 793:86-95.
78. Fiorito S, Genovese S, Taddeo VA, Mathieu V, Kiss R, Epifano F. Novel juglone and plumbagin 5-O derivatives and their in vitro growth inhibitory activity against apoptosis-resistant cancer cells. *Bioorg Med Chem Lett* 2016, 26:334-337.
79. Wang F, Wang Q, Zhou ZW, Yu SN, Pan ST, He ZX, Zhang X, Wang D, Yang YX, Yang T, et al. Plumbagin induces cell cycle arrest and autophagy and suppresses epithelial to mesenchymal transition involving PI3K/Akt/mTOR-mediated pathway in human pancreatic cancer cells. *Drug Des Devel Ther* 2015, 9:537-560.
80. Hafeez BB, Jamal MS, Fischer JW, Mustafa A, Verma AK. Plumbagin, a plant derived natural agent inhibits the growth of pancreatic cancer cells in in vitro and in vivo via targeting EGFR, Stat3 and NF-kappaB signaling pathways. *Int J Cancer* 2012, 131:2175-2186.
81. Joo MK, Park JJ, Kim SH, Yoo HS, Lee BJ, Chun HJ, Lee SW, Bak YT. Antitumorigenic effect of plumbagin by induction of SH2-containing protein tyrosine phosphatase 1 in human gastric cancer cells. *Int J Oncol* 2015, 46:2380-2388.
82. Li J, Shen L, Lu FR, Qin Y, Chen R, Li J, Li Y, Zhan HZ, He YQ. Plumbagin inhibits

- cell growth and potentiates apoptosis in human gastric cancer cells in vitro through the NF-kappaB signaling pathway. *Acta Pharmacol Sin* 2012, **33**:242-249.
83. Wei Y, Yang Q, Zhang Y, Zhao T, Liu X, Zhong J, Ma J, Chen Y, Zhao C, Li J. Plumbagin restrains hepatocellular carcinoma angiogenesis by suppressing the migration and invasion of tumor-derived vascular endothelial cells. *Oncotarget* 2017, **8**:15230-15241.
84. Hwang GH, Ryu JM, Jeon YJ, Choi J, Han HJ, Lee YM, Lee S, Bae JS, Jung JW, Chang W, et al. The role of thioredoxin reductase and glutathione reductase in plumbagin-induced, reactive oxygen species-mediated apoptosis in cancer cell lines. *Eur J Pharmacol* 2015, **765**:384-393.
85. Shih YW, Lee YC, Wu PF, Lee YB, Chiang TA. Plumbagin inhibits invasion and migration of liver cancer HepG2 cells by decreasing productions of matrix metalloproteinase-2 and urokinase- plasminogen activator. *Hepatol Res* 2009, **39**:998-1009.
86. Sinha S, Pal K, Elkhanany A, Dutta S, Cao Y, Mondal G, Iyer S, Somasundaram V, Couch FJ, Shridhar V, et al. Plumbagin inhibits tumorigenesis and angiogenesis of ovarian cancer cells in vivo. *Int J Cancer* 2013, **132**:1201-1212.
87. Tian L, Yin D, Ren Y, Gong C, Chen A, Guo FJ. Plumbagin induces apoptosis via the p53 pathway and generation of reactive oxygen species in human osteosarcoma cells. *Mol Med Rep* 2012, **5**:126-132.



88. Li J, Shen Q, Peng R, Chen R, Jiang P, Li Y, Zhang L, Lu J. Plumbagin enhances TRAIL-mediated apoptosis through up-regulation of death receptor in human melanoma A375 cells. *J Huazhong Univ Sci Technolog Med Sci* 2010, 30:458-463.
89. Bae KJ, Lee Y, Kim SA, Kim J. Plumbagin exerts an immunosuppressive effect on human T-cell acute lymphoblastic leukemia MOLT-4 cells. *Biochem Biophys Res Commun* 2016, 473:272-277.
90. Fu C, Gong Y, Shi X, Sun Z, Niu M, Sang W, Xu L, Zhu F, Wang Y, Xu K. Plumbagin reduces chronic lymphocytic leukemia cell survival by downregulation of Bcl-2 but upregulation of the Bax protein level. *Oncol Rep* 2016, 36:1605-1611.
91. Uttarkar S, Piontek T, Dukare S, Schomburg C, Schlenke P, Berdel WE, Muller-Tidow C, Schmidt TJ, Klempnauer KH. Small-Molecule Disruption of the Myb/p300 Cooperation Targets Acute Myeloid Leukemia Cells. *Mol Cancer Ther* 2016, 15:2905-2915.
92. Wu H, Dai X, Wang E. Plumbagin inhibits cell proliferation and promotes apoptosis in multiple myeloma cells through inhibition of the PI3K/Akt-mTOR pathway. *Oncol Lett* 2016, 12:3614-3618.
93. Qiu JX, He YQ, Wang Y, Xu RL, Qin Y, Shen X, Zhou SF, Mao ZF. Plumbagin induces the apoptosis of human tongue carcinoma cells through the mitochondria-mediated pathway. *Med Sci Monit Basic Res* 2013, 19:228-236.

94. Ono T, Ota A, Ito K, Nakaoka T, Karnan S, Konishi H, Furuhashi A, Hayashi T, Yamada Y, Hosokawa Y, Kazaoka Y. **Plumbagin suppresses tumor cell growth in oral squamous cell carcinoma cell lines.** *Oral Dis* 2015, **21**:501-511.
95. Pan ST, Qin Y, Zhou ZW, He ZX, Zhang X, Yang T, Yang YX, Wang D, Qiu JX, Zhou SF. **Plumbagin induces G2/M arrest, apoptosis, and autophagy via p38 MAPK- and PI3K/Akt/mTOR-mediated pathways in human tongue squamous cell carcinoma cells.** *Drug Des Devel Ther* 2015, **9**:1601-1626.
96. Raghu D, Karunakaran D. **Plumbagin downregulates Wnt signaling independent of p53 in human colorectal cancer cells.** *J Nat Prod* 2014, **77**:1130-1134.
97. Eldhose B, Gunawan M, Rahman M, Latha MS, Notario V. **Plumbagin reduces human colon cancer cell survival by inducing cell cycle arrest and mitochondria-mediated apoptosis.** *Int J Oncol* 2014, **45**:1913-1920.
98. Chen MB, Zhang Y, Wei MX, Shen W, Wu XY, Yao C, Lu PH. **Activation of AMP-activated protein kinase (AMPK) mediates plumbagin-induced apoptosis and growth inhibition in cultured human colon cancer cells.** *Cell Signal* 2013, **25**:1993-2002.
99. Subramaniya BR, Srinivasan G, Sadullah SS, Davis N, Subhadara LB, Halagowder D, Sivasitambaram ND. **Apoptosis inducing effect of plumbagin on colonic cancer cells depends on expression of COX-2.** *PLoS One* 2011, **6**:e18695.
100. Rattarom R, Sakpakdeejaroen I, Hansakul P, Itharat A. **Cytotoxic activity against**

- small cell lung cancer cell line and chromatographic fingerprinting of six isolated compounds from the ethanolic extract of Benjakul. *J Med Assoc Thai* 2014, 97 Suppl 8:S70-75.
101. Li YC, He SM, He ZX, Li M, Yang Y, Pang JX, Zhang X, Chow K, Zhou Q, Duan W, et al. Plumbagin induces apoptotic and autophagic cell death through inhibition of the PI3K/Akt/mTOR pathway in human non-small cell lung cancer cells. *Cancer Lett* 2014, 344:239-259.
102. Xu TP, Shen H, Liu LX, Shu YQ. Plumbagin from *Plumbago Zeylanica* L induces apoptosis in human non-small cell lung cancer cell lines through NF- $\kappa$ B inactivation. *Asian Pac J Cancer Prev* 2013, 14:2325-2331.
103. Shieh JM, Chiang TA, Chang WT, Chao CH, Lee YC, Huang GY, Shih YX, Shih YW. Plumbagin inhibits TPA-induced MMP-2 and u-PA expressions by reducing binding activities of NF- $\kappa$ B and AP-1 via ERK signaling pathway in A549 human lung cancer cells. *Mol Cell Biochem* 2010, 335:181-193.
104. Hafeez BB, Zhong W, Mustafa A, Fischer JW, Witkowsky O, Verma AK. Plumbagin inhibits prostate cancer development in TRAMP mice via targeting PKCepsilon, Stat3 and neuroendocrine markers. *Carcinogenesis* 2012, 33:2586-2592.
105. Hafeez BB, Fischer JW, Singh A, Zhong W, Mustafa A, Meske L, Sheikhani MO, Verma AK. Plumbagin Inhibits Prostate Carcinogenesis in Intact and Castrated PTEN Knockout Mice via Targeting PKCepsilon, Stat3, and Epithelial-to-

**Mesenchymal Transition Markers.** *Cancer Prev Res (Phila)* 2015, 8:375-386.

106. Qiu JX, Zhou ZW, He ZX, Zhao RJ, Zhang X, Yang L, Zhou SF, Mao ZF. Plumbagin elicits differential proteomic responses mainly involving cell cycle, apoptosis, autophagy, and epithelial-to-mesenchymal transition pathways in human prostate cancer PC-3 and DU145 cells. *Drug Des Devel Ther* 2015, 9:349-417.
107. Zhang XQ, Yang CY, Rao XF, Xiong JP. Plumbagin shows anti-cancer activity in human breast cancer cells by the upregulation of p53 and p21 and suppression of G1 cell cycle regulators. *Eur J Gynaecol Oncol* 2016, 37:30-35.
108. Sameni S, Hande MP. Plumbagin triggers DNA damage response, telomere dysfunction and genome instability of human breast cancer cells. *Biomed Pharmacother* 2016, 82:256-268.
109. Dandawate P, Ahmad A, Deshpande J, Swamy KV, Khan EM, Khetmalas M, Padhye S, Sarkar F. Anticancer phytochemical analogs 37: synthesis, characterization, molecular docking and cytotoxicity of novel plumbagin hydrazones against breast cancer cells. *Bioorg Med Chem Lett* 2014, 24:2900-2904.
110. Yan W, Tu B, Liu YY, Wang TY, Qiao H, Zhai ZJ, Li HW, Tang TT. Suppressive Effects of Plumbagin on Invasion and Migration of Breast Cancer Cells via the Inhibition of STAT3 Signaling and Down-regulation of Inflammatory Cytokine Expressions. *Bone Res* 2013, 1:362-370.

111. Sun G, Shan MH, Ma BL, Geng ZL, Alibiyati A, Zhong H, Wang J, Ren GH, Li HT, Dong C. Identifying crosstalk of mTOR signaling pathway of lobular breast carcinomas. *Eur Rev Med Pharmacol Sci* 2012, **16**:1355-1361.
112. Lee JH, Yeon JH, Kim H, Roh W, Chae J, Park HO, Kim DM. The natural anticancer agent plumbagin induces potent cytotoxicity in MCF-7 human breast cancer cells by inhibiting a PI-5 kinase for ROS generation. *PLoS One* 2012, **7**:e45023.
113. Kawiak A, Zawacka-Pankau J, Lojkowska E. Plumbagin induces apoptosis in Her2-overexpressing breast cancer cells through the mitochondrial-mediated pathway. *J Nat Prod* 2012, **75**:747-751.
114. Sagar S, Esau L, Moosa B, Khashab NM, Bajic VB, Kaur M. Cytotoxicity and apoptosis induced by a plumbagin derivative in estrogen positive MCF-7 breast cancer cells. *Anticancer Agents Med Chem* 2014, **14**:170-180.
115. Yan W, Wang TY, Fan QM, Du L, Xu JK, Zhai ZJ, Li HW, Tang TT. Plumbagin attenuates cancer cell growth and osteoclast formation in the bone microenvironment of mice. *Acta Pharmacol Sin* 2014, **35**:124-134.
116. Gowda R, Sharma A, Robertson GP. Synergistic inhibitory effects of Celecoxib and Plumbagin on melanoma tumor growth. *Cancer Lett* 2017, **385**:243-250.
117. Qiao H, Wang TY, Yan W, Qin A, Fan QM, Han XG, Wang YG, Tang TT. Synergistic suppression of human breast cancer cells by combination of plumbagin and zoledronic acid In vitro. *Acta Pharmacol Sin* 2015, **36**:1085-1098.

118. Gowda R, Kardos G, Sharma A, Singh S, Robertson GP. **Nanoparticle-Based Celecoxib and Plumbagin for the Synergistic Treatment of Melanoma.** *Mol Cancer Ther* 2017, **16**:440-452.
119. Qiao H, Wang TY, Yu ZF, Han XG, Liu XQ, Wang YG, Fan QM, Qin A, Tang TT. Structural simulation of adenosine phosphate via plumbagin and zoledronic acid competitively targets JNK/Erk to synergistically attenuate osteoclastogenesis in a breast cancer model. *Cell Death Dis* 2016, **7**:e2094.
120. Lai L, Liu J, Zhai D, Lin Q, He L, Dong Y, Zhang J, Lu B, Chen Y, Yi Z, Liu M. Plumbagin inhibits tumour angiogenesis and tumour growth through the Ras signalling pathway following activation of the VEGF receptor-2. *Br J Pharmacol* 2012, **165**:1084-1096.
121. Reshma RS, Sreelatha KH, Somasundaram V, Satheesh Kumar S, Nadhan R, Nair RS, Srinivas P. **Plumbagin, a naphthaquinone derivative induces apoptosis in BRCA 1/2 defective castrate resistant prostate cancer cells as well as prostate cancer stem-like cells.** *Pharmacol Res* 2016, **105**:134-145.
122. Pan ST, Qin Y, Zhou ZW, He ZX, Zhang X, Yang T, Yang YX, Wang D, Zhou SF, Qiu JX. Plumbagin suppresses epithelial to mesenchymal transition and stemness via inhibiting Nrf2-mediated signaling pathway in human tongue squamous cell carcinoma cells. *Drug Des Devel Ther* 2015, **9**:5511-5551.
123. Zhou ZW, Li XX, He ZX, Pan ST, Yang Y, Zhang X, Chow K, Yang T, Qiu JX, Zhou

- Q, et al. Induction of apoptosis and autophagy via sirtuin1- and PI3K/Akt/mTOR-mediated pathways by plumbagin in human prostate cancer cells. *Drug Des Devel Ther* 2015, **9**:1511-1554.
124. Hsieh YJ, Lin LC, Tsai TH. Measurement and pharmacokinetic study of plumbagin in a conscious freely moving rat using liquid chromatography/tandem mass spectrometry. *J Chromatogr B Analyt Technol Biomed Life Sci* 2006, **844**:1-5.
125. Sumsakul W, Plengsuriyakarn T, Na-Bangchang K. Pharmacokinetics, toxicity, and cytochrome P450 modulatory activity of plumbagin. *BMC Pharmacol Toxicol* 2016, **17**:50.
126. Chen A, Zhou X, Tang S, Liu M, Wang X. Evaluation of the inhibition potential of plumbagin against cytochrome P450 using LC-MS/MS and cocktail approach. *Sci Rep* 2016, **6**:28482.
127. Vijayakumar R, Senthilvelan M, Ravindran R, Devi RS. Plumbago zeylanica action on blood coagulation profile with and without blood volume reduction. *Vascul Pharmacol* 2006, **45**:86-90.
128. Ahmad A, Banerjee S, Wang Z, Kong D, Sarkar FH. Plumbagin-induced apoptosis of human breast cancer cells is mediated by inactivation of NF-kappaB and Bcl-2. *J Cell Biochem* 2008, **105**:1461-1471.
129. Aziz MH, Dreckschmidt NE, Verma AK. Plumbagin, a medicinal plant-derived naphthoquinone, is a novel inhibitor of the growth and invasion of hormone-

- refractory prostate cancer. *Cancer Res* 2008, **68**:9024-9032.
130. Kuete V, Omosa LK, Tala VR, Midiwo JO, Mbaveng AT, Swaleh S, Karaosmanoglu O, Sivas H. Cytotoxicity of Plumbagin, Rapanone and 12 other naturally occurring Quinones from Kenyan Flora towards human carcinoma cells. *BMC Pharmacol Toxicol* 2016, **17**:60.
131. Horvay K, Casagrande F, Gany A, Hime GR, Abud HE. Wnt signaling regulates Snai1 expression and cellular localization in the mouse intestinal epithelial stem cell niche. *Stem Cells Dev* 2011, **20**:737-745.
132. Kuo PL, Hsu YL, Cho CY. Plumbagin induces G2-M arrest and autophagy by inhibiting the AKT/mammalian target of rapamycin pathway in breast cancer cells. *Mol Cancer Ther* 2006, **5**:3209-3221.
133. Bailey-Downs LC, Thorpe JE, Disch BC, Bastian A, Hauser PJ, Farasyn T, Berry WL, Hurst RE, Ihnat MA. Development and characterization of a preclinical model of breast cancer lung micrometastatic to macrometastatic progression. *PLoS One* 2014, **9**:e98624.
134. Jonsson PI, Letertre L, Juliusson SJ, Gudmundsdottir BR, Francis CW, Onundarson PT. During warfarin induction, the Fiix-prothrombin time reflects the anticoagulation level better than the standard prothrombin time. *J Thromb Haemost* 2017, **15**:131-139.
135. Lemini C, Jaimez R, Franco Y. Gender and inter-species influence on coagulation



- tests of rats and mice. *Thromb Res* 2007, **120**:415-419.
136. Zhang M, Li Z, Zhang X, Chang Y. Cancer stem cells as a potential therapeutic target in breast cancer. *Stem Cell Investig* 2014, **1**:14.
137. Bilir B, Kucuk O, Moreno CS. Wnt signaling blockage inhibits cell proliferation and migration, and induces apoptosis in triple-negative breast cancer cells. *J Transl Med* 2013, **11**:280.
138. Su Y, Simmen RC. Soy isoflavone genistein upregulates epithelial adhesion molecule E-cadherin expression and attenuates beta-catenin signaling in mammary epithelial cells. *Carcinogenesis* 2009, **30**:331-339.
139. Nair R, Roden DL, Teo WS, McFarland A, Junankar S, Ye S, Nguyen A, Yang J, Nikolic I, Hui M, et al. c-Myc and Her2 cooperate to drive a stem-like phenotype with poor prognosis in breast cancer. *Oncogene* 2014, **33**:3992-4002.
140. Zhang Y, Zhang GL, Sun X, Cao KX, Ma C, Nan N, Yang GW, Yu MW, Wang XM. Establishment of a murine breast tumor model by subcutaneous or orthotopic implantation. *Oncol Lett* 2018, **15**:6233-6240.
141. Osborne CK. Tamoxifen in the treatment of breast cancer. *N Engl J Med* 1998, **339**:1609-1618.
142. Xu J, Chen Y, Huo D, Khramtsov A, Khramtsova G, Zhang C, Goss KH, Olopade OI. beta-catenin regulates c-Myc and CDKN1A expression in breast cancer cells. *Mol Carcinog* 2016, **55**:431-439.

143. Wang Z, Li B, Zhou L, Yu S, Su Z, Song J, Sun Q, Sha O, Wang X, Jiang W, et al. **Prodigiosin inhibits Wnt/beta-catenin signaling and exerts anticancer activity in breast cancer cells.** *Proc Natl Acad Sci U S A* 2016, **113**:13150-13155.
144. Srinivasan A, Thangavel C, Liu Y, Shoyele S, Den RB, Selvakumar P, Lakshmikuttyamma A. **Quercetin regulates beta-catenin signaling and reduces the migration of triple negative breast cancer.** *Mol Carcinog* 2016, **55**:743-756.
145. Jang GB, Kim JY, Cho SD, Park KS, Jung JY, Lee HY, Hong IS, Nam JS. **Blockade of Wnt/beta-catenin signaling suppresses breast cancer metastasis by inhibiting CSC-like phenotype.** *Sci Rep* 2015, **5**:12465.
146. Tian X, Liu Z, Niu B, Zhang J, Tan TK, Lee SR, Zhao Y, Harris DC, Zheng G. **E-cadherin/beta-catenin complex and the epithelial barrier.** *J Biomed Biotechnol* 2011, **2011**:567305.
147. Solanas G, Porta-de-la-Riva M, Agusti C, Casagolda D, Sanchez-Aguilera F, Larriba MJ, Pons F, Peiro S, Escriva M, Munoz A, et al. **E-cadherin controls beta-catenin and NF-kappaB transcriptional activity in mesenchymal gene expression.** *J Cell Sci* 2008, **121**:2224-2234.
148. Shan S, Lv Q, Zhao Y, Liu C, Sun Y, Xi K, Xiao J, Li C. **Wnt/beta-catenin pathway is required for epithelial to mesenchymal transition in CXCL12 over expressed breast cancer cells.** *Int J Clin Exp Pathol* 2015, **8**:12357-12367.
149. Lieu C, Heymach J, Overman M, Tran H, Kopetz S. **Beyond VEGF: inhibition of the**

- fibroblast growth factor pathway and antiangiogenesis. *Clin Cancer Res* 2011, 17:6130-6139.
150. Sasich LD, Sukkari SR. The US FDAs withdrawal of the breast cancer indication for Avastin (bevacizumab). *Saudi Pharm J* 2012, 20:381-385.
151. Aukes K, Forsman C, Brady NJ, Astleford K, Blixt N, Sachdev D, Jensen ED, Mansky KC, Schwertfeger KL. Breast cancer cell-derived fibroblast growth factors enhance osteoclast activity and contribute to the formation of metastatic lesions. *PLoS One* 2017, 12:e0185736.
152. Kottakis F, Polytarchou C, Foltopoulou P, Sanidas I, Kampranis SC, Tsihliis PN. FGF-2 regulates cell proliferation, migration, and angiogenesis through an NDY1/KDM2B-miR-101-EZH2 pathway. *Mol Cell* 2011, 43:285-298.
153. Alessi P, Leali D, Camozzi M, Cantelmo A, Albini A, Presta M. Anti-FGF2 approaches as a strategy to compensate resistance to anti-VEGF therapy: long-pentraxin 3 as a novel antiangiogenic FGF2-antagonist. *Eur Cytokine Netw* 2009, 20:225-234.
154. Katoh M, Katoh M. Cross-talk of WNT and FGF signaling pathways at GSK3beta to regulate beta-catenin and SNAIL signaling cascades. *Cancer Biol Ther* 2006, 5:1059-1064.
155. Zhang H, Qi Y, Geng D, Shi Y, Wang X, Yu R, Zhou X. Expression profile and clinical significance of Wnt signaling in human gliomas. *Oncol Lett* 2018, 15:610-

617.



จุฬาลงกรณ์มหาวิทยาลัย  
**CHULALONGKORN UNIVERSITY**

## APPENDIX

### Buffers and Reagents

#### 1. Incomplete MEM medium 1 liter

MEM powder	10.4	g
NaHCO <sub>3</sub>	3.7	g
Ultrapure H <sub>2</sub> O	900	mL

Adjust pH to 7.3 with 1 N HCl or 2 N NaOH.

Add ultrapure H<sub>2</sub>O to 1 liter and sterilize by filtering through a 0.2 sterile membrane filter.

#### 2. Completed MEM medium 100 mL

Incomplete MEM solution	94	mL
Fetal bovine serum	5.0	mL
Penicillin/Streptomycin	1.0	mL

Store the refrigerator temperature at or below 4°C.

Warm the solution to 37°C before use.

#### 3. Freezing MEM medium 100 mL

Incomplete MEM solution	69	mL
Fetal bovine serum	20	mL

Dimethyl sulfoxide	10	mL
Penicillin/Streptomycin	1.0	mL

Store the refrigerator temperature at or below 4°C.

#### 4. 10x Phosphate Buffered Saline (PBS) 1 liter

NaCl	80.65	g
KCl	2.0	g
KH <sub>2</sub> PO <sub>4</sub>	2.0	g
Na <sub>2</sub> HPO <sub>4</sub>	11.5	g
Ultrapure H <sub>2</sub> O	900	mL

Adjust pH to 7.4 with 1N HCl or 2N NaOH.

Add ultrapure H<sub>2</sub>O to 1 liter and sterilize by autoclaving.

#### 5. Crystal violet staining (0.1% w/v) solution 100 mL

Crystal violet dyes	0.05	g
Ultrapure H <sub>2</sub> O	50.0	mL

Add ultrapure H<sub>2</sub>O to 100 mL and sterilize by filtering through a 0.2 membrane filter.

Store the room temperature at 25°C.

## 6. Formaldehyde (3.7% v/v) solution 1 liter

37% Formaldehyde solution	100	mL
Ultrapure ddH <sub>2</sub> O	900	mL

Sterilize by autoclaving.

Store the room temperature at 25°C.

## 7. SDS Buffer 10% (w/v) solution 100 mL

SDS	10.0	g
Ultrapure H <sub>2</sub> O	50.0	mL

Add ultrapure H<sub>2</sub>O to 200 mL and store the room temperature at 25°C.

Prepare the solution in a ventilated fume hood due to SDS powder is hazardous.

## 8. 10X Tris-Glycine SDS Running Buffer 1 liter

Tris base	30.0	g
Glycine	144.0	g
SDS	10.0	g
Ultrapure H <sub>2</sub> O	900	mL

Adjust pH to 8.3 with 1N HCl or 2N NaOH.

Add ultrapure H<sub>2</sub>O to 200 mL and store at 4°C and dilute to 1X before use.

## 9. 10X Tris Buffered Saline (TBS) 1 liter

Tris base	24.2	g
NaCl	87.7	g
Ultrapure H <sub>2</sub> O	900	mL

Adjust pH to 7.6 with 1N HCl or 2N NaOH.

Add ultrapure H<sub>2</sub>O to 1 liter and store at 4°C and dilute to 1X before use.

## 10. 1X Tris Buffered Saline with Tween 20 (TBST) 1 liter

10X TBS	100	mL
Tween 20	1.0	mL
Ultrapure H <sub>2</sub> O	900	mL

Add ultrapure H<sub>2</sub>O to 1 liter.

Store the room temperature at 25°C.

จุฬาลงกรณ์มหาวิทยาลัย  
CHULALONGKORN UNIVERSITY

## 11. Nonfat Dried Milk 5% (w/v) solution 100 mL

Nonfat dried milk	5.0	g
TBST	100	mL

Store the room temperature at 25°C



## 12. 1X SDS Protein Lysis Buffer 100 mL

10% SDS	15.0	mL
1 M Tris, pH 6.8	1.0	mL
Ultrapure H <sub>2</sub> O	50	mL

Add ultrapure H<sub>2</sub>O to 100 mL and store the room temperature at 25°C.

Add protease and phosphatase inhibitor cocktail of a protein lysis buffer to produce a 1X final concentration.

## 13. 1 M Tris, pH 6.8 200 mL

Tris base	24.22	g
Ultrapure H <sub>2</sub> O	100	mL

Adjust pH to 6.8 with 1N HCl or 2N NaOH.

Add ultrapure H<sub>2</sub>O to 200 mL and store at 4 °C up to 1 month.

CHULALONGKORN UNIVERSITY

## 14. 1.5 M Tris, pH 8.8 200 mL

Tris base	36.33	g
Ultrapure H <sub>2</sub> O	100	mL

Adjust pH to 8.8 with 1N HCl or 2N NaOH.

Add ultrapure H<sub>2</sub>O to 200 mL and store at 4 °C up to 1 month.

## 15. Ponceau S (0.5% w/v) solution 100 mL

Ponceau S	0.5	g
Acetic Acid	5.0	mL
Ultrapure H <sub>2</sub> O	50	mL

Add ultrapure H<sub>2</sub>O to 100 mL and store at 4 °C until use.

Protect from the light by wrapping a bottle in aluminum foil.

## 16. Bromophenol Blue (1% w/v) solution 100 mL

Bromophenol Blue	0.1	g
Ultrapure H <sub>2</sub> O	90	mL

Add ultrapure H<sub>2</sub>O to 100 mL

Store the room temperature at 25°C.

## 17. 5X SDS Loading Buffer 50 mL

10% SDS	3.75	g
Glycerol	15.0	mL
1 M Tris, pH 6.8	2.5	mL
1% Bromophenol Blue	0.5	mL
Ultrapure H <sub>2</sub> O	40	mL

Add ultrapure H<sub>2</sub>O to 50 mL and store in aliquots of 1 cc at 4 °C.

## 18. 1X Transfer Buffer 1 liter

Tris Base	5.82	g
Glycine	2.93	g
Methanol	200	mL
Ultrapure H <sub>2</sub> O	900	mL

Add ultrapure H<sub>2</sub>O to 1 liter and store at 4°C until use.



## VITA

**NAME** Nithidol Sakunrangsit

**DATE OF BIRTH** 1 June 1988

**PLACE OF BIRTH** Bangkok

**PUBLICATION** Sakunrangsit N, Ketchart W. Plumbagin inhibits cancer stem-like cells, angiogenesis and suppresses cell proliferation and invasion by targeting Wnt/ $\beta$ -catenin pathway in endocrine resistant breast cancer. Under Revision.

Manmuan S, Sakunrangsit N, Ketchart W. Salinomycin overcomes acquired tamoxifen resistance through AIB1 and inhibits cancer cell invasion in endocrine resistant breast cancer. Clin Exp Pharmacol Physiol. 2017;44:1042-1052.

Sakunrangsit N, Kalpongkul N, Pisitkun T, Ketchart W. Plumbagin enhances tamoxifen sensitivity and inhibits tumor invasion in endocrine resistant breast cancer through EMT regulation. Phytother Res. 2016;30:1968-1977.

.

**AWARD RECEIVED** The 100th Anniversary Chulalongkorn University for Doctoral Scholarship 2015-2017.